CHAPTER 7

Leqooa Valley results

7.1 INTRODUCTION

The deposits identified at Leqooa Valley are unique, as this is the only site where two deposits occur in close proximity of one another. They both occur on a south-facing slope approximately halfway between the crest of the mountain range and the river in the lower portions of the valley. The deposits are situated approximately 1 km from the Great escarpment. This chapter will describe the morphological, sedimentological and micromorphological results of the Leqooa Valley western and eastern deposits.

7.2 MORPHOLOGY

The Leqooa Valley Site ridges are 308 m (western ridge) and 230 m (eastern ridge) in length and vary in width between 15 m and 67 m and 34m and 56 m respectively (Figures 7.1, 7.2 and 7.3). The maximum heights for the deposits are 12 m for the western ridge and 10 m for the eastern ridge. The altitudinal range of the western ridge is 3054 m a.s.l. to 3112 m a.s.l., whilst that for the eastern ridge is 3057 m a.s.l. to 3108 m a.s.l. The distance between the ridges increases from 290 m at the lower end to 480 m at the upper end of the deposits. The eastern slope deposit has two additional ridges on its eastern flank, the largest being 170 m long, 33 m wide and varies in height between 2 m to 6 m. The western slope deposit has a fairly uniform gradient on both its eastern and western aspects, ranging from 20º (cross section C-C; Figure 7.3) to 26° (cross sections B-B and D-D; Figure 7.3). The longitudinal profile indicates that the slope gradient of the deposit averages 11º. The eastern ridge gradients vary from 10º to 15° on the western aspect and 15º to 21º on the eastern aspect (cross sections F-F, G-G and H-H; Figure 7.3). The longitudinal profile (cross section E-E; Figure 7.3) indicates that the slope gradient varies between 10º and 24° and the average gradient for the deposit is 12º.

Cross section I-I represents the slope profile relating to the western ridge, containing a range of units related to various types of processes (see Figure 2.2 for comparison to a

Figure 7.1 The Leqooa Valley western slope deposit (photo by N. Mulder).

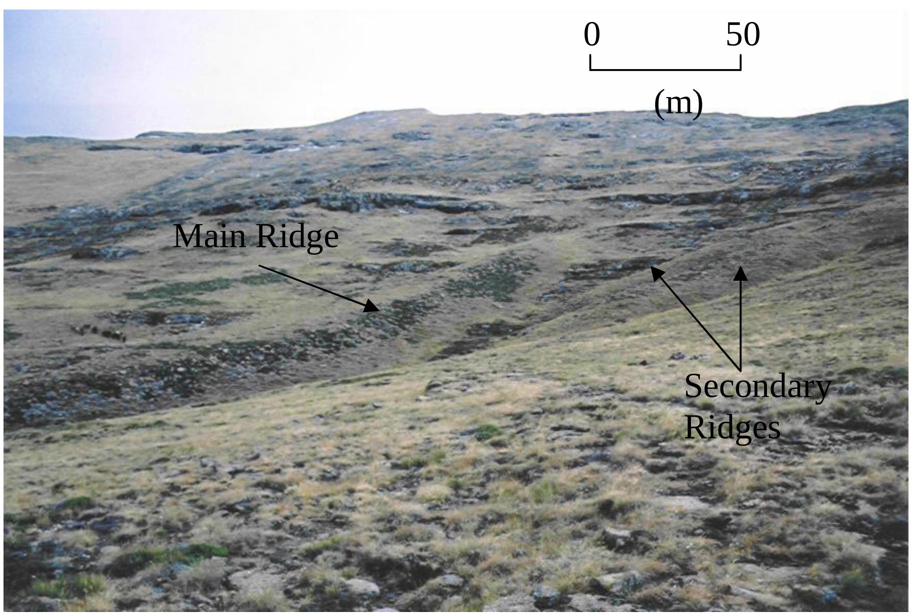

Figure 7.2 The Leqooa Valley eastern slope deposit (photo by S. Mills).

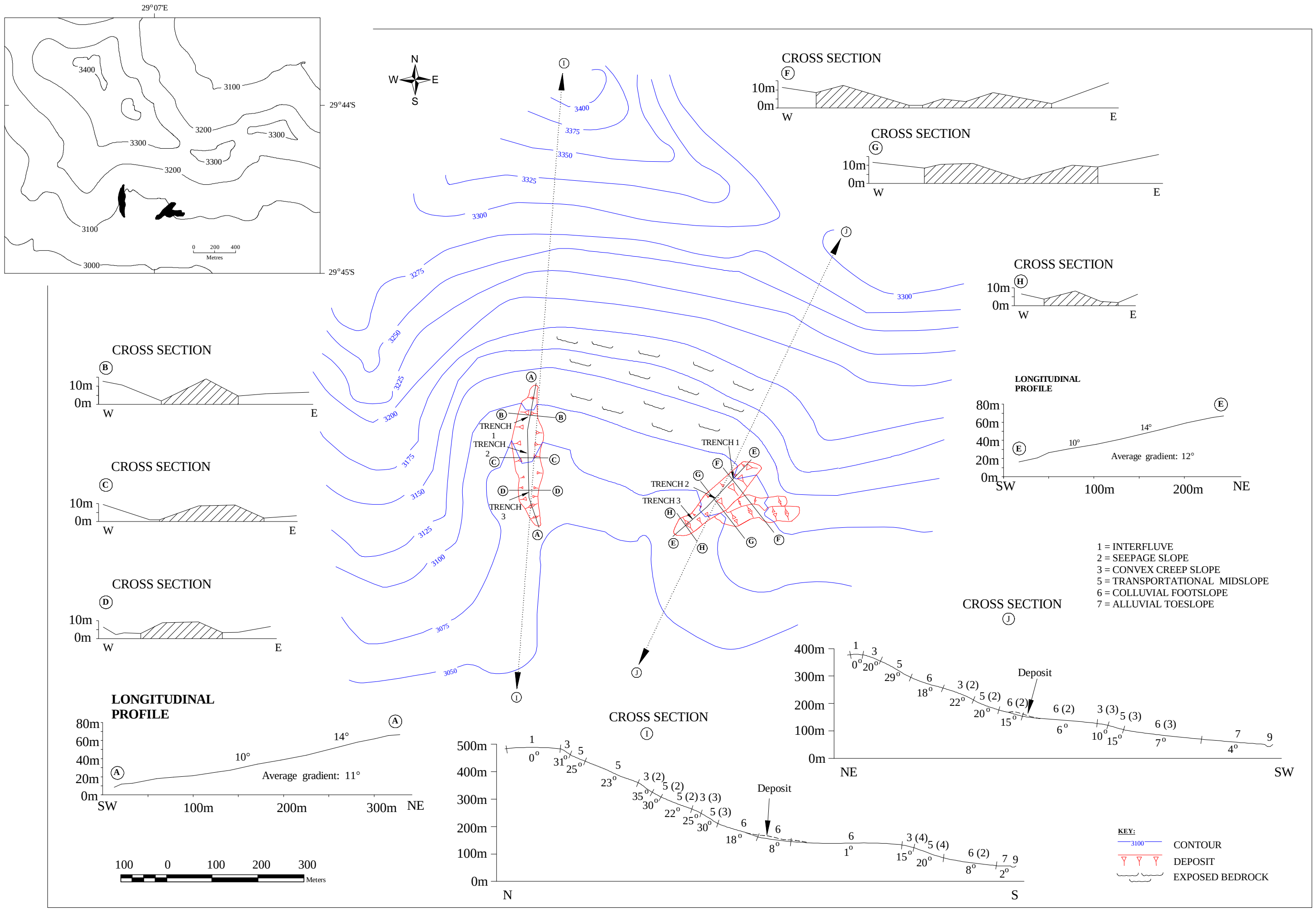

Figure 7.3 Morphological map of the Leqooa Valley deposits.

theoretical slope profile). The slope profile begins with an interfluve unit, which has a slope angle of 0º. The slope angle then increases to 31º on the convex creep slope and ranges between 23º and 25º on the transportational midslope. There is then a second convex slope unit with a gradient of 35º, and a second transportational midslope with a slope angle ranging between 22º and 30º (Figure 7.3). There is a third convex slope unit present, with a slope gradient of 25º, increasing to 30º in the transportational midslope. The colluvial footslope follows this unit and ranges between 1º and 18º. There is then a fourth convex slope unit which has a slope angle of 15º, increasing to 20º on the transportational midslope. The colluvial footslope has a slope angle of 8º, which then levels off to 2º on the alluvial toeslope. The slope deposit occurs within the colluvial footslope and the total slope length is 1.9 km down to the Leqooa River.

Cross section J-J is also a complex slope profile (Figure 7.3). It begins with an interfluve unit, where the slope angle is 0º, followed by a convex slope unit with a slope angle of 20º. The transportational midslope follows this, where the slope angle reaches 29º, and then becomes gentler in the colluvial footslope where the slope angle is 18º. There is then a second convex slope unit with a slope angle of 22º, followed by the transportational midslope, where the slope angle ranges from 15º to 6º. There is a third convex slope unit with a slope angle of 10º, which merges into the transportational midslope where the slope angle is 15º. The colluvial footslope follows this with a slope angle of 7º, followed by the alluvial toeslope where the slope angle is 4º. The deposit occurs within the colluvial footslope and the slope length is 1.6 km down to the Leqooa River.

7.3 FIELD OBSERVATIONS

7.3.1 Western slope deposit

The lithofacies at this site consists of present-day soil which is underlain by a diamict. Although the excavation was to a depth between 120 cm and 150 cm, this is not the depth at which bedrock was reached, but the depth at which it became increasingly difficult to excavate boulders. Within this diamict a variety of different sized clasts and boulders are present, ranging in size from 2 cm to over 100 cm in length, and which are held together by a sandy matrix. There are considerably fewer large boulders present in these deposits in comparison to the Tsatsa-La-Mangaung and Sekhokong deposits. The diamict unit in trenches 1 and 2 (Figures 7.4 and 7.5) is very

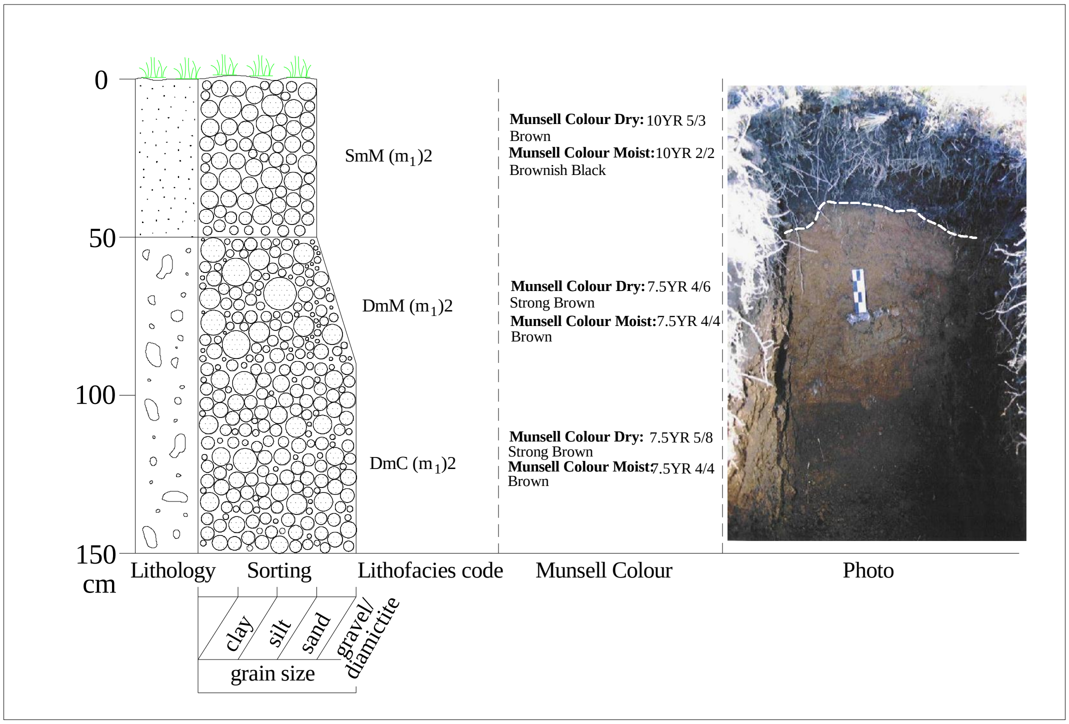

Figure 7.4 Sedimentological and stratigraphical data for trench 1 of the western slope deposit, Leqooa Valley.

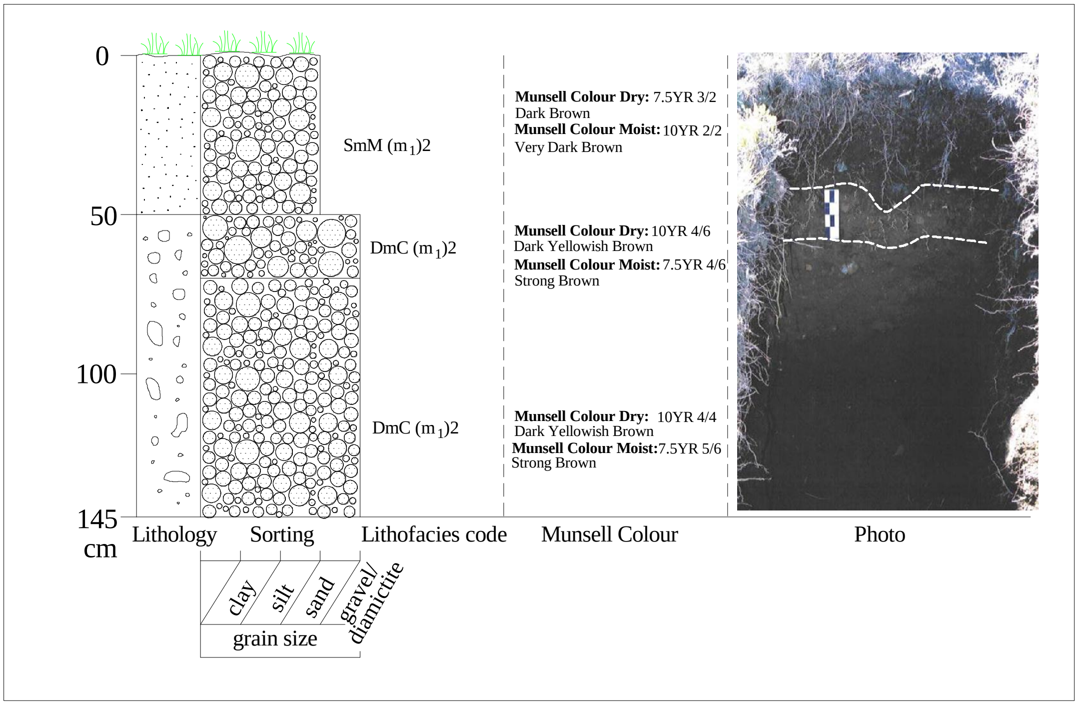

Figure 7.5 Sedimentological and stratigraphical data for trench 2 of the western slope deposit, Leqooa Valley.

similar and is predominantly coarse- grained, massive, poorly sorted, friable and matrix-supported with few clasts. The diamict unit in trench 3 (Figure 7.6) is slightly different. The upper part of this diamict unit massive, medium grained, matrix-supported with few clasts, friable and moderately sorted. The soil is dark brown when dry. Alternatively, the lower part of the unit is more coarse-grained and yellowish brown in colour.

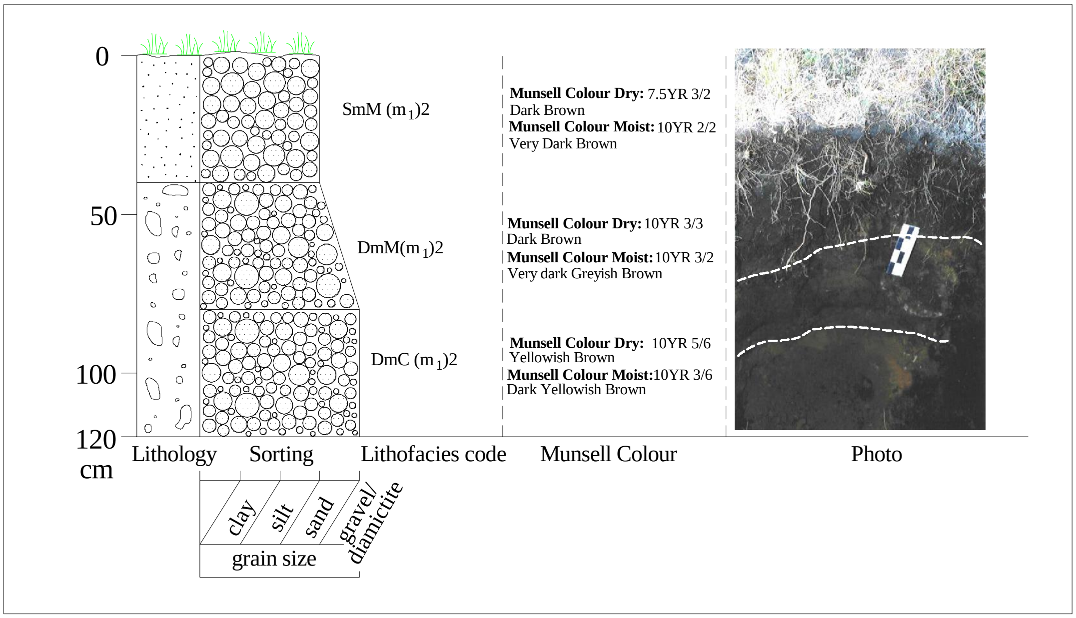

Figure 7.6 Sedimentological and stratigraphical data for trench 3 of the western slope deposit, Leqooa Valley.

7.3.2 Eastern slope deposit

The eastern slope deposit consists of similar lithofacies to the western ridge, in terms of a present-day soil horizon, overlying a gravelly diamict. The diamict unit in trench 1 (Figure 7.7) is uniform throughout. The sediment is massive, medium grained, matrix supported with moderate clasts, friable and poorly sorted. The soil is yellowish brown when dry. In contrast, the diamict unit in trench 2 (Figure 7.8) becomes coarser, loose and more poorly sorted with depth. Trench 3 (Figure 7.9) consists of two units below the present-day soil horizon, which are identified by a change

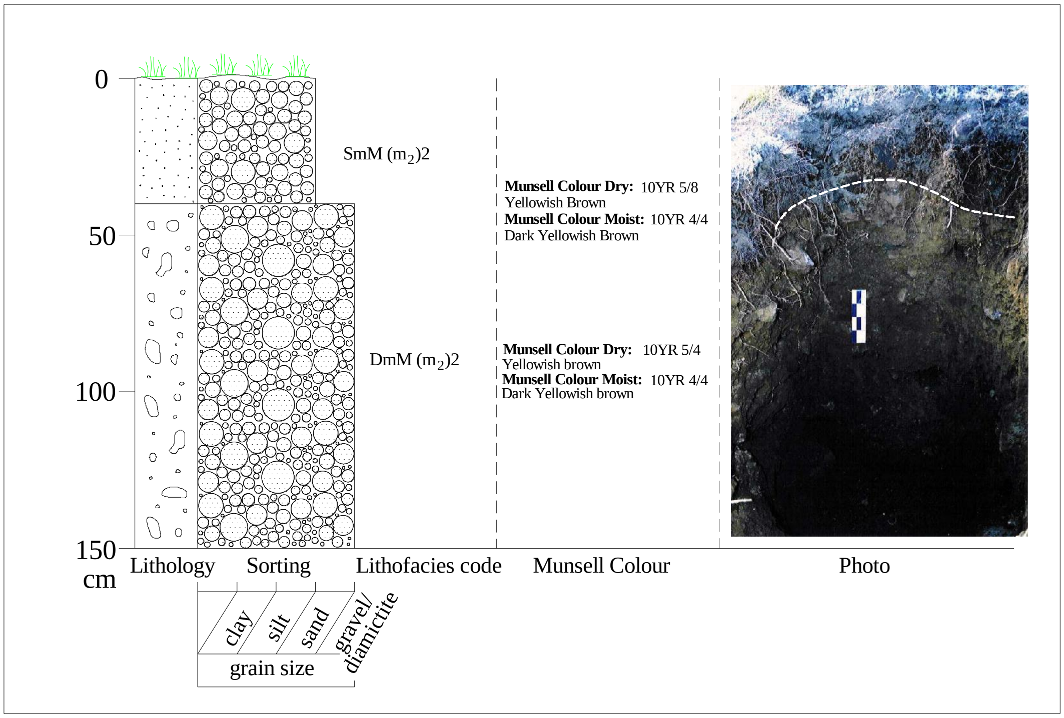

Figure 7.7 Sedimentological and stratigraphical data for trench 1 of the eastern slope deposit, Leqooa Valley.

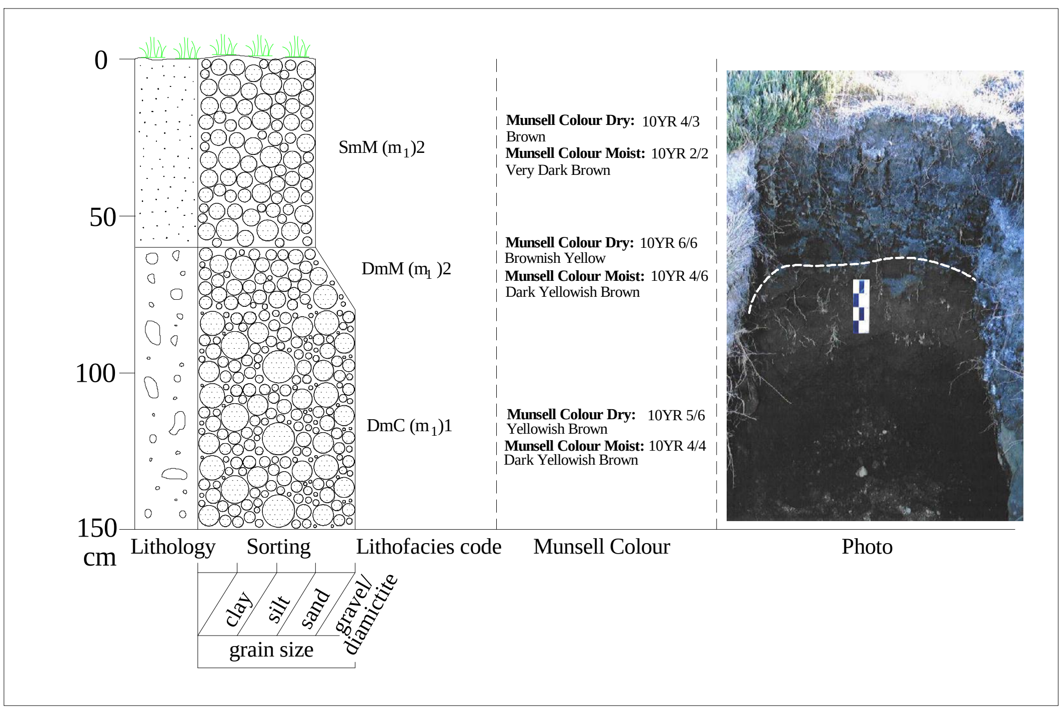

Figure 7.8 Sedimentological and stratigraphical data for trench 2 of the eastern slope deposit, Leqooa Valley.

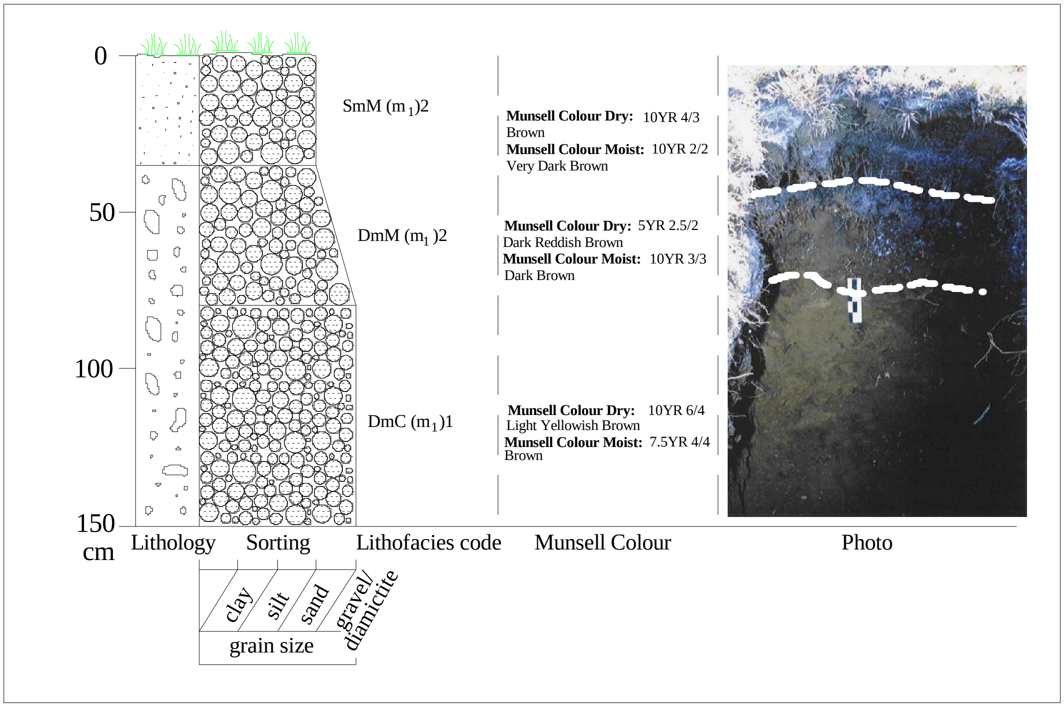

Figure 7.9 Sedimentological and stratigraphical data for trench 3 of the eastern slope deposit, Leqooa Valley.

in colour and consistence. The first unit is massive, matrix supported with few clasts, medium grained, friable and moderately sorted. The soil is dark reddish brown when dry. In contrast, the lower unit is loose and light yellowish brown when dry.

7.4 PARTICLE SIZE ANALYSIS

7.4.1 Western slope deposit

Particle size analysis results for the western slope deposit indicate that gravel is the main constituent in trench 1 at 40 cm and 120 cm depth, representing between 50% and 59% of the sample (Figures 7.10 to 7.12 and Table 7.1). In contrast, at 80 cm and 150 cm depth, sand is the main constituent and makes up more than 43% of the total sample. Particle size in trench 2 consists of approximately 40% gravel and 40% sand, with the exception at 80 cm depth, where gravel constitutes 51%. Trench 3 contains less than 23% gravel at 40 cm and 80 cm depth as opposed to 61% at 120 cm depth. This concurs with the lithology description of this trench (Figure 7.9), which indicates the presence of a medium-grained unit below the present-day soil. Clay represents less than 2% of the samples at this site. There is the presence of a secondary peak at 4 phi,

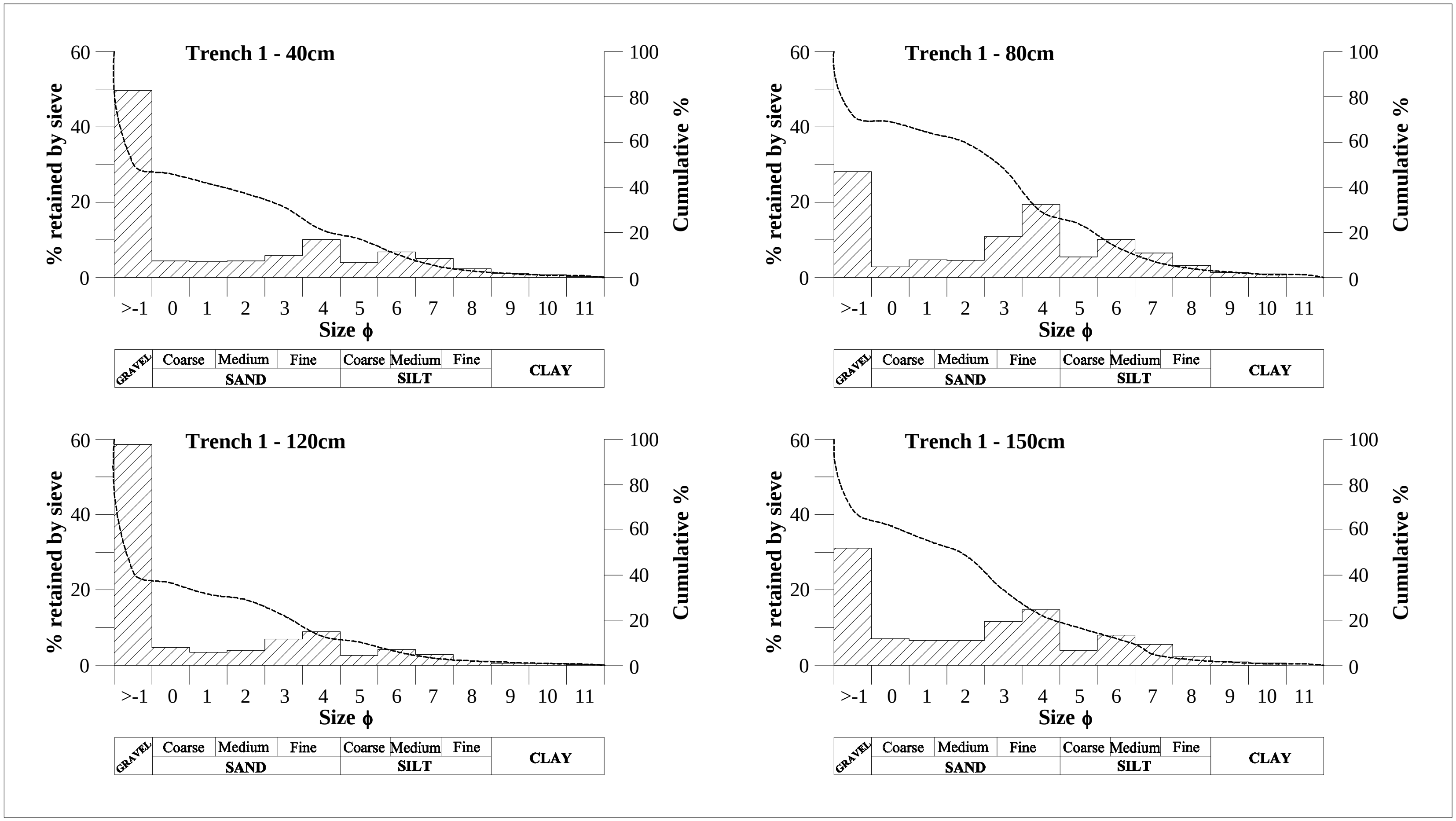

Figure 7.10 Grain size distributions for the sediment from trench 1 of the western slope deposit.

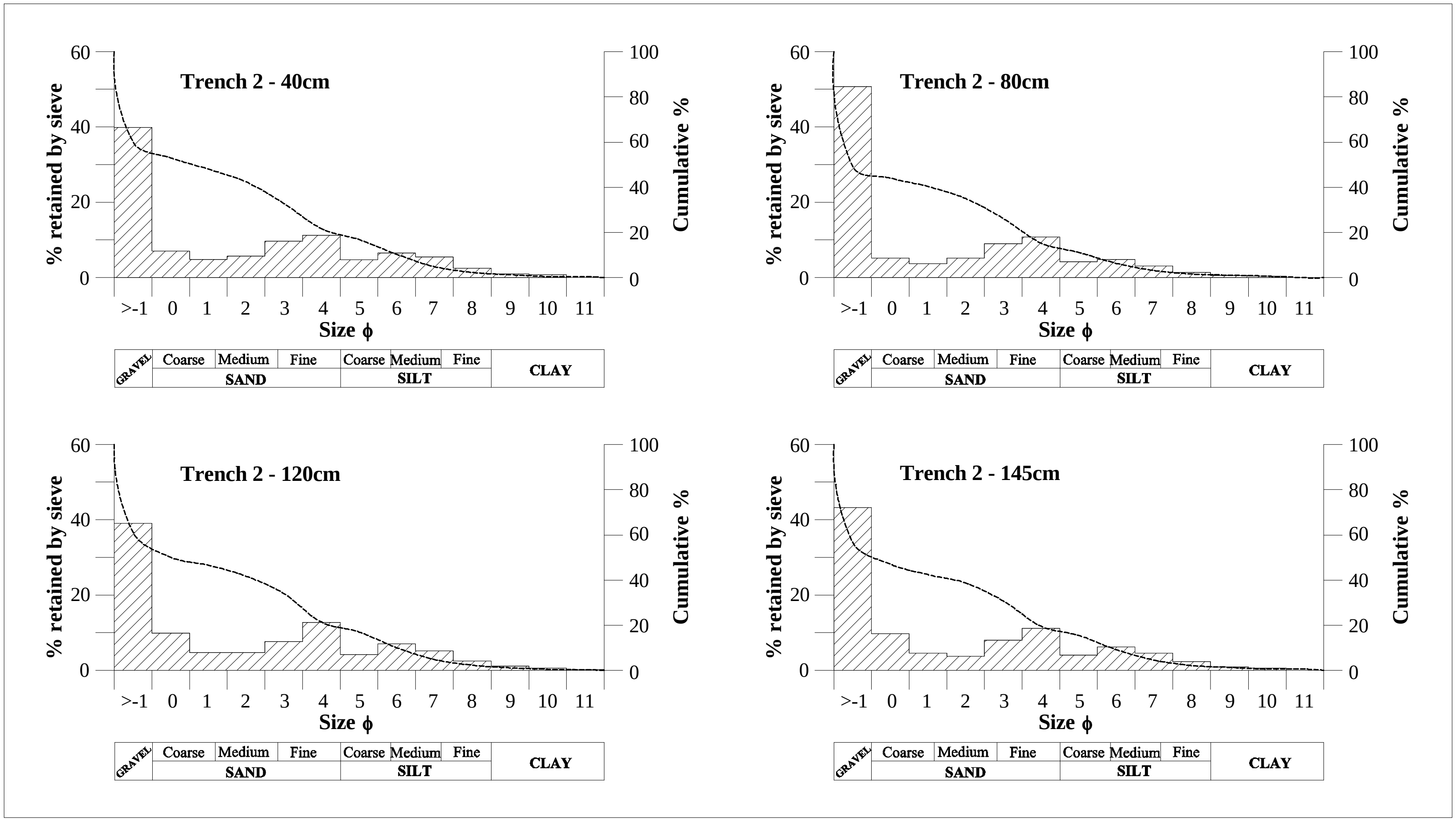

Figure 7.11 Grain size distributions for the sediment from trench 2 of the western slope deposit.

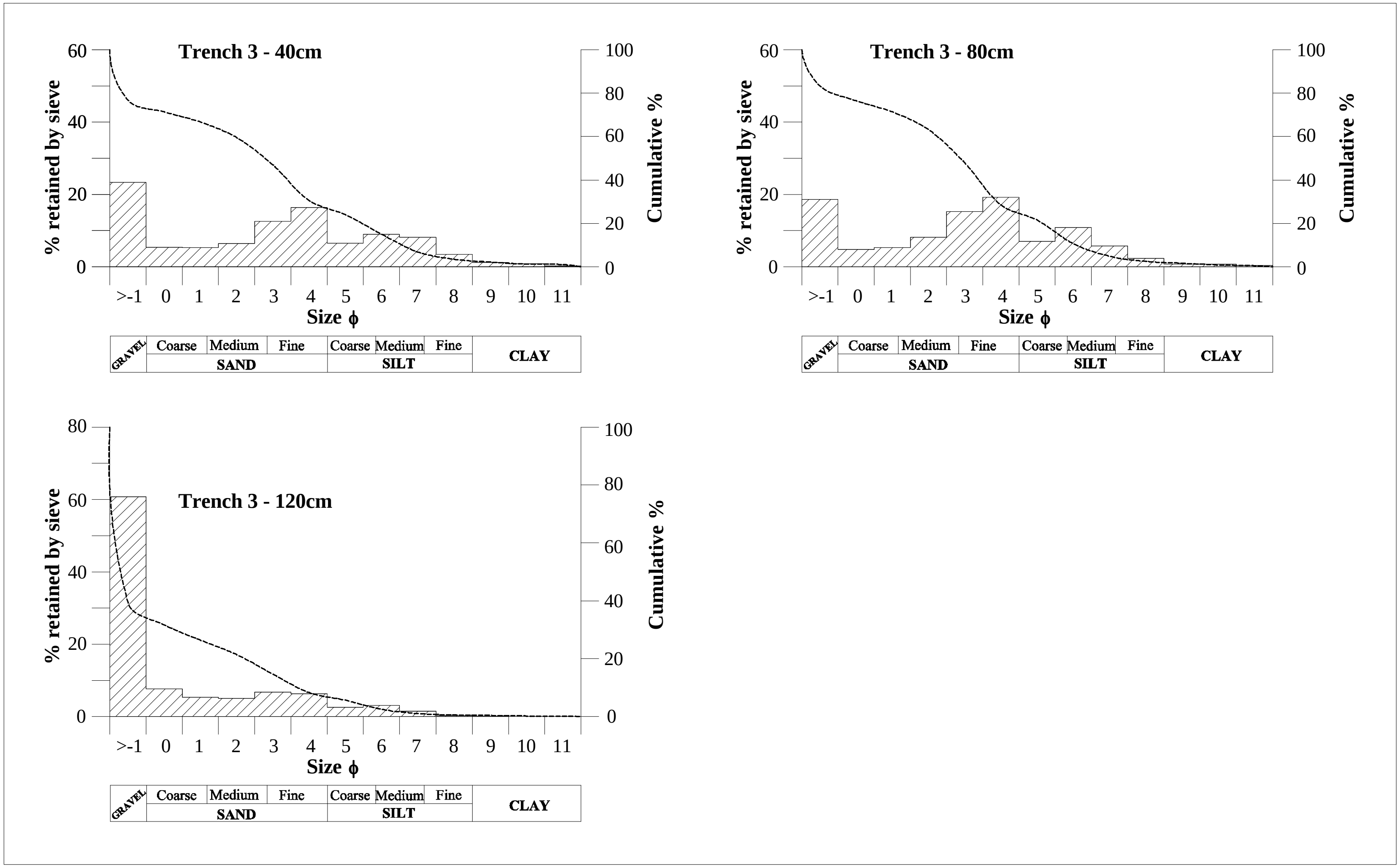

Figure 7.12 Grain size distributions for the sediment from trench 3 of the western slope deposit.

Table 7.1 Particle size statistical analysis for western slope deposit.

Sample	Depth	Gravel (%)	Sand (%)	Silt (%)	Clay (%)	Mean (phi)	Mode (phi)	Peaks (phi)	Bimodality Index (B*)
Trench 1	40 cm	50	29	19	2	1.09	-1	-1, 4, 6	1, 1.4
	80 cm	28	43	27	2	2.54	-1	-1, 4, 6	3.4, 1
	120 cm	59	28	12	1	0.53	-1	-1, 4	0.76
	150 cm	31	47	21	1	2.04	-1	-1, 4, 6	2.4, 1.1
Trench 2	40 cm	40	39	20	1	1.59	-1	-1, 4	1.4
	80 cm	51	34	14	1	0.63	-1	-1, 4	1.1
	120 cm	39	40	20	1	1.46	-1	-1, 4	1.6
	145 cm	44	37	18	1	1.17	-1	-1, 4	1.3
Trench 3	40 cm	24	46	28	2	2.56	-1	-1, 4, 6	3.5, 1.1
	80 cm	18	53	27	2	2.44	4	-1, 4, 6	4.9, 1.1
	120 cm	61	31	8	0	0.25	-1	-1, 3	0.4

with the exception of trench 3 at 120 cm depth where the secondary peak is at 3 phi. Grain size distributions in trench 1 at 80 cm and 140 cm depth are bimodal, however the presence of a peak at 6 phi is not significant enough to produce a polymodal distribution. The sediment in trench 2 is bimodal at 120 cm depth, however this result falls in the transitional range (Hoey 2004). Grain size distributions in trench 3 are bimodal at 40 cm and 80 cm depth and once again the presence of a peak at 6 phi is not significant enough to produce a polymodal distribution.

The graphic mean (Table 7.1) for the three trenches within the western slope deposit indicates that sediment at 120 cm depth is coarsest in trenches 1 and 3, whereas sediment is coarsest at 80 cm depth in trench 2. The mode indicates that all samples have a modal class of -1 phi, which represents gravel, with the exception of trench 3 at 80 cm depth which has a modal class of 4 phi, which represents very fine sand. Further statistical analyses have been undertaken in the form of sorting, skewness and kurtosis (Tables 7.2 and 5.3). The sediment sorting in the three trenches is poorly to very poorly-sorted. Skewness in trenches 1 and 3 ranges from very coarse skewed to nearly symmetrical, whilst the sediment in trench 2 is all very coarse skewed (Table 7.2). This characterises the presence of slightly coarser material within trench 2. Kurtosis ranges from very platykurtic to platykurtic for the three trenches. The mean values in Table 7.3 indicate that the three trenches are similar in terms of their mean particle size which represents medium to coarse sand. The sediment within the three trenches is very poorly sorted, coarse-skewed and platykurtic.

7.4.2 Eastern slope deposit

Particle size analysis results (Figures 7.13 to 7.15 and Table 7.4) for the eastern slope deposit yield similar results to those described for the western slope deposit. Gravel constitutes <44% in trench 1, with sand and silt making up the majority of constituents in the samples (55% to 69%). In contrast, trench 2 contains a higher percentage of gravel than trench 1, such that at 150 cm depth it constitutes 64% of the sample. Trench 3 is similar to trench 1 where sand is the main constituent and accounts for >49% of the samples. There is <13% silt in all the units below the present-day soil horizon at this site and <2% clay. There is a secondary peak in the grain size distribution in all samples and trench 3 at 40 cm depth has two secondary peaks.

Table 7.2 Further particle size statistical analysis for the western slope deposit.

Sample		Sorting	Skewness	Kurtosis
Trench 1	40 cm	2.77	-0.97	0.72
	80 cm	3.00	0.02	0.60
	120 cm	2.26	-1	0.82
	150 cm	2.78	-0.20	0.68
Trench 2	40 cm	2.74	-0.53	0.71
	80 cm	2.33	-1	0.73
	120 cm	2.74	-0.64	0.69
	145 cm	2.67	-0.82	0.72
Trench 3	40 cm	3.01	-0.01	0.62
	80 cm	2.82	0.08	0.76
	120 cm	1.87	-1	1.11

Table 7.3 Mean and Standard deviation for the particle size statistical analysis for the western slope deposit.

Trench	Mean		Mode		Sorting		Skewness		Kurtosis	
	x	*s*	*x*	*s*	*x*	*s*	*x*	*s*	*x*	*s*
Trench 1	1.55	0.91	-1	0	2.70	0.31	-0.54	0.53	0.71	0.09
Trench 2	1.21	0.43	-1	0	2.62	0.20	-0.75	0.20	0.71	0.02
Trench 3	1.75	1.30	0.67	2.89	2.57	0.61	-0.31	0.60	0.83	0.25

These peaks predominantly occur at -1 phi and 4 phi in trenches 1 and 2 and -1 phi and 3 phi in trench 3. The grain size distribution in trench 1 is bimodal throughout with values ranging between 1.5 and 3.0. In contrast trenches 2 and 3 are unimodal with the exception of trench 3 at 40 cm depth. The graphic mean (Table 7.4) of the diamict unit in the three trenches ranges between 1.3 phi and 0.24 phi, which represents medium to coarse sand. The mode indicates that the three trenches are predominantly composed of gravel with the exception of trench 2 at 40 cm depth which has a modal class of 4 phi, which represents very fine sand.

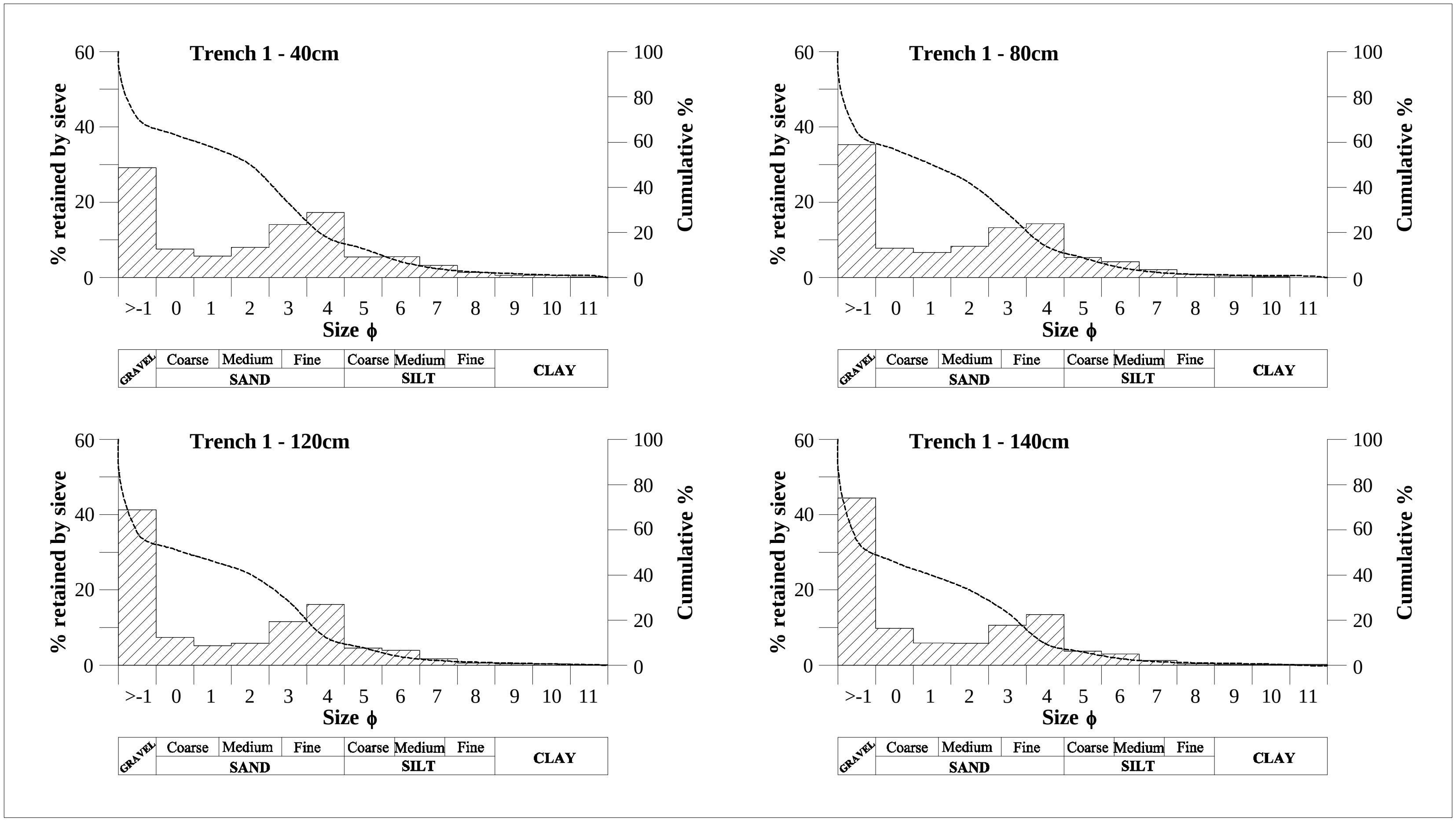

Figure 7.13 Grain size distributions for the sediment from trench 1 of the eastern slope deposit.

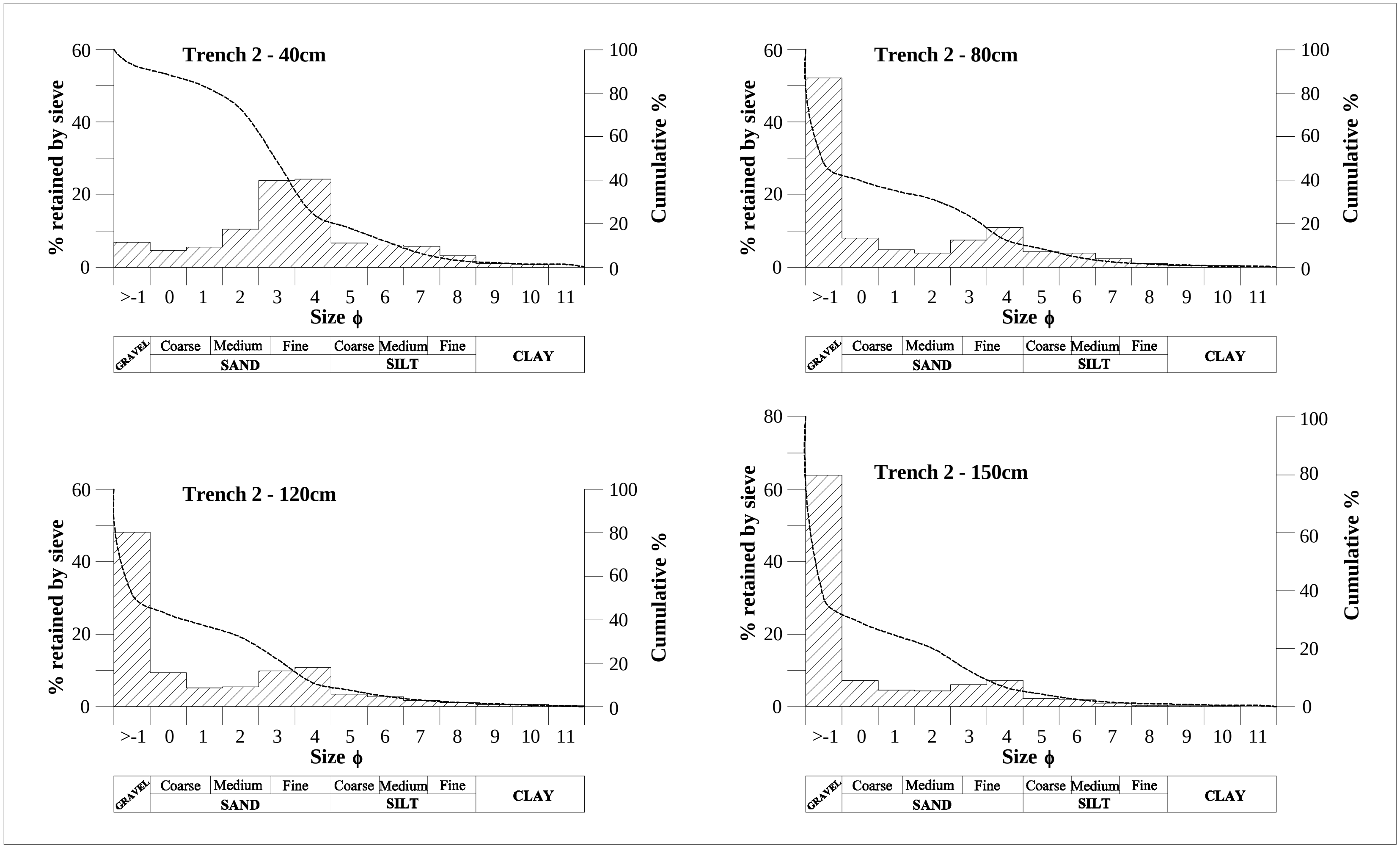

Figure 7.14 Grain size distributions for the sediment from trench 2 of the eastern slope deposit.

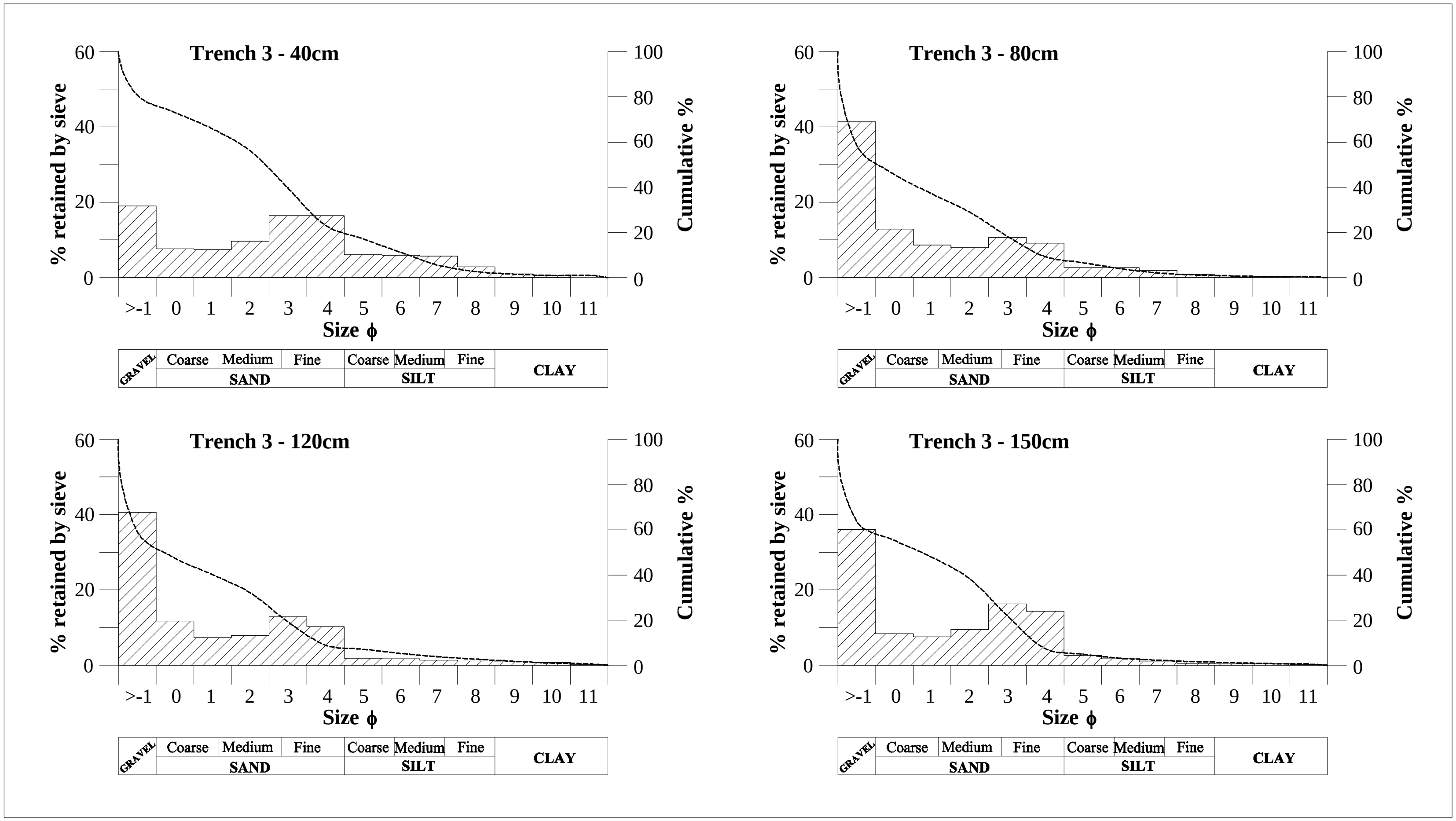

Figure 7.15 Grain size distributions for the sediment from trench 3 of the eastern slope deposit.

Table 7.4 Particle size statistical analysis for the eastern slope deposit.

Sample	Depth	Gravel (%)	Sand (%)	Silt (%)	Clay (%)	Mean (phi)	Mode (phi)	Peaks (phi)	Bimodality Index (B^*)
Trench 1	40 cm	29	53	16	2	1.8	-1	-1, 4	3.0
	80 cm	35	51	13	1	1.3	-1	-1, 4	2.0
	120 cm	41	46	12	1	1.0	-1	-1, 4	2.0
	140 cm	44	46	9	1	0.65	-1	-1, 4	1.5
Trench 2	40 cm	7	69	22	2	3.02	4	3, 4	1.0
	80 cm	52	35	12	1	0.56	-1	-1, 4	1.
	120 cm	48	41	10	1	0.55	-1	-1, 4	1.1
	150 cm	64	29	6	1	0.24	-1	-1, 4	0.6
Trench 3	40 cm	19	58	22	1	2.19	-1	-1, 3, 4	3.4, 1.0
	80 cm	41	49	9	1	0.62	-1	-1, 3	1.0
	120 cm	41	50	7	2	0.67	-1	-1, 3	1.3
	150 cm	36	56	7	1	1.03	-1	-1, 3	1.4

Further statistical analyses have been undertaken in the form of sorting, skewness and kurtosis (Table 7.5). Sediment sorting within the three trenches is predominantly very poorly sorted. Skewness within the eastern slope deposit is symmetrical at 40 cm depth and then ranges from negatively (coarse) skewed to very negatively (coarse) skewed (Table 7.5). The sediment in trenches 1 and 3 ranges from very platykurtic to platykurtic (Table 7.5), whereas the sediment in trench 2 ranges from very leptokurtic to platykurtic. The mean values in Table 7.6 indicate that the sediment within the eastern slope deposit at Leqooa Valley is composed of medium sand which is very poorly sorted and very negatively skewed. The mean grain size indicates that trench 2 contains slightly coarser material than trenches 1 and 3. This is further reinforced by the mean skewness value which indicate that trench 2 is more negatively (coarse) skewed than trenches 1 and 3. Kurtosis is platykurtic in trenches 1 and 3 and mesokurtic in trench 2.

Table 7.5 Further particle size statistical analysis for the eastern slope deposit.

Sample		Sorting	Skewness	Kurtosis
Trench 1	40 cm	2.51	-0.07	0.68
	80 cm	2.26	-0.29	0.66
	120 cm	2.20	-0.56	0.64
	140 cm	2.06	-0.82	0.67
Trench 2	40 cm	2.36	-0.07	1.63
	80 cm	2.21	-1	0.74
	120 cm	2.17	-0.94	0.77
	150 cm	1.80	-1	1.27
Trench 3	40 cm	2.78	-0.04	0.81
	80 cm	2.06	-0.76	0.79
	120 cm	2.16	-0.73	0.82
	150 cm	2.00	-0.31	0.65

Table 7.6 Mean and Standard deviation for the particle size statistical analysis of the eastern slope deposit.

Trench	Mean		Mode		Sorting		Skewness		Kurtosis	
	x	*s*	*x*	*s*	*x*	*s*	*x*	*s*	*x*	*s*
Trench 1	1.19	0.49	-1	0	2.26	0.19	-0.43	0.32	0.66	0.01
Trench 2	1.09	1.29	0.25	2.5	2.14	0.24	-0.75	0.46	1.10	0.43
Trench 3	1.13	0.73	-1	0	2.25	0.36	-0.46	0.35	0.77	0.08

7.5 CLAST FABRIC AND FABRIC EIGENVALUES

7.5.1 Western slope deposit

Due to the lack of available clasts of the given size range for clast fabric analysis and comparison between deposits, it was not possible to satisfy the sample number of 50. Clast a-axis orientation and dip were plotted as an equal-area stereographic scatter plot and an equal-area stereographic contour plot (Figure 7.16). Orientation of the clasts measured within trenches 1 and 2 indicates preferred orientation down-slope in the direction of the ridge crest. In contrast, clasts in trench 3 display orientations slightly more transverse to the ridge crest. Clasts tend to dip between 0º to 30º in all three trenches. The chi-square test was used in order to determine whether clast orientation is statistically significant. Clasts in trench 1 have a statistically significant orientation (<0.05%), whilst clasts in trenches 2 and 3 have a probability of being randomly distributed at a level >0.05%. Although clasts in trench 3 are randomly oriented at >0.05%, they have a statistically significant orientation at <0.10%.

S_1 values, which measure the strength of clustering about the mean axis for the three sites are fairly high and range from 0.766 at trench 3 to 0.813 at trench 1. S_2 and S_3 values are much lower, which indicates that the clast fabrics represent linear clusters, whereby all observations are approximately parallel and $S_1 \gg S_2 \approx S_3$. The normalised S_1 eigenvalues were then plotted onto a general shape diagram (Figure 7.17), and indicate that the sediment in all three trenches has low isotropy (between 0.03 and 0.05) and high elongation values (between 0.74 and 0.80). Fabric shape ellipsoids are compared with plotted data from various published sources (Figure 7.17C) which indicate the sediment from all three trenches falls within the basal ice envelope. The sediment in trenches 2 and 3 also fall within the undeformed lodgement till envelope. When compared with Figure 7.17D, the sediment in all three trenches falls within the boundaries of melt-out till.

A triangular plot of normalised eigenvalues was also generated (Figure 7.18) in order to further compare the western slope deposit eigenvalues to envelopes produced by various authors for a variety of deposits. The sediment in all three trenches falls within the melt-out till and rock glacier internal fabric envelopes. In addition, the

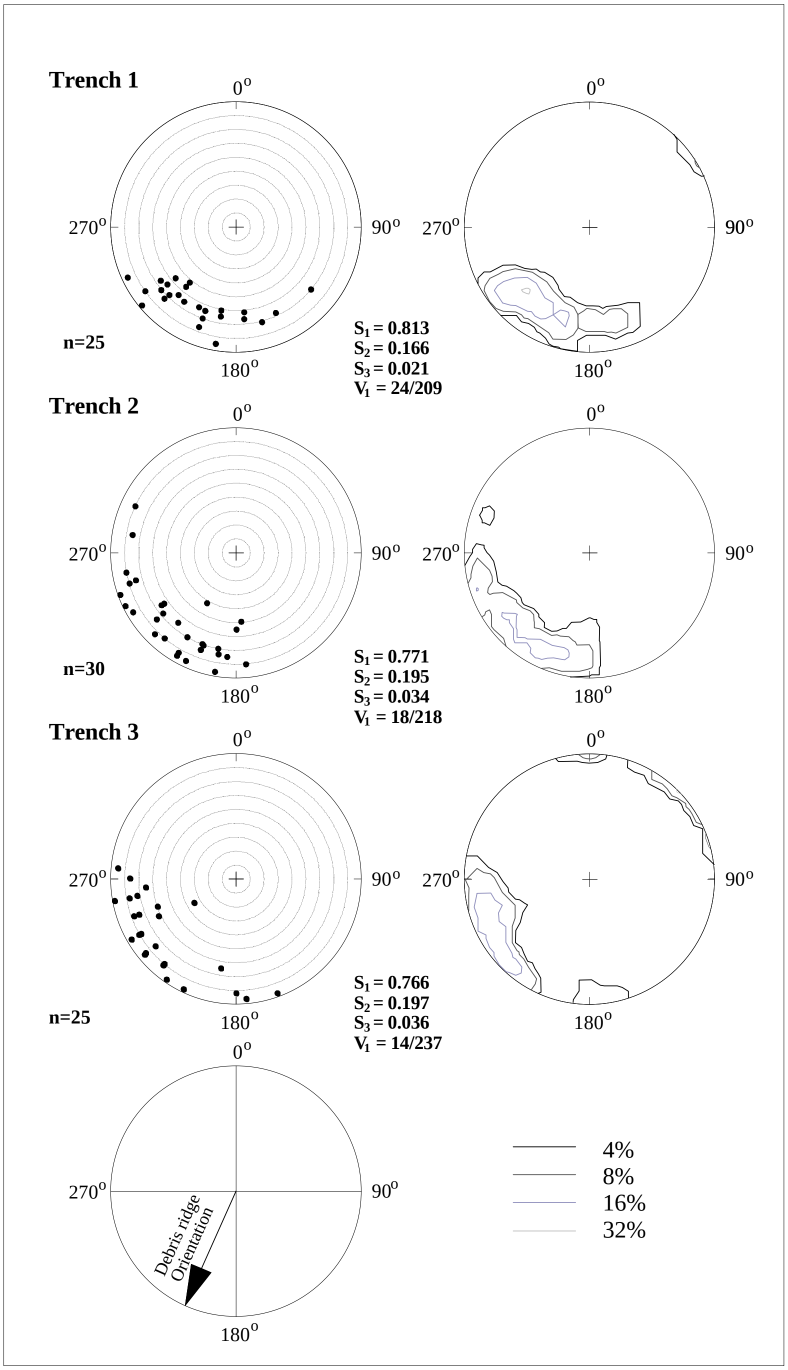

Figure 7.16 Clast orientation, dip and contouring at trenches 1, 2 and 3 at the western slope deposit, Leqooa Valley.

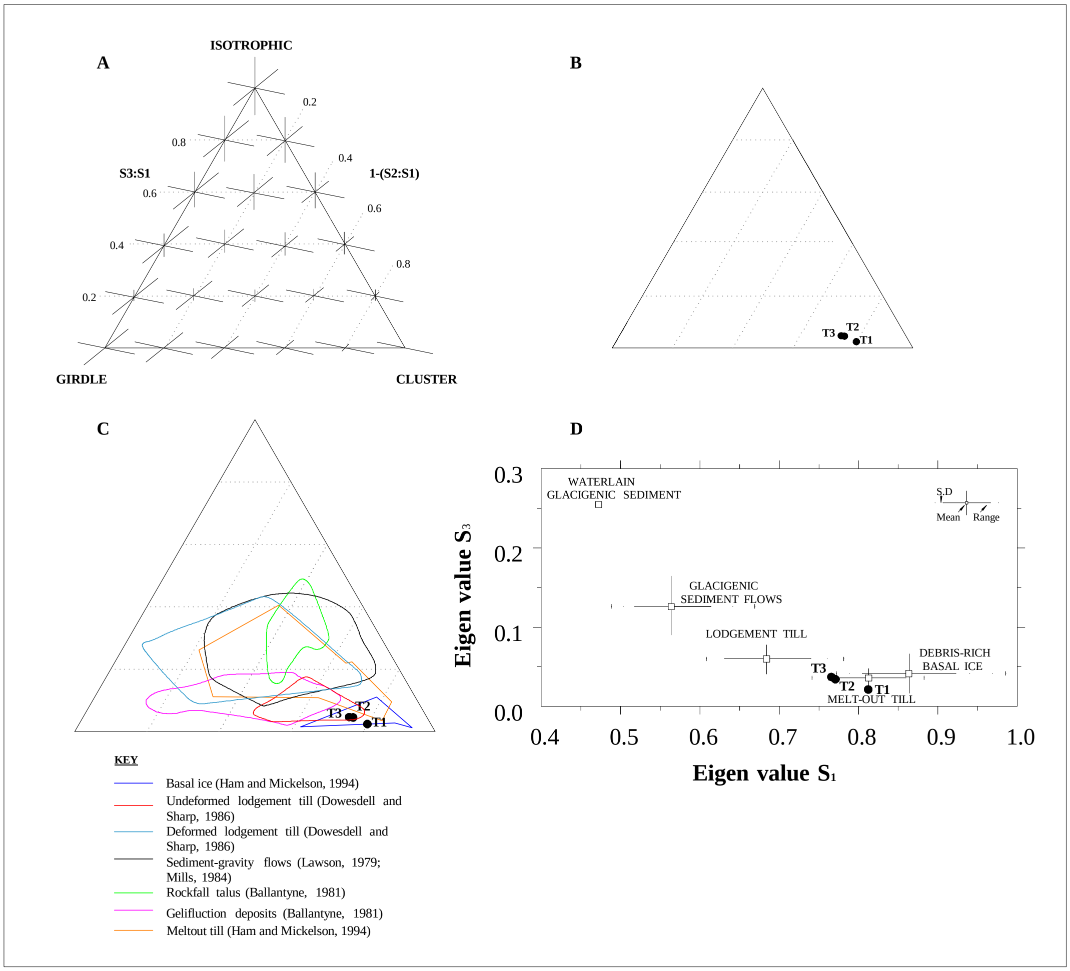

Figure 7.17 Till fabric using eigenvalue data for the western slope deposit in the Leqooa Valley. (A) The range of orthorhombic fabric shapes. (B) Fabric data from the three trenches. (C) Comparison with envelopes from a range of deposits. (D) Comparison with modern data fabrics from various environments (Dowdeswell *et al.,* 1985).

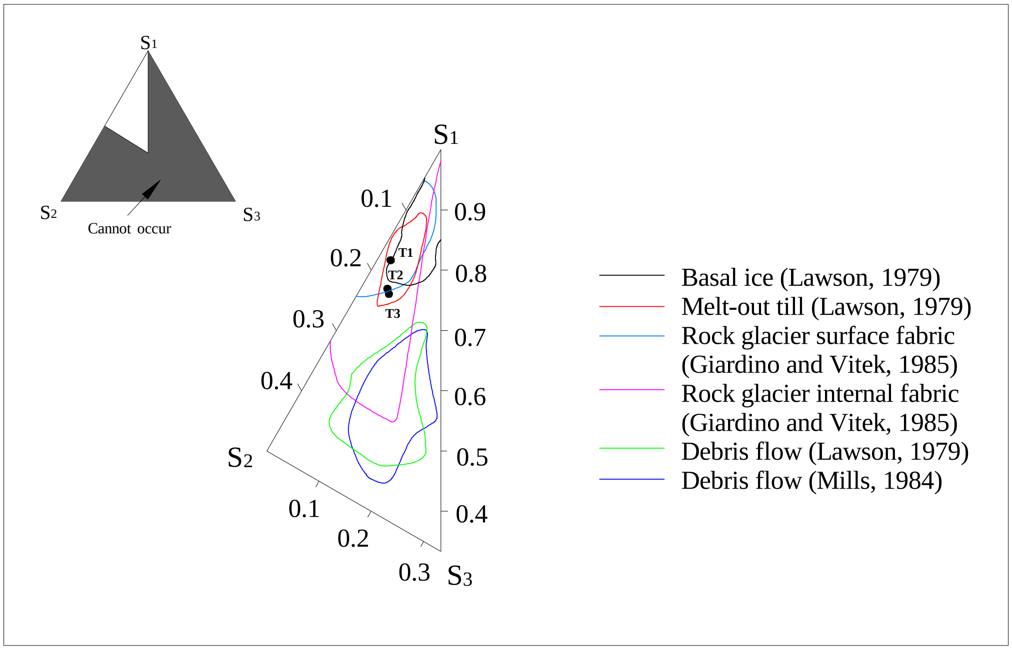

Figure 7.18 Triangular plot of normalised eigenvalues for the western slope deposit, showing envelopes suggested by various authors. The usable field diagram occupies one sixth of the diagram because $S_1 > S_2 > S_3$.

sediment within trench 1 falls on the limit of the basal ice envelope, whilst the sediment within trenches 1 and 2 fall within the rock glacier surface fabric envelope.

7.5.2 Eastern slope deposit

Orientation of clasts measured within trenches 1 and 3 indicates preferred orientation transverse to the ridge crest (Figure 7.19). However, clasts in trench 2 display random orientations. Most clasts within the three trenches dip between 0º to 40º. The chi-square test was used in order to determine whether clast orientation is statistically significant. Clasts in trenches 1 and 3 have a statistically significant orientation (<0.05%), whilst clasts in trench 2 have a probability of being randomly distributed at a level >0.05%.

S_1 values, which measure the strength of clustering about the mean axis for the three sites are fairly high and range from 0.642 at trench 2 to 0.750 at trench 1. S_2 and S_3 values are much lower which indicates that the clast fabrics represent linear clusters, whereby all observations are approximately parallel and $S_1 \gg S_2 \approx S_3$. The normalised

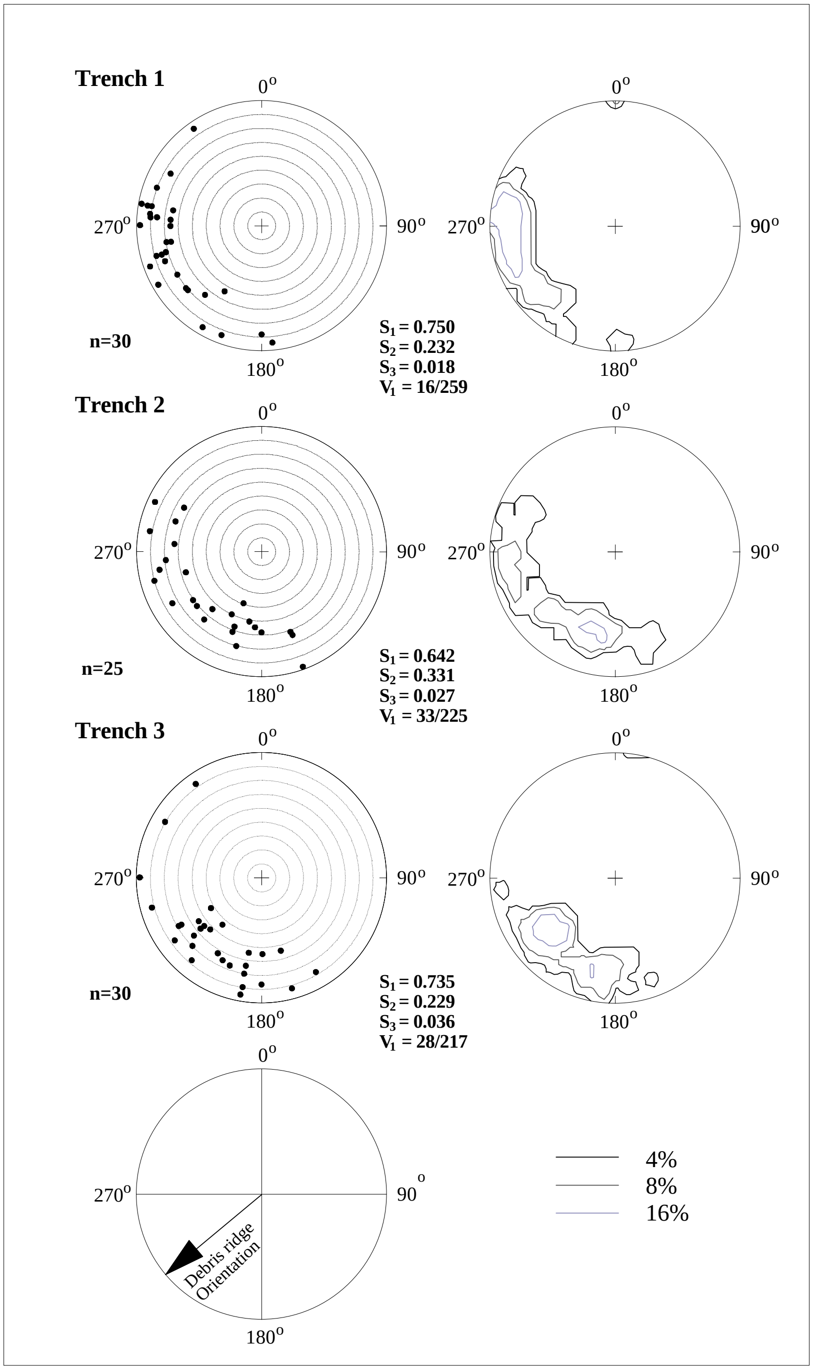

Figure 7.19 Clast orientation, dip and contouring at trenches 1, 2 and 3 at the eastern slope deposit, Leqooa Valley.

eigenvalues were then plotted onto a general shape diagram (Figure 7.20) and indicate that the sediment within all three trenches has low isotropy and moderate to high elongation values. Fabric shape ellipsoids are compared with plotted data from various published sources (Figure 7.20C), which indicates that the sediment within trenches 1 and 3 fall within the basal ice envelope. The sediment within trench 3 also falls within the undeformed lodgement till envelope, whilst the sediment within trench 2 falls on the limit of the undeformed lodgement till and gelifluction deposits envelopes. When compared with Figure 7.20D, the sediment within trench 1 falls close to the melt-out till boundary, whereas the sediment within trench 2 falls close to the lodgement till boundary and the sediment within trench 3 falls within the boundaries of lodgement till. A triangular plot of normalised eigenvalues was also generated (Figure 7.21) in order to further compare the eastern slope deposit eigenvalues to envelopes produced by previous authors for various deposits. The sediment in trenches 1 and 3 falls within the internal rock glacier fabric envelope, whilst the sediment in trench 2 falls on the limit of this envelope.

7.6 PARTICLE SHAPE

7.6.1 Western slope deposit

Particle form was plotted onto triangular diagrams using Tri-plot v1.3 (Graham and Midgley, 2000), which represents the descriptive classes defined by Sneed and Folk (1958) (Figure 7.22) and the isolines of the Oblate-prolate (OP) index of Dobkins and Folk (1970) (Figure 7.23) for the western slope deposit.

All three trenches tend to contain a variety of clast shape (Figure 7.22 and Table 7.7). The modal class of clast shape is bladed in the case of all three trenches which contain >44% bladed shapes. Trench 1 contains a higher proportion of platy shapes than the other 2 trenches, whilst all three trenches contain very few compact clasts. The wide variety of clast shape within the western slope deposit is also represented in Figure 7.23 which displays the Oblate-prolate index; however mean clast shape is bladed. The maximum projection sphericity is represented in Figure 7.24. These results are varied, with the clasts in trenches 1 and 2 falling between 0.2 and 0.9 and those in trench 3 falling between 0.3 and 0.9. A further indication of the varied nature

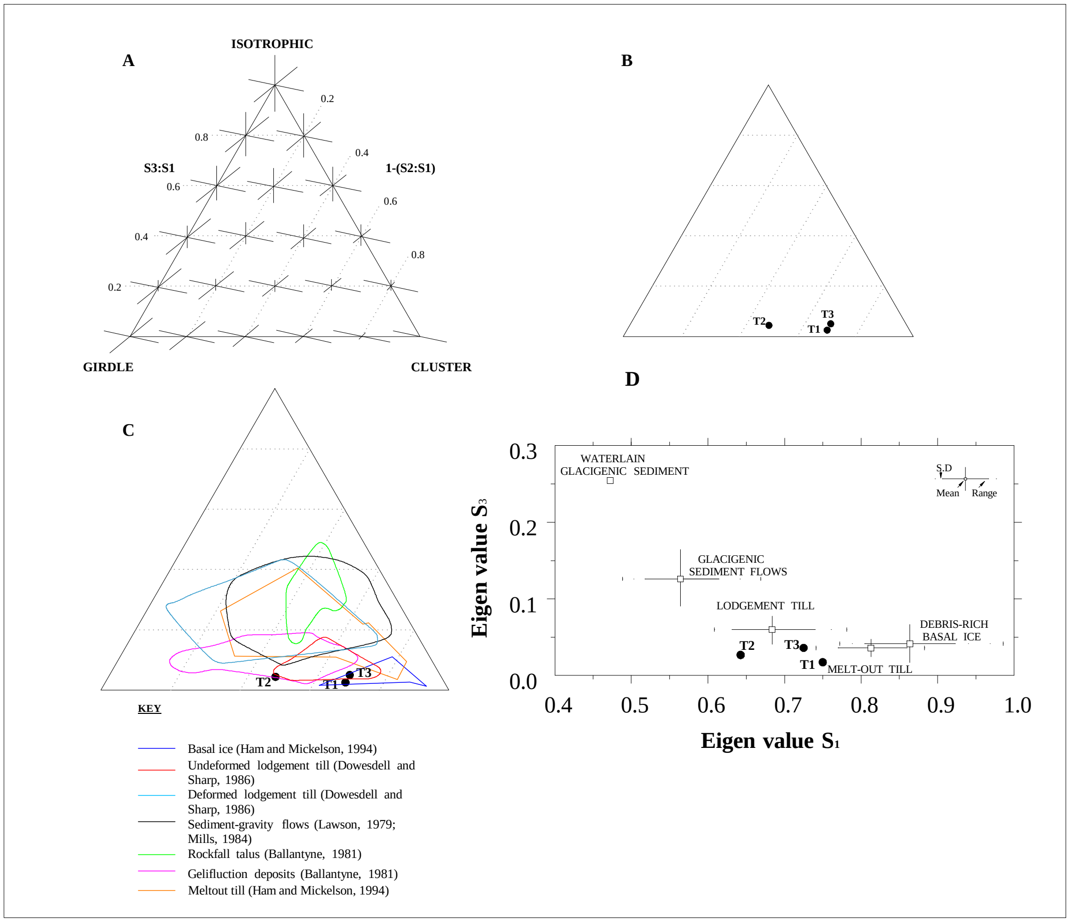

Figure 7.20 Till fabric using eigenvalue data for the eastern slope deposit in the Leqooa Valley. (A) The range of orthorhombic fabric shapes. (B) Fabric data from the three trenches. (C) Comparison with envelopes from a range of deposits. (D) Comparison with modern data fabrics from various environments (Dowdeswell *et al.*, 1985).

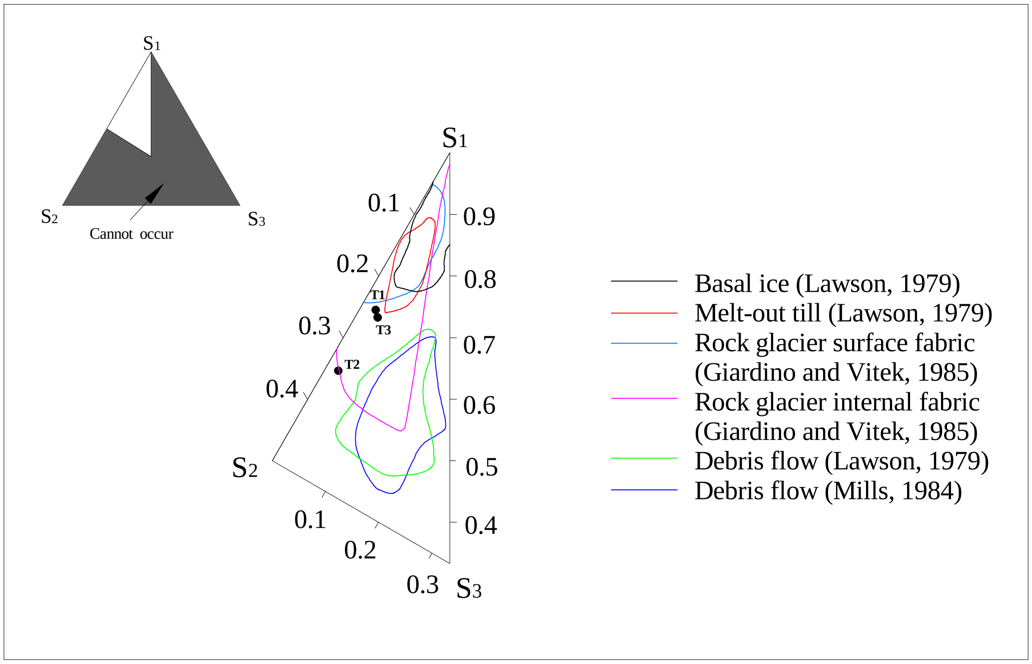

Figure 7.21 Triangular plot of normalised eigenvalues for the eastern slope deposit, showing envelopes suggested by various authors. The usable field diagram occupies one sixth of the diagram because $S_1 > S_2 > S_3$.

of the clasts in terms of maximum projection sphericity is indicated in Table 7.8, where the mean value ranges from 0.62 in trench 2 to 0.66 in trench 3.

Clast roundness is represented in Figure 7.25 and Table 7.9. The majority of clasts within the three trenches fall within the angular and subangular categories of roundness. Trenches 2 and 3 have a subangular modal class, whilst trench 1 has an angular modal class. Subangular clasts range from 40% in trench 1 to 46% in trench 2, whilst trench 3 contains the highest proportion of subrounded clasts (24%). Average roundness ranges from 1.5 in trench 1 to 1.9 in trench 3 (Table 7.8), which places the results in trench 1 between the angular and subangular categories and the results in trench 3 in the subangular category. It should be noted that there is a slight increase in roundness towards the snout of the deposit.

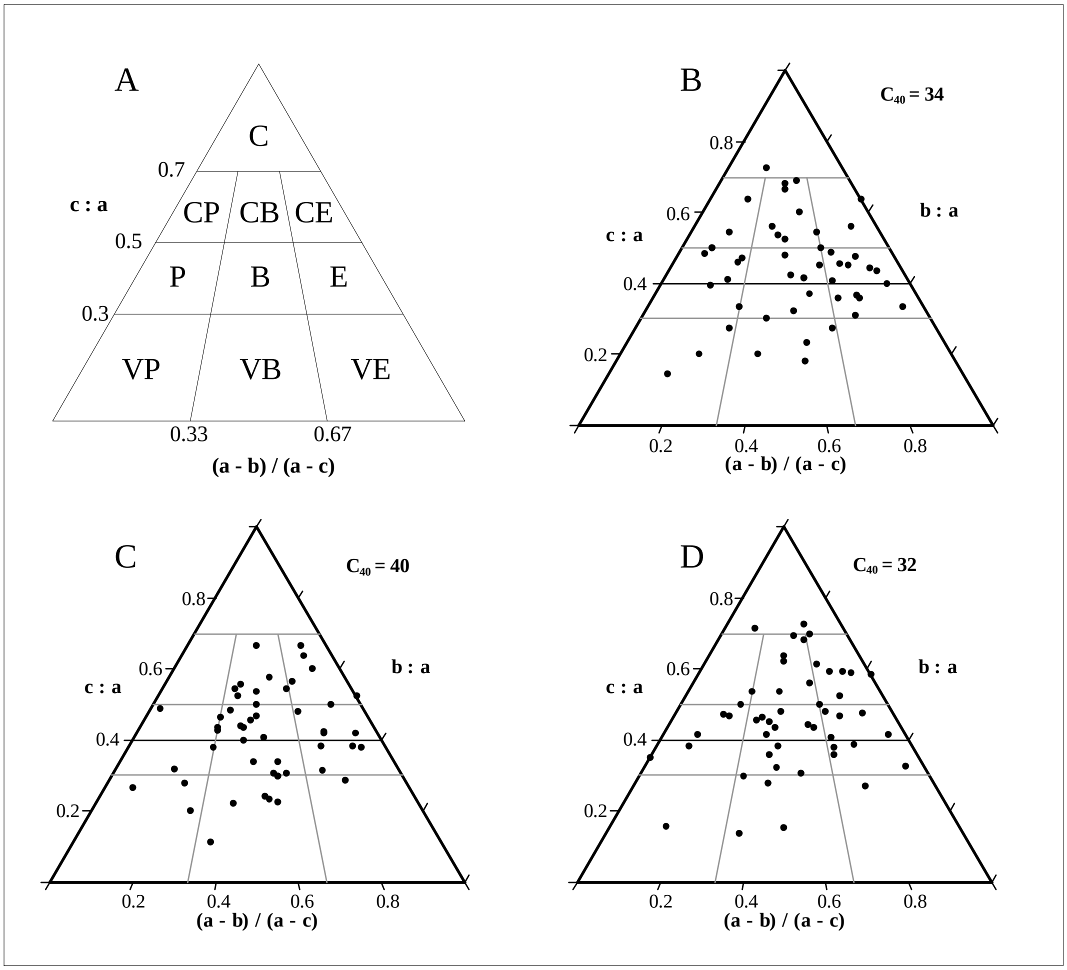

Figure 7.22 Triangular diagrams after Sneed and Folk (1958). (A) The descriptive classes according to Sneed and Folk (1958) where C = compact, P = platy, B = bladed, E = elongate and V = very. (B-D) Triangular diagrams for trenches 1, 2 and 3 respectively at the western slope deposit. C_{40} is the percentage of sample with c:a ≤ 0.4 (Benn and Ballantyne, 1993) (n = 50).

Table 7.7 The percentage of clasts falling within the various shape categories for the western slope deposit.

Shape	Trench 1 (%)	Trench 2 (%)	Trench 3 (%)
Compact	2	-	4
Platy	24	14	16
Bladed	40	56	44
Elongate	34	30	36

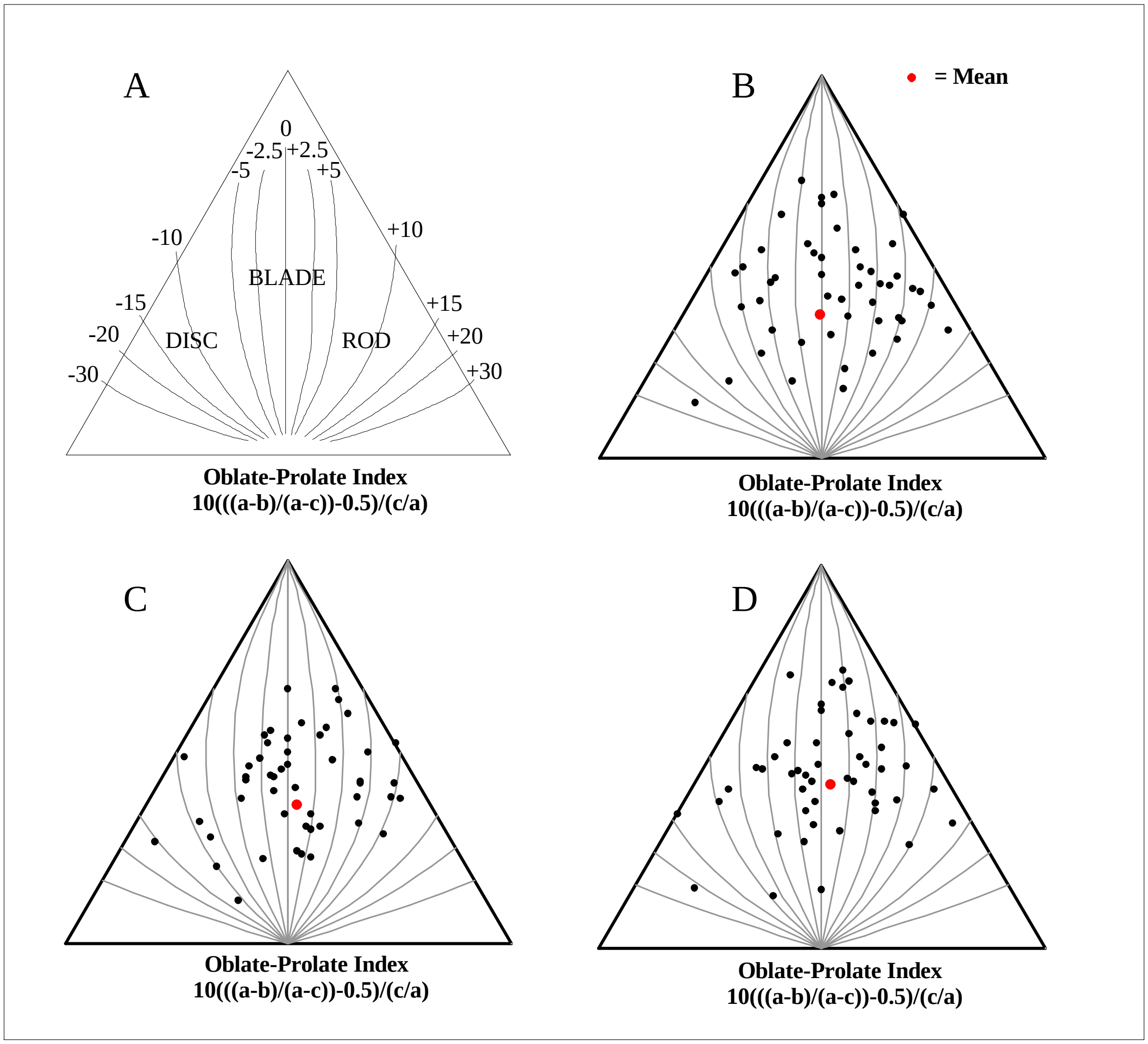

Figure 7.23 Triangular diagrams after Sneed and Folk (1958). (A) Isolines of the Oblate-prolate index according to Dobkins and Folk (1970). Triangular diagrams for Trenches 1, 2 and 3 respectively at the western slope deposit (n = 50).

Table 7.8 The shape of clasts measured at the Leqooa western slope deposit. (*x* = mean, *s* = standard deviation).

	Number In Sample	**Oblate-prolate Index**		**Maximum Projection Sphericity**		**Visual Roundness (Powers, 1953)**	
		x	*s*	*x*	*s*	*x*	*s*
Trench 1	50	0.55	6.53	0.65	0.13	1.5	0.79
Trench 2	50	0.64	5.83	0.62	0.13	1.7	0.85
Trench 3	50	0.48	6.16	0.66	0.13	1.9	0.83

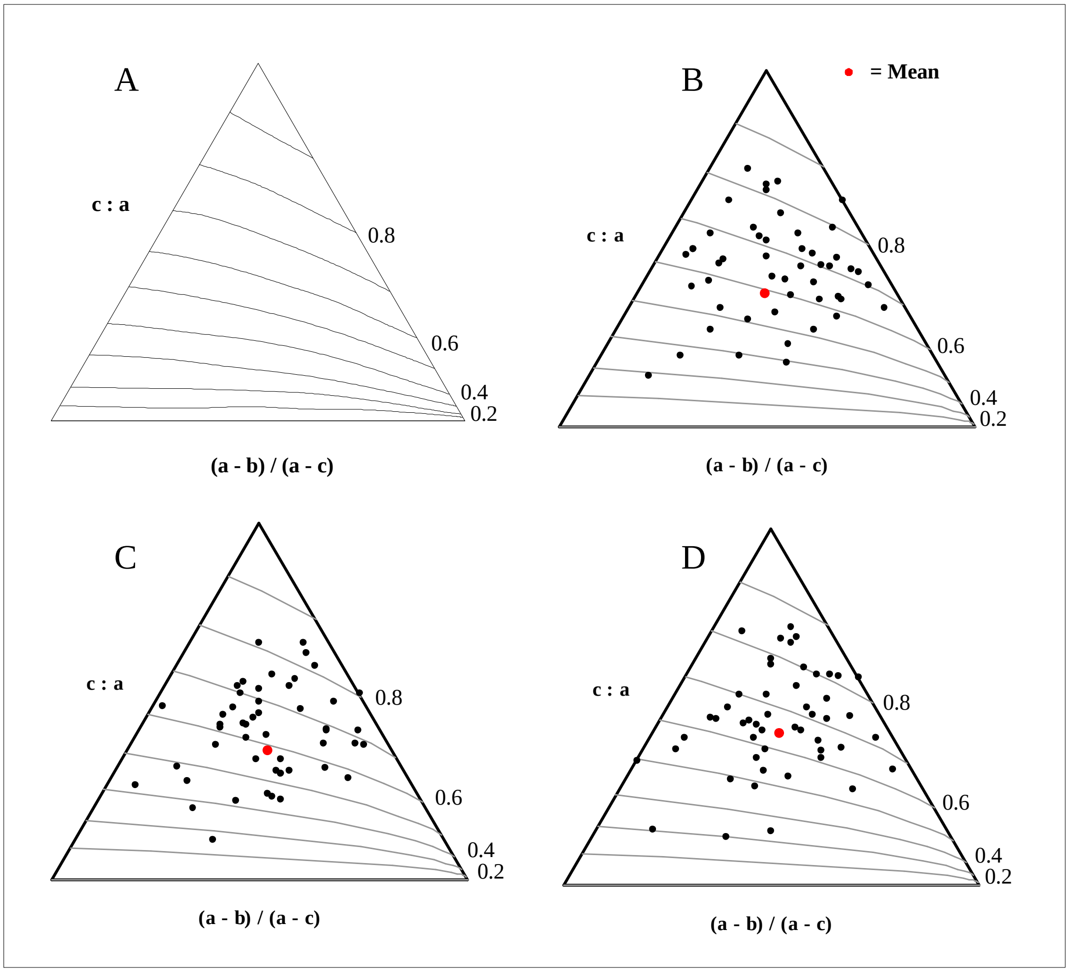

Figure 7.24 Triangular diagrams after Sneed and Folk (1958). (A) Isolines of the maximum projection sphericity according to Sneed and Folk (1958). (B-D) Triangular diagrams for Trenches 1, 2 and 3 respectively at the western slope deposit (n = 50).

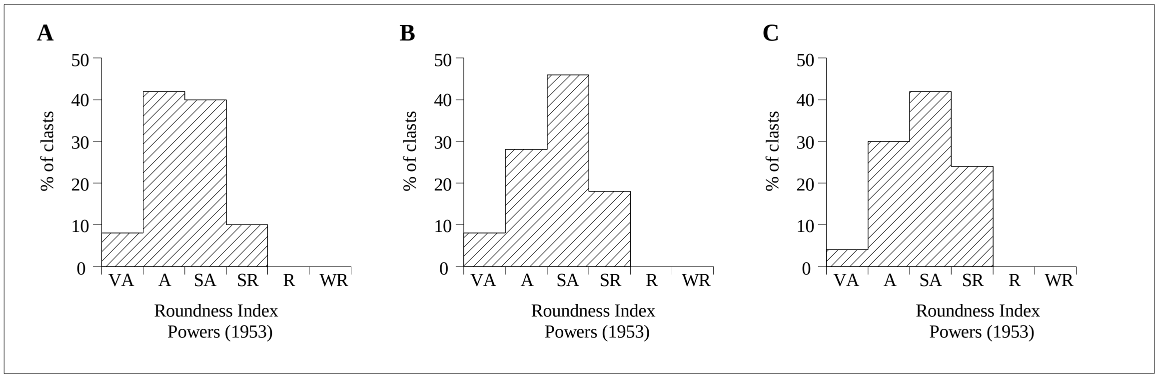

Figure 7.25 Graphs representing visual roundness of clasts (after Powers 1953) in trenches 1 (A), 2 (B) and 3 (C) at the western slope deposit. VA = Very Angular, A = Angular, SA = Sub Angular, SR = Sub Rounded, R = Rounded, WR = Well Rounded (n = 50).

Table 7.9 The percentage of clasts falling in the roundness categories at the western slope deposit.

	VA (%)	A (%)	SA (%)	SR (%)	R (%)	WR (%)
Trench 1	8	42	40	10	-	-
Trench 2	8	28	46	18	-	-
Trench 3	4	30	42	24	-	-

The t-test was performed in order to determine whether the sediment samples in the three trenches for form, sphericity and roundness was statistically significant (<0.05%), and whether there was a relationship between the sediment in the trenches (Table 7.10) and between deposits (Table 7.11). The results for clast shape in the three trenches are statistically significant in all but visual roundness, where the results are not significant between trenches 1 and 3 (Table 7.10). Results indicate that the Oblate-prolate index is not significant between the western slope deposit in trench 3 and the Tsatsa-La-Mangaung deposit in trench 2 (Table 7.11). The maximum projection sphericity is statistically significant in all cases, except between trench 2 of the western slope deposit and trench 3 of the Sekhokong Site 2 deposit. In contrast, visual roundness is not significant when comparing trench 3 of the various deposits with trenches 1 and 2. This may be attributed to the increase in roundness towards the snout of the deposit as discussed previously.

Table 7.10 The statistical significance calculated by the t-test of the shape of clasts sampled in the three trenches in the western slope deposit (SS = Statistically significant. NS = Not significant).

Trenches	Oblate Prolate Index	Maximum Projection Sphericity	Visual Roundness
T1-T2	**SS**	**SS**	**SS**
T1-T3	**SS**	**SS**	NS
T2-T3	**SS**	**SS**	**SS**

Table 7.11 The statistical significance calculated by the t-test of the shape of clasts sampled in the three trenches for the western slope deposit, Tsatsa-La-Mangaung and Sekhokong Sites 1 and 2 deposits (SS = Statistically significant, NS = Not significant).

Site and Trenches	Oblate Prolate Index	Maximum Projection Sphericity	Visual Roundness
LeqWT1-TsatsaT1	**SS**	**SS**	**SS**
LeqWT1-TsatsaT2	**SS**	**SS**	**SS**
LeqWT1-TsatsaT3	**SS**	**SS**	**SS**
LeqWT2-TsatsaT1	**SS**	**SS**	**SS**
LeqWT2-TsatsaT2	**SS**	**SS**	**SS**
LeqWT2-TsatsaT3	**SS**	**SS**	**SS**
LeqWT3-TsatsaT1	**SS**	**SS**	NS
LeqWT3-TsatsaT2	NS	**SS**	NS
LeqWT3-TsatsaT3	**SS**	**SS**	**SS**
LeqWT1-Sek1T1	**SS**	**SS**	**SS**
LeqWT1-Sek1T2	**SS**	**SS**	**SS**
LeqWT1-Sek1T3	**SS**	**SS**	**SS**
LeqWT2-Sek1T1	**SS**	**SS**	NS
LeqWT2-Sek1T2	**SS**	**SS**	**SS**
LeqWT2-Sek1T3	**SS**	**SS**	**SS**
LeqWT3-Sek1T1	**SS**	**SS**	NS
LeqWT3-Sek1T2	**SS**	**SS**	NS
LeqWT3-Sek1T3	**SS**	**SS**	**SS**
LeqWT1-Sek2T1	**SS**	**SS**	**SS**
LeqWT1-Sek2T2	**SS**	**SS**	**SS**
LeqWT1-Sek2T3	**SS**	**SS**	NS
LeqWT2-Sek2T1	**SS**	**SS**	**SS**
LeqWT2-Sek2T2	**SS**	**SS**	**SS**
LeqWT2-Sek2T3	**SS**	NS	NS
LeqWT3-Sek2T1	**SS**	**SS**	**SS**
LeqWT3-Sek2T2	**SS**	**SS**	**SS**
LeqWT3-Sek2T3	**SS**	**SS**	NS

7.6.2 Eastern slope deposit

Particle form was plotted onto triangular diagrams using Tri-plot v1.3 (Graham and Midgley, 2000), which represents the descriptive classes defined by Sneed and Folk (1958) (Figure 7.26) and the isolines of the Oblate-prolate (OP) index of Dobkins and Folk (1970) (Figure 7.27) for the western slope deposit.

All three trenches tend to contain a majority of bladed clasts (Figure 7.26 and Table 7.12). Platy clasts are the second most common clast shape in trenches 1 and 3, ranging from 20% to 34%, whilst elongate clasts are the second most common clast shape in trench 2 (24%). Compact clasts are few, with values ranging between 2% in trench 3 to 6% in trenches 1 and 2. The predominance of bladed clasts is also represented in Figure 7.27, which displays the Oblate-prolate index. The sediment from trenches 1 and 2 shows more clustering around the -5 and +5 boundaries of the blade category than trench 3, however all three trenches have a bladed mean clast shape. This is also represented in Table 7.13, where Oblate-prolate mean values range from 1.01 in trench 2 to -0.31 in trench 3, which places the mean clast shape in the bladed category.

The maximum projection sphericity is represented in Figure 7.28. These results are varied, with clasts in trench 1 ranging between 0.4 and 1 and clasts in trenches 2 and 3 ranging between 0.4 and 0.9. A further indication of the varied nature of the clasts in terms of maximum projection sphericity is indicated in Table 7.13, where the mean value ranges from 0.64 in trench 1 to 0.66 in trench 2.

Clast roundness is represented in Figure 7.29 and Table 7.14. The majority of clasts from the three trenches fall within the angular and subangular categories of roundness. Trench 1 contains the highest percentage of very angular clasts (10%), whereas trench 3 contains the most subrounded clasts (14%). The percentage of angular clasts ranges from 56% in trench 1 to 42% in trench 3 and all three trenches have an angular modal class. The presence of subangular and subrounded clasts increases towards trench 3. Table 7.13 indicates that average roundness ranges from 1.3 in trench 1 to 1.6 in trench 3, which places these results between the angular and subangular

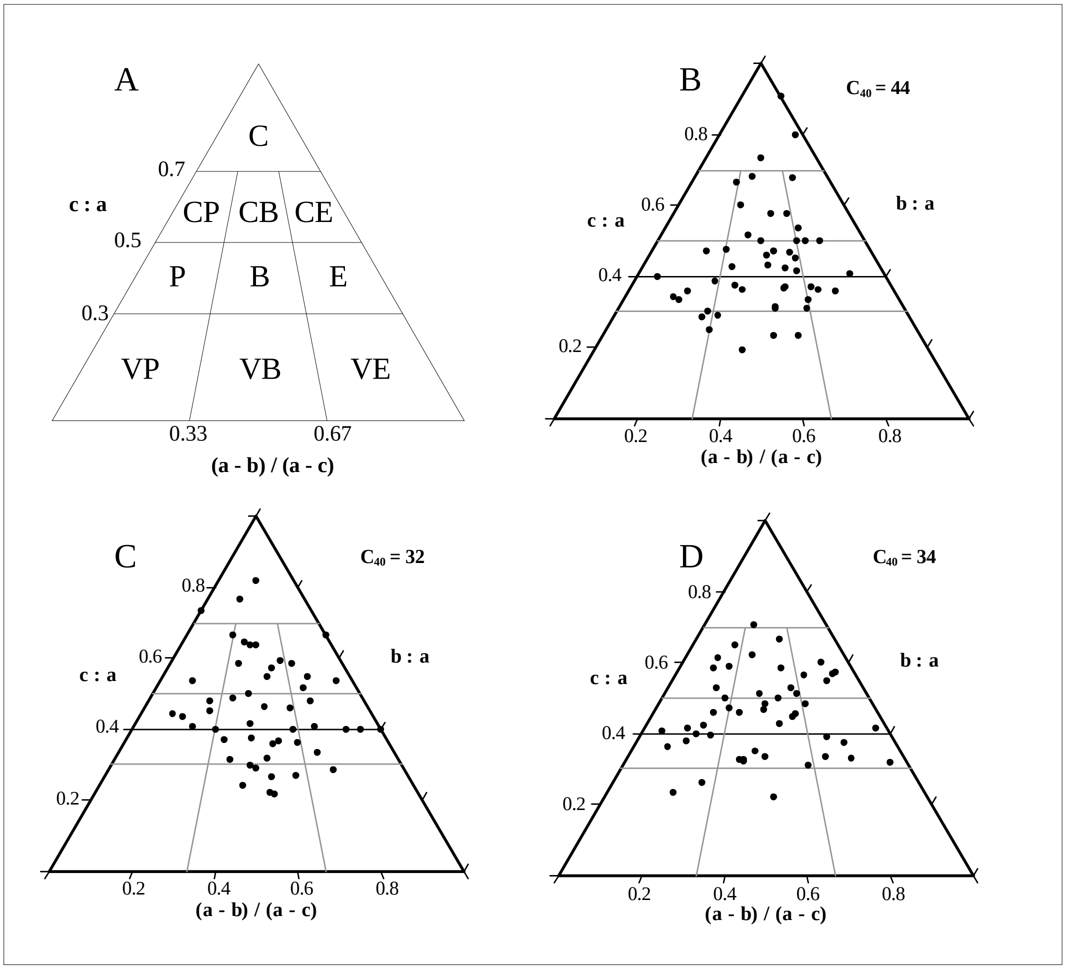

Figure 7.26 Triangular diagrams after Sneed and Folk (1958). (A) The descriptive classes according to Sneed and Folk (1958) where C = compact, P = platy, B = bladed, E = elongate and V = very. (B-D) Triangular diagrams for Trenches 1, 2 and 3 respectively at the eastern slope deposit. C_{40} is the percentage of sample with c:a ≤ 0.4 (Benn and Ballantyne, 1993) (n = 50).

Table 7.12 The percentage of clasts falling within the various shape categories for the eastern slope deposit.

Shape	Trench 1 (%)	Trench 2 (%)	Trench 3 (%)
Compact	6	6	2
Platy	20	14	34
Bladed	56	56	40
Elongate	18	24	24

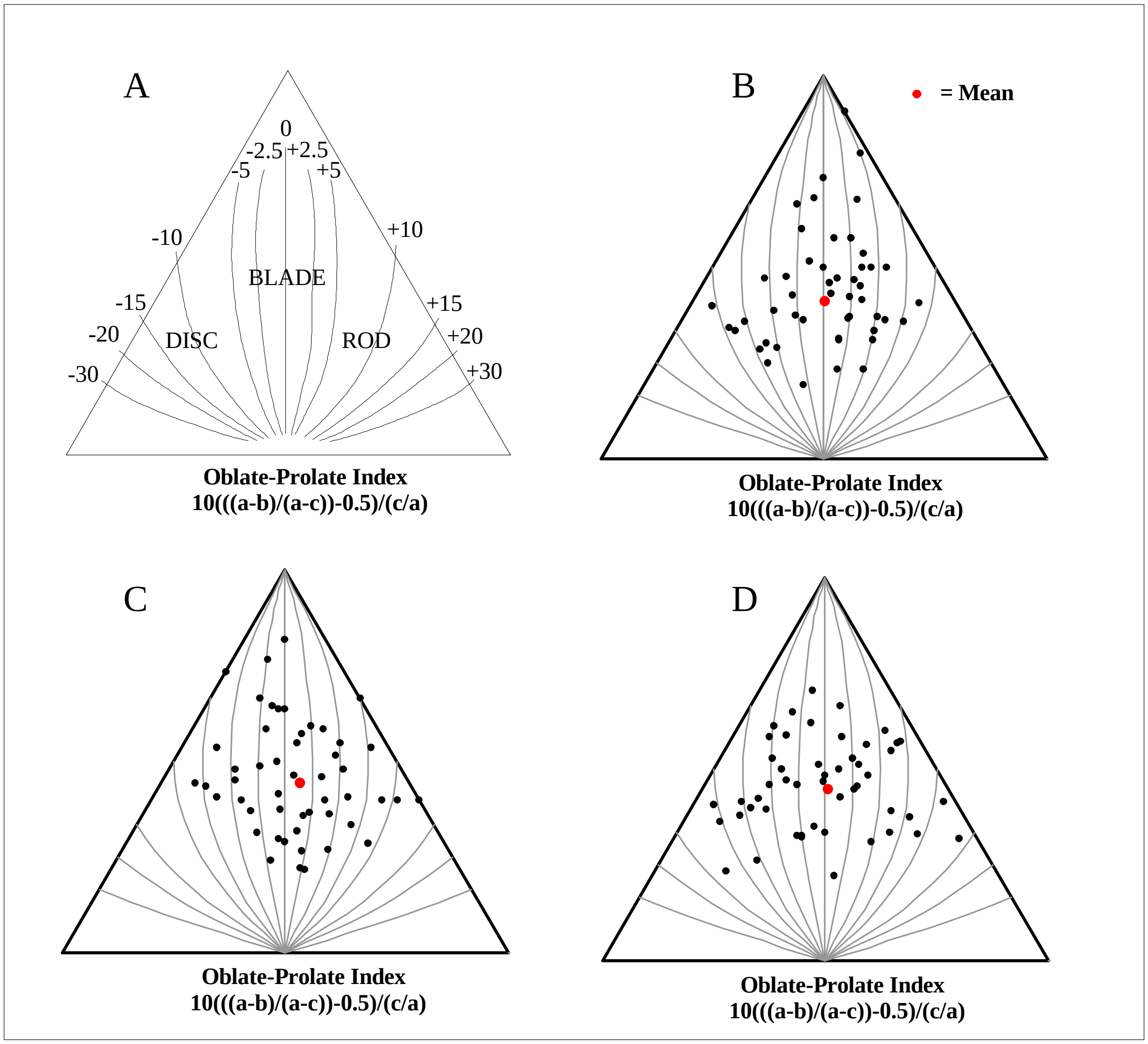

Figure 7.27 Triangular diagrams after Sneed and Folk (1958). (A) Isolines of the Oblate-prolate index according to Dobkins and Folk (1970). Triangular diagrams for Trenches 1, 2 and 3 respectively at the eastern slope deposit (n = 50).

Table 7.13 The shape of clasts measured at the Leqooa eastern slope deposit. (*x* = mean, *s* = standard deviation).

	Number In Sample	Oblate-prolate Index		Maximum Projection Sphericity		Modified Wentworth Roundness	
		x	*s*	*x*	*s*	*x*	*s*
Trench 1	50	0.11	4.64	0.64	0.12	1.3	0.66
Trench 2	50	1.01	4.65	0.66	0.12	1.4	0.73
Trench 3	50	-0.31	5.78	0.65	0.11	1.6	0.84

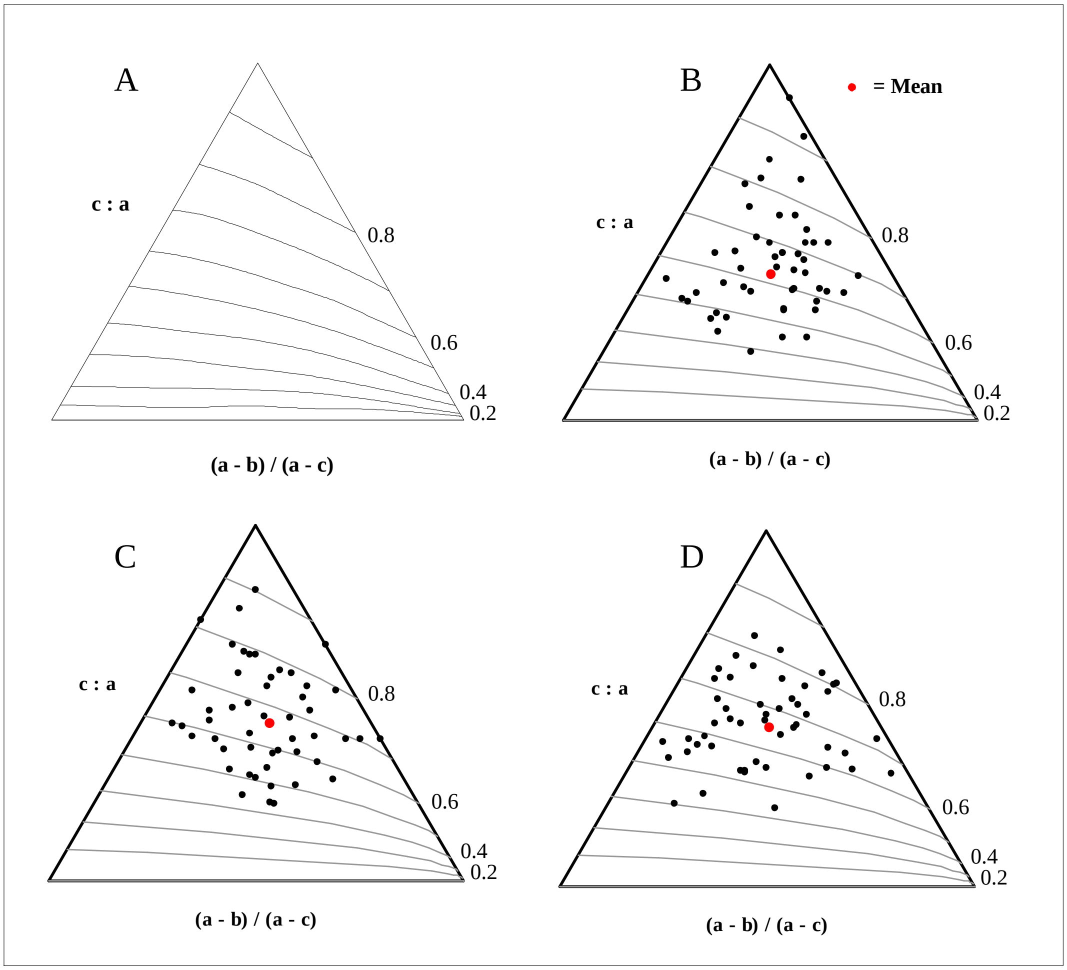

Figure 7.28 Triangular diagrams after Sneed and Folk (1958). (A) Isolines of the maximum projection sphericity according to Sneed and Folk (1958). (B-D) Triangular diagrams for trenches 1, 2 and 3 respectively at the eastern slope deposit (n = 50).

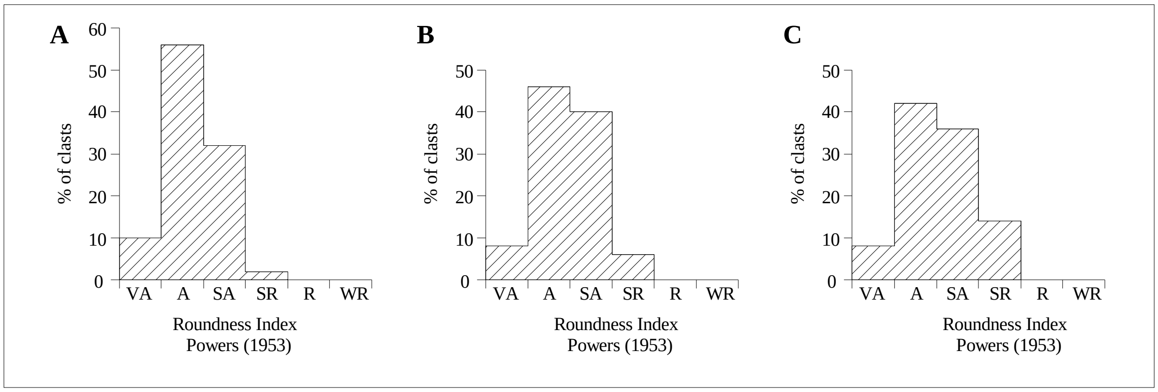

Figure 7.29 Graphs representing visual roundness of clasts (after Powers 1953) in trenches 1 (A), 2 (B) and 3 (C) at the eastern slope deposit. VA = Very Angular, A = Angular, SA = Sub Angular, SR = Sub Rounded, R = Rounded, WR = Well Rounded (n = 50).

Table 7.14 The percentage of clasts falling in the roundness categories at the eastern slope deposit.

	VA (%)	A (%)	SA (%)	SR (%)	R (%)	WR (%)
Trench 1	10	56	32	2	-	-
Trench 2	8	46	40	6	-	-
Trench 3	8	42	36	14	-	-

categories. It should also be noted that there is a slight increase in roundness towards the snout of the deposit in trench 3.

The t-test was performed in order to determine whether the sediment samples in the three trenches for form, sphericity and roundness was statistically significant (<0.05%), and whether there was a relationship between the sediment in the trenches (Table 7.15) and between deposits (Table 7.16). It is clear from Table 7.15 that the results for clast shape in the three trenches are statistically significant in all but visual roundness, where the results are not significant between trenches 1 and 3. Table 7.16 indicates that the oblate prolate index is not significant between the eastern slope deposit in trench 1 and the Tsatsa-La-Mangaung deposit in trench 1, the eastern slope deposit in trench 2 and the Tsatsa-La-Mangaung deposit in trench 2 and the eastern slope deposit in trench 2 and the Sekhokong Site 2 deposit in trench 2. The maximum projection sphericity is statistically significant in all cases, except between trench 2 of

Table 7.15 The statistical significance calculated by the t-test of the shape of clasts sampled in the three trenches in the eastern slope deposit (SS = Statistically significant. NS = Not significant).

Trenches	Oblate Prolate Index	Maximum Projection Sphericity	Visual Roundness
T1-T2	**SS**	**SS**	**SS**
T1-T3	**SS**	**SS**	NS
T2-T3	**SS**	**SS**	**SS**

the eastern slope deposit and trench 2 of the Tsatsa-La-Mangaung deposit and between trench 3 of the eastern slope deposit and trench 1 of the Tsatsa-La-Mangaung deposit. In contrast, visual roundness is not significant when comparing trench 3 of the various deposits with trenches 1 and 2. This may be attributed to the increase in roundness towards the snout of the deposit as discussed previously.

7.7 MICROMORPHOLOGY

7.7.1 Western slope deposit

Samples were collected within trench 2 at 140 cm depth and trench 3 at 70 cm depth and descriptions of the microstructure of the samples is presented in Table 7.17. The fabric pattern for both samples is random and particles have a broad angle with a weakly expressed quantity of oriented clasts. The c/f related distribution is double spaced porphyric in trench 2, whilst it is open porphyric in trench 3. The dominant size fraction is coarse sand in trench 2 and medium sand in trench 3. Particles are poorly sorted to unsorted, blocky in shape, subangular with a smooth to undulating surface in trench 2 and an undulating surface in trench 3. Peds are spheroidal and weakly separated. Voids are vughy and channel in both samples and the predominant microstructure is vughy. The total percentage area occupied by voids is 20% in both samples.

The main rock type is basalt and average size of particles is 2900 µm in trench 2 and 1700 µm in trench 3. The colour of the fine material is yellowish brown in trench 2 and brown in trench 3 and limpidity is speckled. The c/f related distribution indicates that trench 3 contains a greater proportion of clasts <2 mm than trench 2. The c/f related distribution of the finer particles is double spaced porphyric. Cappings are

Table 7.16 The statistical significance calculated by the t-test of the shape of clasts sampled in the three trenches for the eastern slope deposit, western slope deposit, Tsatsa-La-Mangaung and Sekhokong Sites 1 and 2 deposits (SS = Statistically significant, NS = Not significant).

Site and Trenches	Oblate Prolate Index	Maximum Projection Sphericity	Visual Roundness
LeqET1-LeqWT1	**SS**	**SS**	**SS**
LeqET1-LeqWT2	**SS**	**SS**	NS
LeqET1-LeqWT3	**SS**	**SS**	NS
LeqET2-LeqWT1	**SS**	**SS**	**SS**
LeqET2-LeqWT2	**SS**	**SS**	**SS**
LeqET2-LeqWT3	**SS**	**SS**	NS
LeqET3-LeqWT1	**SS**	**SS**	**SS**
LeqET3-LeqWT2	**SS**	**SS**	**SS**
LeqET3-LeqWT3	**SS**	**SS**	**SS**
LeqET1-TsatsaT1	NS	**SS**	**SS**
LeqET1-TsatsaT2	**SS**	**SS**	**SS**
LeqET1-TsatsaT3	**SS**	**SS**	NS
LeqET2-TsatsaT1	**SS**	**SS**	**SS**
LeqET2-TsatsaT2	**SS**	NS	**SS**
LeqET2-TsatsaT3	**SS**	**SS**	**SS**
LeqET3-TsatsaT1	**SS**	NS	**SS**
LeqET3-TsatsaT2	NS	**SS**	**SS**
LeqET3-TsatsaT3	**SS**	**SS**	**SS**
LeqET1-Sek1T1	**SS**	**SS**	**SS**
LeqET1-Sek1T2	**SS**	**SS**	**SS**
LeqET1-Sek1T3	**SS**	**SS**	NS
LeqET2-Sek1T1	**SS**	**SS**	**SS**
LeqET2-Sek1T2	**SS**	**SS**	**SS**
LeqET2-Sek1T3	**SS**	**SS**	NS
LeqET3-Sek1T1	**SS**	**SS**	**SS**
LeqET3-Sek1T2	**SS**	**SS**	**SS**
LeqET3-Sek1T3	**SS**	**SS**	**SS**
LeqET1-Sek2T1	**SS**	**SS**	NS
LeqET1-Sek2T2	**SS**	**SS**	NS
LeqET1-Sek2T3	**SS**	**SS**	NS
LeqET2-Sek2T1	**SS**	**SS**	**SS**
LeqET2-Sek2T2	NS	**SS**	**SS**
LeqET2-Sek2T3	**SS**	**SS**	NS
LeqET3-Sek2T1	**SS**	**SS**	**SS**
LeqET3-Sek2T2	**SS**	**SS**	**SS**
LeqET3-Sek2T3	**SS**	**SS**	NS

Table 7.17 Micromorphological description of the Leqooa western deposit samples.

Micromorphological features →	Skeleton									Aggregates		Voids			Parent Material				Groundmass			Pedofeatures					
	Fabric						Shape										Fine								Infillings		
Sample No. ↓	Pattern	Degree of parallelism	Quantity of oriented particles	C/F related distribution	Dominant size fraction	sorting	Shape	Degree of roundness	surface roughness	peds	ped seperation and pedality	Void type	Microstructure	% total area occupied by voids	Rock type	Average size um	Colour	Limpidity	C/F 2mm	C/F 10um	C/F related distribution	Cappings	Texture	laminated	Classification	Descriptive criteria	Crystals
T2 140	R	BA	W-E	DSP	CS	P/U	B	SA	S&U	S	WS	V&C	VM	20	B	2900	YB	SP	7:3	4:1	DSP	•	SL&C	NL	LD	PF	
T3 70	R	BA	W-E	OP	MS	P/U	B	SA	U	S	WS	V&C	VM	20	B	1700	B	SP	3:7	4:1	DSP				LD	PF	•

KEY:

Pattern:
R = Random

Degree of parallelism:
BA = Broad angle

Quantity of oriented particles:
WE = Weakly expressed:<33% of particles are oriented

C/F related distribution:
SSP = Single spaced porphyric
DSP = Double spaced porphyric

Size:
CS = Coarse sand

Sorting:
PS = Poorly sorted
U = Unsorted

Shape:
P = Platy
B = Blocky

Degree of roundness:
A = Angular
SA = Subangular

Surface roughness:
U= Undulating

Peds:
S = Spheroidal Peds

Ped seperation and pedality:
WS = Weakly seperated

Void type:
C = Channels
CM = Chambers
V = Vughs
VCM = Vugh and Chamber
P = Planes

Microstructure:
VM = Vughy microstructure
CM = Channel microstructure

Mineral type
B = Basalt

Colour:
YB = Yellowish Brown

Limpidity:
SP = Speckled

Cappings:
• <10%
•• <10-20%
••• >20%

Texture:
SL = Silt

Laminated:
NL = Nonlaminated
L = Laminated

Infillings classification:
LD = Loose discontinuous

Descriptive criteria:
PF = Passage features

Crystals:
• Few
•• Some
•• Many

Crystal intergrowth:
P = Parallel

only present in trench 2, are predominantly composed of silt and are non-laminated. One particle in the sample also contains a clay capping (Figure 7.30) which has a speckled appearance. The photo indicates a strong alignment of clays which create birefringence. Further pedofeatures include passage features which are loose discontinuous and the presence of few crystals in trench 3. Several rotation structures are also observed in trench 2 at 140 cm depth (Figure 7.31). These are identified by the halo formed around the main clast and the orientation of smaller clasts around the main clast. Also evident in these photos is the loose sediment below the rotation structure which indicates that waterflow has opened up and washed out sediment.

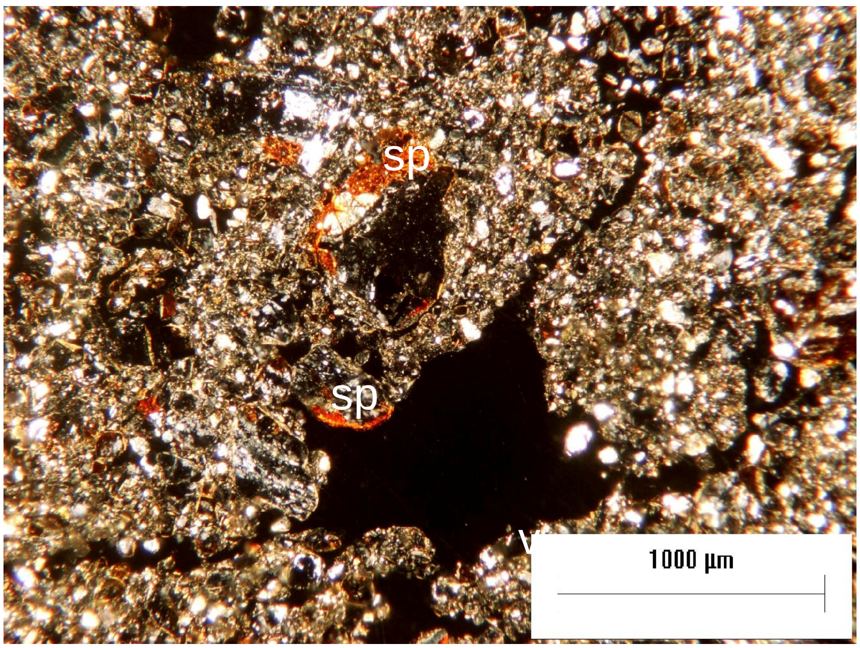

Figure 7.30 Clay capping on clast in trench 2 taken in XPL (sp = speckled, v = void).

7.7.2 Eastern slope deposit

Samples were collected in trench 3 at 55 cm depth and 110 cm depth and their micromorphological characteristics are described in Table 7.18. The fabric pattern in both samples is random and particles have a broad angle with weakly expressed orientation. The c/f related distribution is open porphyric at 55 cm depth and double spaced porphyric at 110 cm depth. The dominant size fraction is medium sand at 55 cm depth and coarse sand at 110 cm depth. Both samples are poorly sorted to unsorted with blocky shaped particles which are subangular, with an undulating surface.

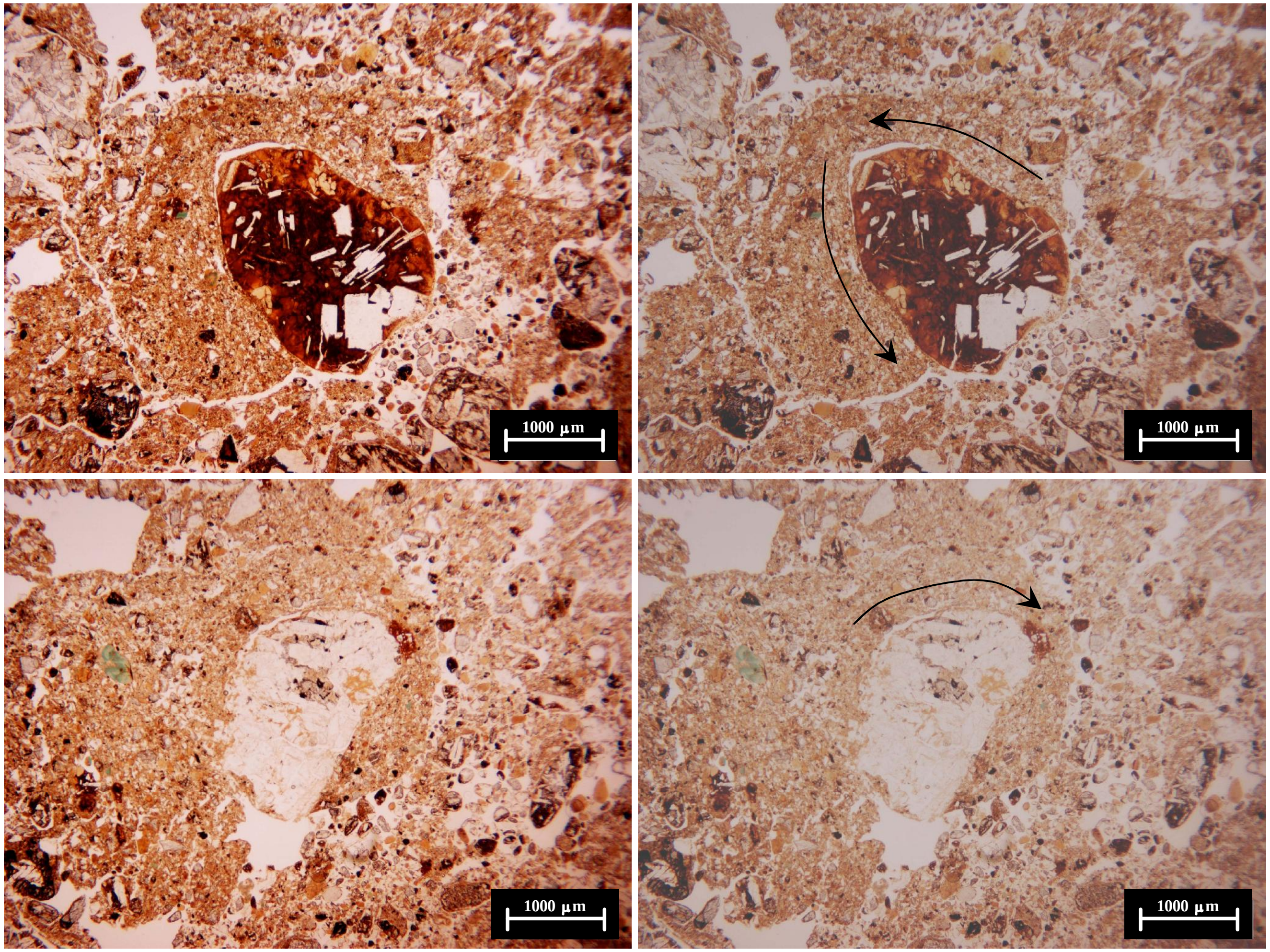

Figure 7.31 Examples of rotational structures about clasts. Note images are paired with original and annotated versions.

Table 7.18 Micromorphological description of the Leqooa eastern deposit samples.

Micromorphological features →	Skeleton									Aggregates		Voids			Parent Material				Groundmass			Pedofeatures					
	Fabric						Shape										Fine								Infillings		
Sample No. ↓	Pattern	Degree of parallelism	Quantity of oriented particles	C/F related distribution	Dominant size fraction	sorting	Shape	Degree of roundness	surface roughness	peds	ped seperation and pedality	Void type	Microstructure	% total area occupied by voids	Rock type	Average size um	Colour	Limpidity	C/F 2mm	C/F 10um	C/F related distribution	Cappings	Texture	laminated	Classification	Descriptive criteria	Crystals
T3 55	R	BA	W-E	OP	MS	P/U	B	SA	U	S	WS	V&C	VM	10	B	2200	B	D	2:3	4:1	DSP				LD	PF	•
T3 110	R	BA	W-E	DSP	CS	P/U	B	SA	U	S	WS	V&C	VM	25	B	2800	YB	SP	9:1	4:1	DSP	•	SL	NL	LD	PF	•

KEY:

Pattern:
R = Random

Degree of parallelism:
BA = Broad angle

Quantity of oriented particles:
WE = Weakly expressed:<33% of particles are oriented

C/F related distribution:
SSP = Single spaced porphyric
DSP = Double spaced porphyric

Size:
CS = Coarse sand

Sorting:
PS = Poorly sorted
U = Unsorted

Shape:
P = Platy
B = Blocky

Degree of roundness:
A = Angular
SA = Subangular

Surface roughness:
U= Undulating

Peds:
S = Spheroidal Peds

Ped seperation and pedality:
WS = Weakly seperated

Void type:
C = Channels
CM = Chambers
V = Vughs
VCM = Vugh and Chamber
P = Planes

Microstructure:
VM = Vughy microstructure
CM = Channel microstructure

Mineral type
B = Basalt

Colour:
YB = Yellowish Brown

Limpidity:
SP = Speckled

Cappings:
• <10%
•• <10-20%
••• >20%

Texture:
SL = Silt

Laminated:
NL = Nonlaminated
L = Laminated

Infillings classification:
LD = Loose discontinuous

Descriptive criteria:
PF = Passage features

Crystals:
• Few
•• Some
•• Many

Crystal intergrowth:
P = Parallel

Peds are spheroidal and weakly separated. Void types are vughy and channel and the predominant microstructure is vughy. The total percentage area occupied by voids ranges from 10% at 55 cm depth to 25% at 110 cm depth.

The rock type is basalt and average size of the coarse fraction ranges from 2200 μm at 55 cm depth to 2800 μm at 110 cm depth. The colour of the fine material is brown at 55 cm depth and yellowish brown at 110 cm depth and limpidity is dotted at 55 cm depth and speckled at 110 cm depth. The c/f ratio indicates that the sediment at 55 cm depth is finer than at 110 cm depth and the c/f related distribution is double spaced porphyric for both samples. Silt cappings only occur at 110 cm depth and these are non-laminated. These cappings are composed of relatively coarse material (Figure 7.32). Further pedofeatures include loose discontinuous passage features and few crystals in both samples.

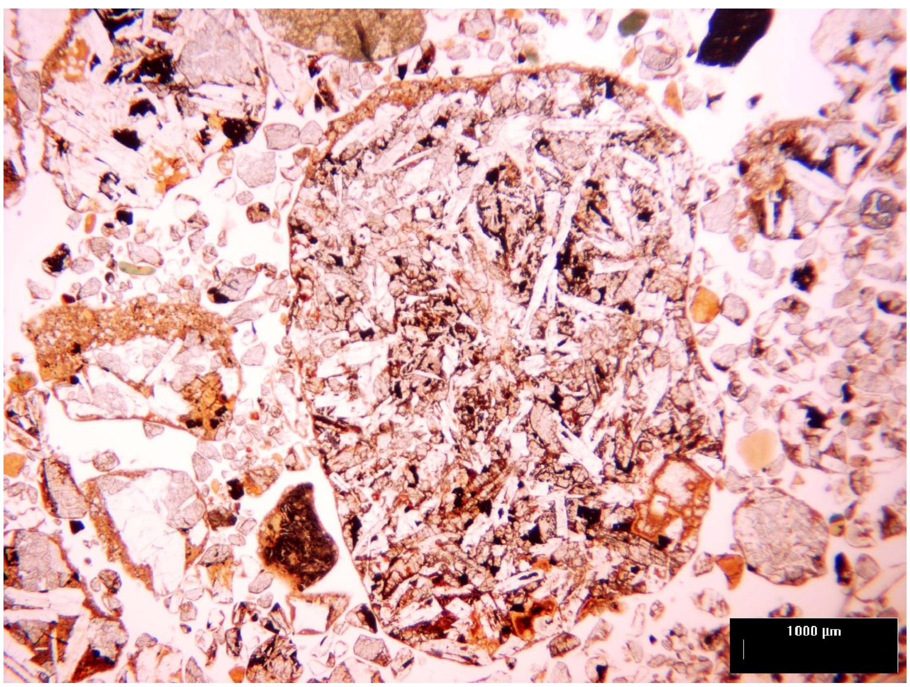

Figure 7.32 Silt cappings and coarse material within trench 3 taken in PPL.

7.8 RADIOCARBON DATING

The AMS ages were obtained at a depth of 1.45 m (trench 2 of the western slope deposit) and 1.50 m (trench 3 of the eastern slope deposit) (Table 7.19). These sampling depths represent the maximum depth of each trench. The ages range from 12 890 ± 60 radiocarbon yrs BP in trench 3 of the eastern slope deposit to 14 400 ± 60 radiocarbon yrs BP in trench 2 of the western slope deposit. The calibrated ages range from 15 390 yrs BP to 17 200 yrs BP.

7.9 SUMMARY

A site summary of the sedimentary characteristics of the Leqooa western and eastern deposits is presented in Tables 7.20 and 7.21. The sediment within the deposits varies, with the western deposit containing slightly finer material than the eastern deposit, especially in trench 3. The sediment within the western deposit contains several bimodal distributions, whilst they are fewer within the eastern deposit. The sediment in both deposits tends to range from very poorly to poorly sorted. Clast orientation is in the direction of the ridge crest in trench 1 of the western deposit and trench 3 of the eastern deposit, whilst it is random in trenches 2 and 3 of the western deposit and trench 2 of the eastern deposit. Clasts tend to dip between 0° and 30° in the western deposit and 0° and 40° in the eastern deposit. Both deposits contain predominantly bladed clasts; however clasts within the western deposit fall in the subangular categories of roundness, whilst those in the eastern deposit are more angular. Silt cappings are few in both deposits; however the western deposit contains several rotational structures. The calibrated AMS ages range from 15 390 yrs BP to 17 200 yrs BP indicating that the deposits are pre-Holocene.

Table 7.19 AMS and calibrated ages for the Leqooa Valley deposits (sampling depths: T2 = 1.45 m, T3 = 1.50 m).

Anal. No. [1] Gr-A	**Sample designation**	**$\delta^{13}C$ (‰ PDB)**	**Radiocarbon Age yrs BP**	**1σ yrs BC**	**2σ yrs BC**	**Calibrated yrs BP**
24891	Leqooa West T2	-18.9	14 400 ± 60	15 314 – 15 176	15 383 – 15 107	17 200
24890	Leqooa East T3	-19.9	12 890 ± 60	13 518 – 13 360	13 597 – 13 281	15 390

Table 7.20 A summary of the sedimentary characteristics at the Leqooa western deposit.

	Trench 1	**Trench 2**	**Trench 3**
Lithofacies	Soil overlying gravely diamict	Soil overlying gravely diamict	Soil overlying a medium - gravely diamict
Particle Size	-1 Phi (Gravel)	-1 Phi (Gravel)	-1 Phi (Gravel), 4 phi (v fine sand)
Sorting	Poorly – very poorly sorted	Poorly – very poorly sorted	Poorly - very poorly sorted
Fabric	In the direction of the ridge crest	Random	Random
Dip	10° - 30°	0° - 20°	0° - 20°
Shape	Bladed	Bladed	Bladed
Roundness	Angular	Sub-angular	Sub-angular
Micromorphology	-	Few silt and clay cappings	Rotation structures
AMS dating		17 200 yrs BP	

Table 7.21 A summary of the sedimentary characteristics at the Leqooa eastern deposit.

	Trench 1	Trench 2	Trench 3
Lithofacies	Soil overlying gravely diamict	Soil overlying gravely diamict	Soil overlying a medium - gravely diamict
Particle Size	-1 Phi (Gravel)	-1 Phi (Gravel)	-1 Phi (Gravel)
Sorting	Very poorly sorted	Very poorly sorted	Very poorly sorted
Fabric	Transverse to ridge crest	Random	In the direction of ridge crest
Dip	0° - 30°	20° - 40°	20° - 40°
Shape	Bladed	Bladed	Bladed
Roundness	Angular	Angular	Angular
Micromorphology	-	No cappings	Few cappings
AMS dating			15 390 yrs BP

CHAPTER 8

Sehonghong Results

8.1 INTRODUCTION

The Sehonghong River Site stretches for approximately 2km along the Sehonghong River (Figure 8.1), which flows in a westerly direction and is flanked by north and south-facing slopes reaching 3465 m a.s.l. Sediment has been exposed through fluvial incision primarily on the south-facing slopes and at a small area on a north-facing slope. Some of the exposures are vegetated and others are composed of loose material.

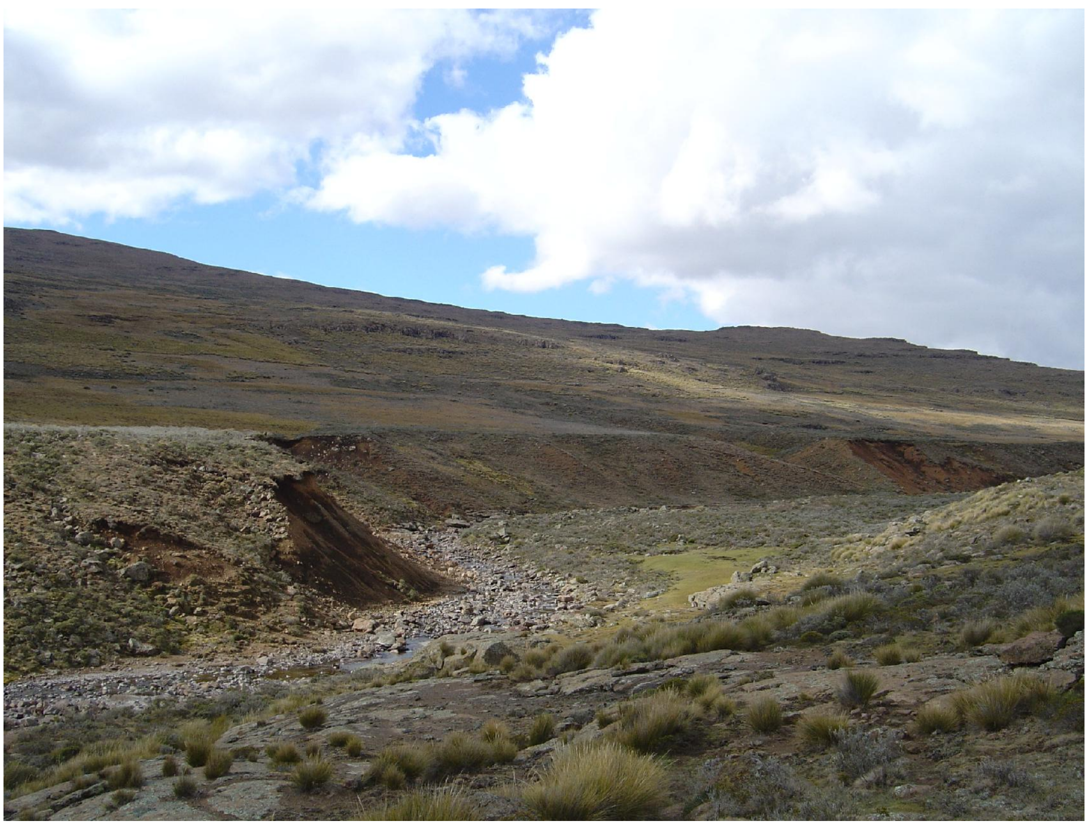

Figure 8.1 The deposits along the south-facing slopes of the Sehonghong River (photo by S. Mills).

8.2 MORPHOLOGY

The debris exposures on the south-facing slopes reach a maximum height of 13 m, whilst those on the north-facing slopes reach a maximum height of 15 m. Site 1 is located at 29º29’29’’S, 29º15’50’’E and the debris exposure is 6 m in height with a slope angle of 15º (cross-section A-A; Figure 8.2 and Figure 8.3). Site 2 is located at 29º29’28’’S, 29º16’5’’E and the debris exposure at this site is 11 m in height with a slope angle of 35º (cross-section B-B; Figure 8.2 and Figure 8.4). Site 3 is located on the north-facing slope at 29º29’32’’S, 29º16’14’’E where the exposure is 15 m in height and the slope angle is 45º, changing to 35º towards the river (cross-section C-C; Figure 8.2 and Figure 8.5). These deposits are different to those described for the Tsatsa-La-Mangaung, Sekhokong and Leqooa Valley deposits, in that they are more terrace-like in morphology and stretch over a greater distance (Figure 5.2, 6.2, 6.20 and 7.3).

Cross sections D-D and E-E represent the slope profiles containing a range of units related to various types of processes (see Figure 2.2 for comparison to a theoretical slope profile). The slope profile for cross section D-D begins with an interfluve unit, which has a slope angle of 1º, gradually increasing to 4º on the seepage slope unit. The slope angle then increases to 11º on the convex creep slope and reaches a maximum of 15º on the transportational midslope (Figure 8.2). The slope gradient then tapers off to 10º along the colluvial footslope. There is then a second convex creep slope, which has a slope angle of 12º, increasing to 14º on the second colluvial toeslope. The slope gradient then levels off to 4º on the alluvial toeslope, where it reaches the Sehonghong River. The total slope length is 2.1 km. Cross section E-E represents the slope profile for the north-facing slope and begins with an interfluve unit, which has a slope angle of 1º. This slope angle gradually increases to 4º on the seepage slope unit and reaches a maximum of 17º on the convex creep slope (Figure 8.2). The slope angle then levels off to 5º on the colluvial footslope and becomes even gentler on the alluvial toeslope where it is 3º. The total slope length down to the Sehonghong River is 2.5 km. The north-facing slope profile is much gentler than the south-facing slope profile.

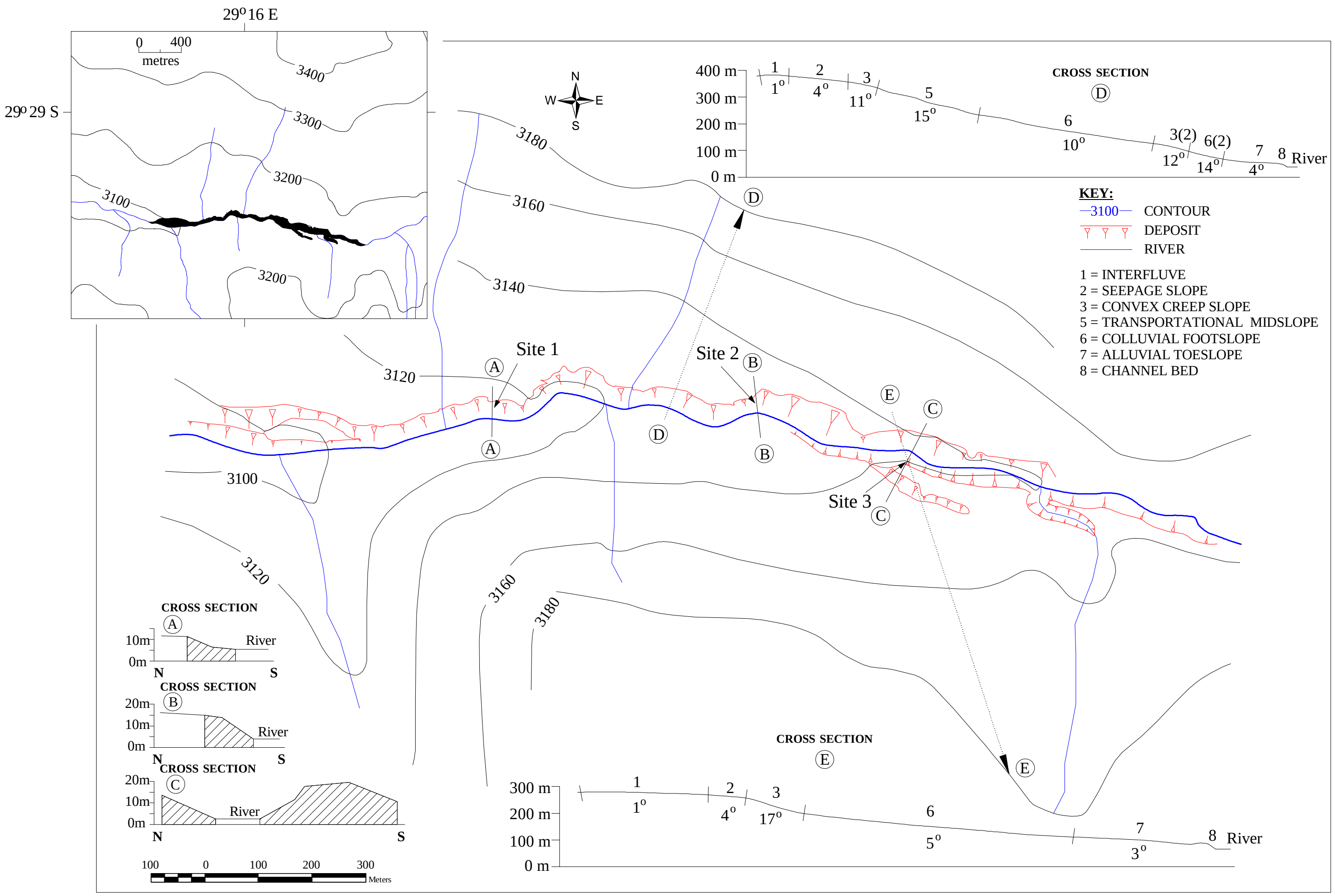

Figure 8.2 Morphological map of the Sehonghong River Valley deposits.

Figure 8.3 Site 1 along the Sehonghong River (photo by S. Mills).

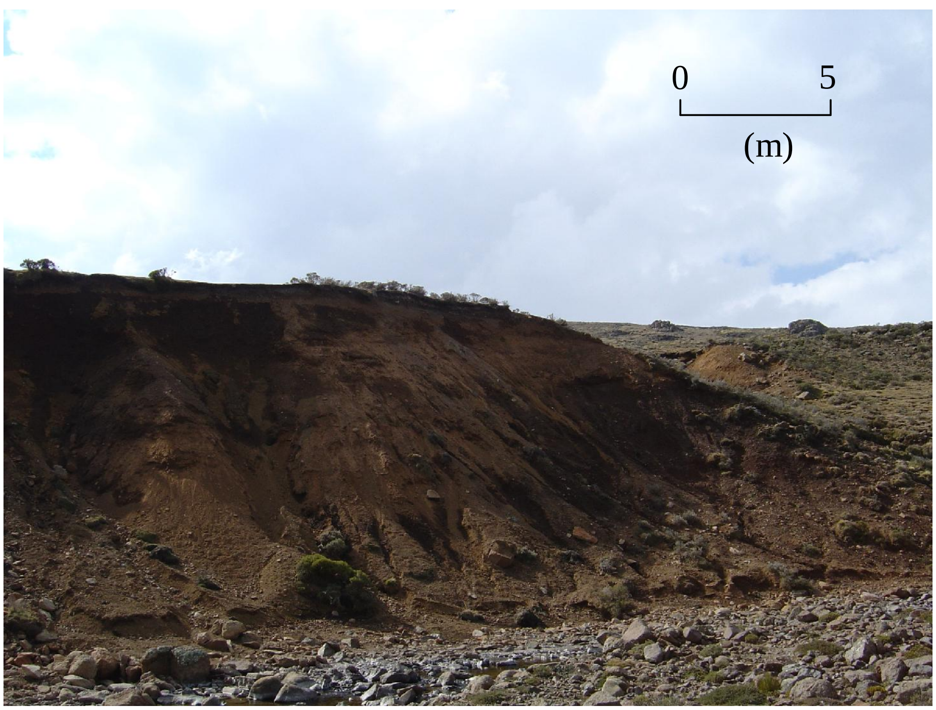

Figure 8.4 Site 2 along the Sehonghong River (photo by S. Mills).

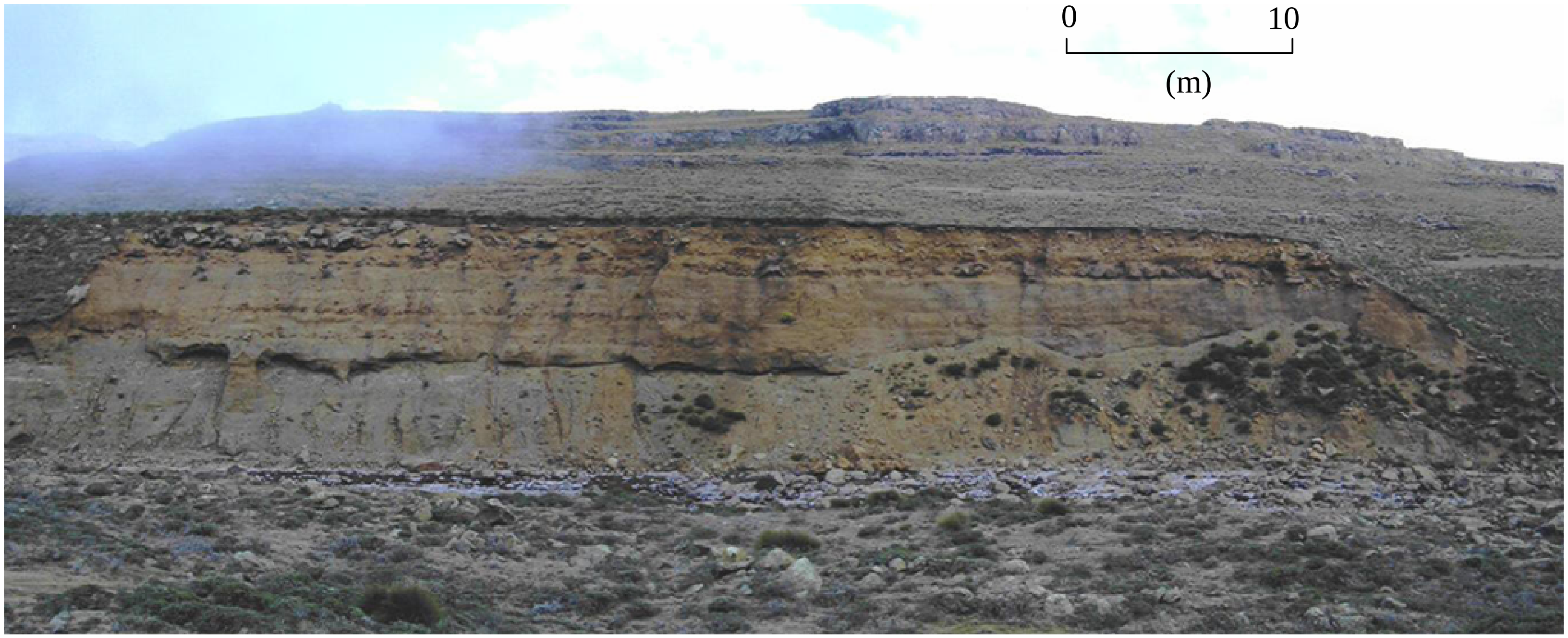

Figure 8.5 Site 3 along the Sehonghong River (photo by S. Mills).

8.3 FIELD OBSERVATIONS

Soil profile data collected for the three sites were reproduced as logs for each individual trench using a modified graphic chart after Krüger and Kjær (1999). The lithofacies at this site is completely different to that of the linear slope deposits. Three units have been identified at Site 1 below the present-day soil horizon (Figure 8.6). The first unit consists of sand which is massive and matrix supported with few clasts. The sediment in this unit is friable, poorly-sorted, yellowish brown in colour when dry and brown when wet, with yellowish red mottles. It was impossible to clear the face below 220 cm due to the nature of the loose material below. The second unit also consists of sand and was identified based on a change in colour, which is gray when dry. Moderate clasts are also present in this unit. The third unit consists of boulders, which are matrix-supported. The material in this unit is friable, moderately-sorted and strong brown in colour when wet and dry.

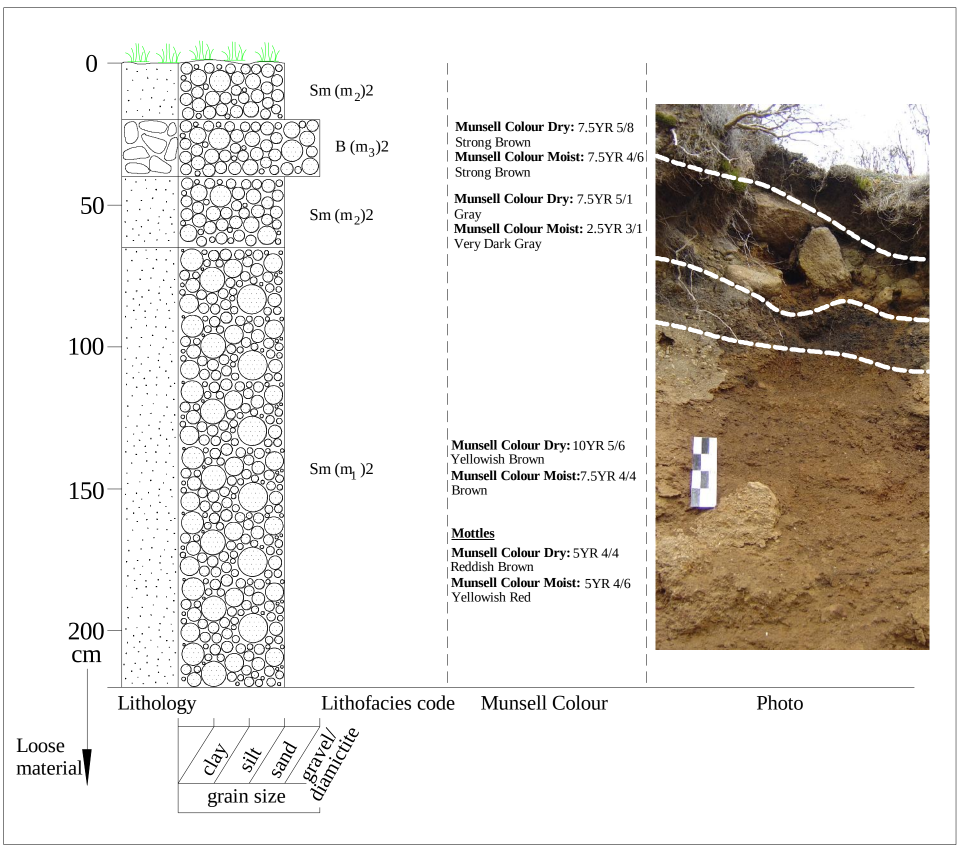

Figure 8.6 Sedimentological and stratigraphical data for Site 1 along the Sehonghong River.

The lithofacies at site 2 is similar to that at site 1 in terms of the clastic unit underlain by finer material (Figure 8.7). The sandy unit is massive with moderate clasts, friable and moderately sorted. The soil is light yellowish brown when dry. As in the case of Site 1 the material on the face of the deposit was extremely loose and it was impossible to sample below 120 cm depth. In contrast, the clastic unit is matrix-supported and clast rich. The sediment within this unit is friable, moderately-sorted and gray in colour when dry. There is also the presence of sediment which is light yellowish brown in colour when dry.

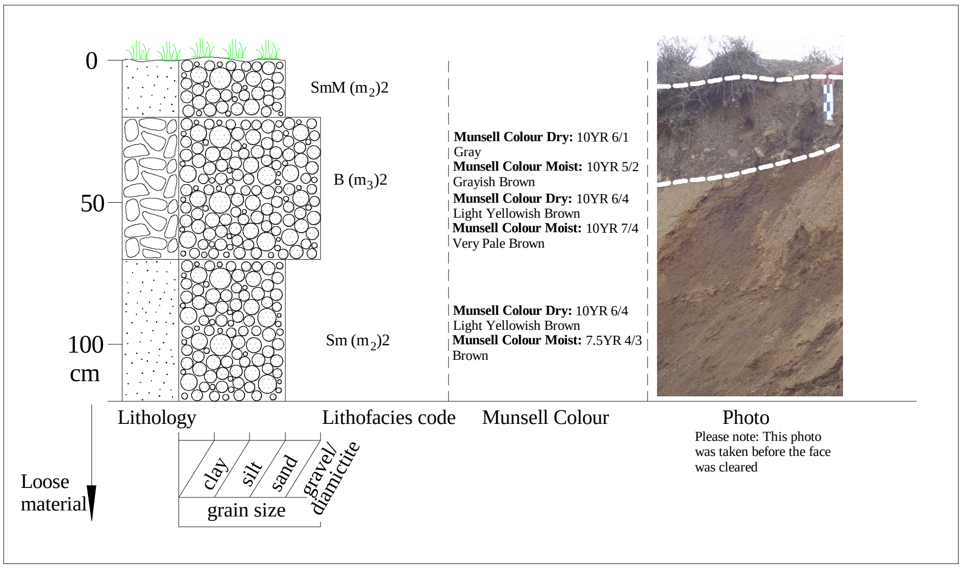

Figure 8.7 Sedimentological and stratigraphical data for Site 2 along the Sehonghong River.

Site 3 is located on a north-facing slope and contains a very different lithofacies to the other two sites. There is still the presence of a bouldery unit, however this unit is much larger and the material below it is much finer (Figure 8.8). Four units have been identified at this site below the present-day soil horizon. The first unit is made up of silt which contains a moderate quantity of clasts. It is moderately sorted, extremely firm and light grayish brown in colour when dry. The second unit contains large clasts which are matrix supported. This unit is poorly-sorted, firm and yellowish brown in colour when dry. The third unit consists of gravel which is massive. This unit is matrix supported and clast rich, moderately-sorted, firm and yellowish brown in colour when wet and dry. The fourth unit contains very large clasts. The boulders are

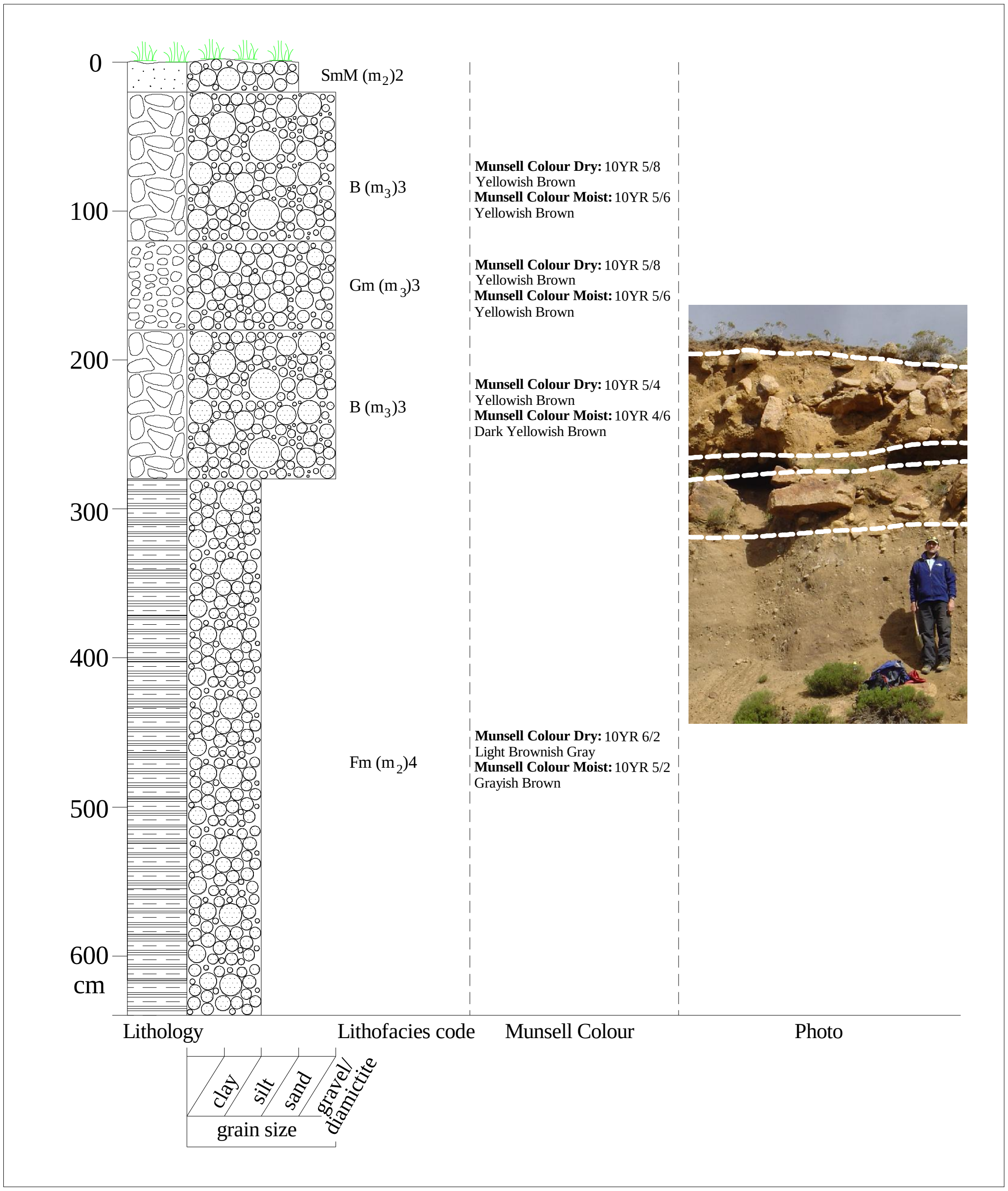

Figure 8.8 Sedimentological and stratigraphical data for Site 3 along the Sehonghong River.

matrix supported and this matrix is friable, poorly sorted and yellowish brown in colour when wet and dry.

8.4 PARTICLE SIZE ANALYSIS

Particle size analysis results (Figures 8.9 to 8.11 and Table 8.1) for Site 1 indicate that at 40 cm and 220 cm depth, gravel is the main constituent (>47%). Sand accounts for 35% and 33% at 45 cm and 220 cm respectively, whilst silt and clay make up <20%. In contrast, the sediment at 60 cm depth consists of almost equal quantities of gravel, sand and silt. The sediment at 45 cm and 60 cm depth is bimodal, with peaks at -1, 3 and 6 phi, whilst the sediment at 220 cm depth is unimodal. The results for Site 2 indicate the presence of two distinct units. At 50 cm depth, the sediment contains >60% gravel, whilst it only makes up 32% of the total sample at 120 cm depth. The sediment at site 2 at 120 cm depth contains almost equal quantities of gravel, sand and silt, whereas very little silt is present at 50 cm depth (5%). The sediment is unimodal at 50 cm depth; however is polymodal at 120 cm depth.

Particle size analysis results at Site 3 are fairly similar at 40 cm and 150 cm depth, where sand makes up the greater percentage of the sample (>44%). The secondary particle size mode is gravel, which constitutes >29% of the sample, whilst combined silt and clay values constitute <22% of the total samples. Sand is also the main constituent at 260 cm depth, where it accounts for 41% of the total sample. In contrast, at 430 cm and 640 cm depth, silt makes up between 56% and 79% of the total sample. All samples contain <2% clay. The sediment at 40 cm depth at site 3 falls within the transitional range of bimodality, however the sediment is bimodal at 150 cm and 260 cm depth. In contrast, the sediment below this depth is unimodal.

The graphic mean at Site 1 confirms the difference in the three units identified, where at 45 cm and 220 cm depth, the mean value falls in the coarse sand category, whereas at 60 cm depth, the sediment falls in the fine sand category. In contrast, the modal class is -1 phi in all three samples. The graphic mean results at Sites 2 and 3 indicate that the material becomes finer with depth. At Site 3, the sediment at 40 cm and 150 cm, the sediment constitutes medium sand, whilst at 430 cm, it constitutes medium silt. The presence of finer material at these depths is also reflected in the mode, which indicates that at 430 cm and 640 cm depth, the mode is 6 phi and 4 phi respectively (Table 8.1).

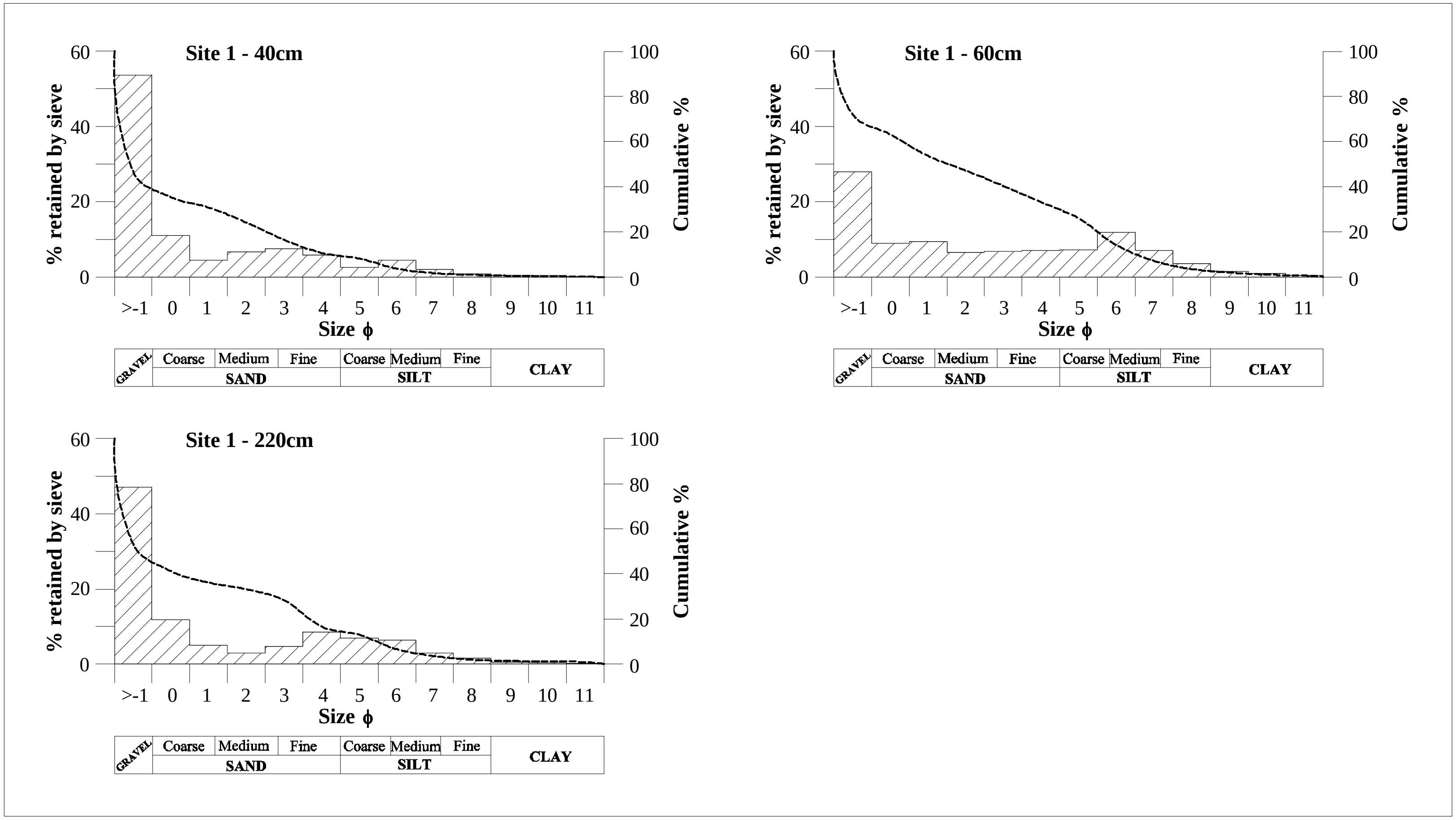

Figure 8.9 Grain size distributions for the sediment from Site 1 along the Sehonghong River.

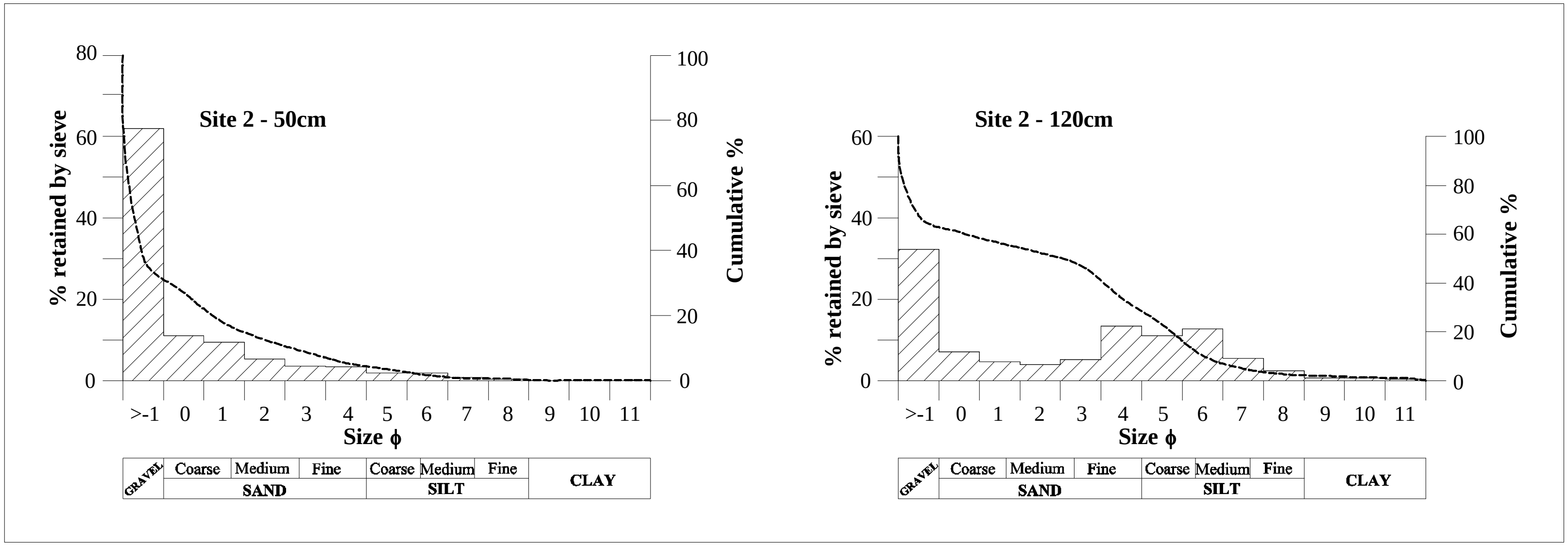

Figure 8.10 Grain size distributions for the sediment from Site 2 along the Sehonghong River.

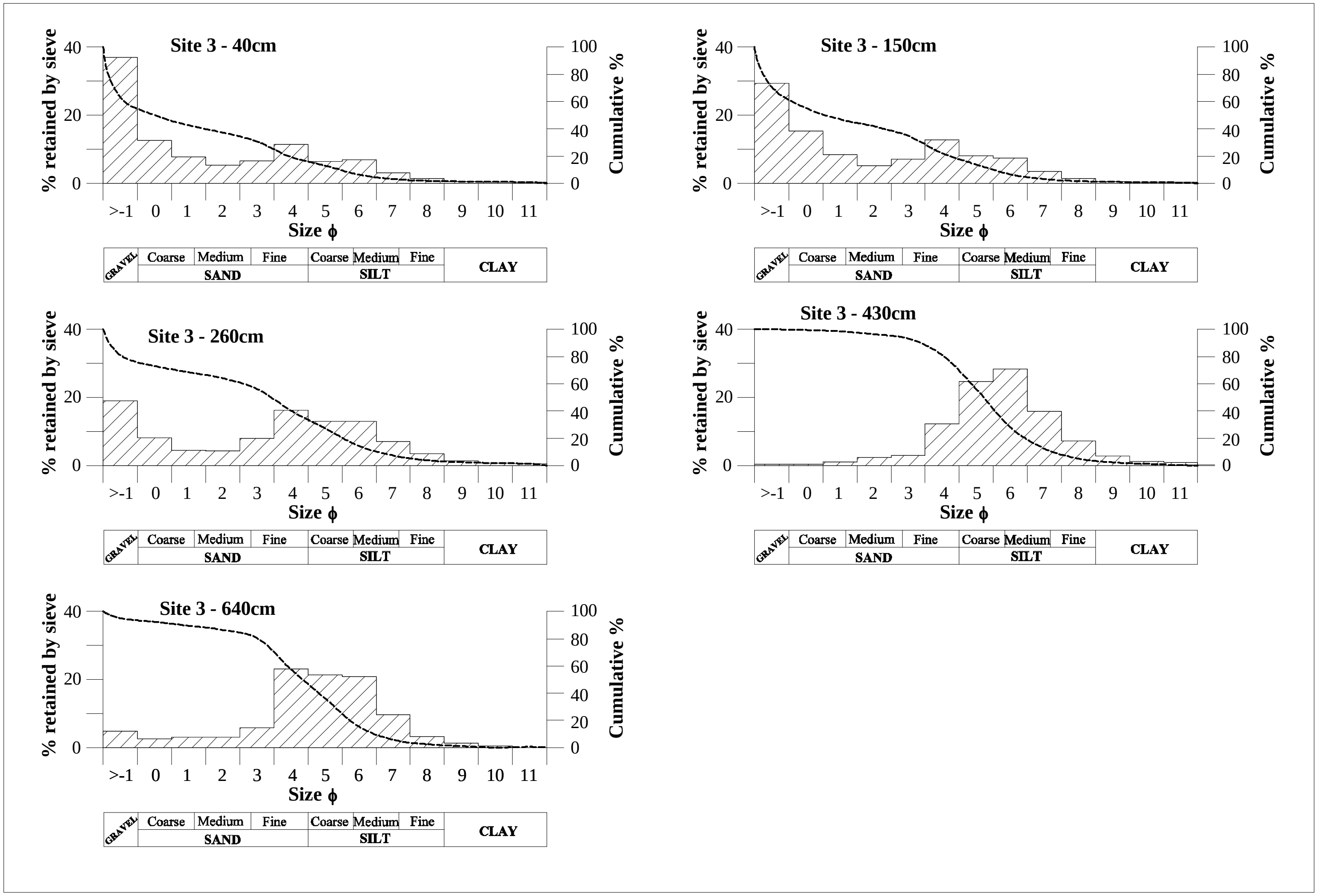
Site 3 - 40cm
Site 3 - 150cm
Site 3 - 260cm
Site 3 - 430cm
Site 3 - 640cm
% retained by sieve
Cumulative %
Size ϕ
>-1 0 1 2 3 4 5 6 7 8 9 10 11
GRAVEL
Coarse
Medium
Fine
SAND
SILT
CLAY

Figure 8.11 Grain size distributions for the sediment from Site 3 along the Sehonghong River.

Table 8.1 Particle size statistical values for the Sehonghong River deposits.

Sample	Depth	Gravel (%)	Sand (%)	Silt (%)	Clay (%)	Mean (phi)	Mode (phi)	Peaks (phi)	Bimodality Index (B^*)
Site 1	40 cm	54	35	10	1	0.37	-1	-1, 3, 6	0.56, 1.77
	60 cm	28	39	31	2	2.12	-1	-1, 6	3.0
	220 cm	47	33	19	1	0.94	-1	-1, 4	0.90
Site 2	50 cm	62	33	5	0	-0.19	-1	-1	-
	120 cm	32	34	32	2	2.39	-1	-1, 4, 6	2.06, 1.91
Site 3	40 cm	37	44	18	1	1.22	-1	-1, 4	1.54
	150 cm	29	49	21	1	1.46	-1	-1, 4	2.18
	260 cm	19	41	38	2	2.75	-1	-1, 4	4.26
	430 cm	0	19	79	2	5.22	6	6	-
	640 cm	5	38	56	1	4.33	4	4	-

Further statistical analyses have been undertaken in the form of sorting, skewness and kurtosis (Tables 8.2 and 5.3). The sediment sorting at the three sites ranges from poorly to very poorly-sorted. The sediment sampled at Site 1 is very coarse skewed, whilst at Site 2, skewness ranges from very coarse skewed to nearly symmetrical. In contrast, at Site 3, the sediment range from very coarse skewed to fine skewed. Kurtosis is highly variable within the samples at the three sites and ranges from very platykurtic to leptokurtic. The mean values in Table 8.3 indicate that the sediment at Site 1 is composed of medium sand, is very platykurtic, very coarse skewed and mesokurtic, whilst the sediment at Site 2 is very similar, however is leptokurtic. In contrast, the sediment at Site 3 is composed of very fine sand, is very poorly sorted, coarse skewed and mesokurtic.

Table 8.2 Particle size statistical values for the Sehonghong River deposits.

Sample		Sorting	Skewness	Kurtosis
Site 1	45 cm	2.04	-0.1	0.96
	60 cm	3.00	-0.33	1.13
	220 cm	2.49	-0.94	0.66
Site 2	50 cm	1.40	-1	1.77
	120 cm	2.85	0	0.56
Site 3	40 cm	2.51	-0.67	0.67
	150 cm	2.55	-0.50	0.64
	260 cm	3.00	0.17	0.64
	430 cm	1.56	-0.02	1.26
	640 cm	2.06	0.21	1.57

Table 8.3 Mean and Standard deviation for the particle size statistical analysis at the Sehonghong River deposits.

Site	Mean		Mode		Sorting		Skewness		Kurtosis	
	x	*s*	*x*	*s*	*x*	*s*	*x*	*s*	*x*	*s*
Site 1	1.14	0.89	-1	0	2.51	0.48	-0.76	0.37	0.92	0.24
Site 2	1.1	1.82	-1	0	2.13	1.03	-0.50	0.71	1.17	0.86
Site 3	3.00	1.75	1.4	3.4	2.34	0.55	-0.16	0.40	0.96	0.43

8.5 CLAST FABRIC AND FABRIC EIGENVALUES

Clast a-axis orientation and dip were plotted as an equal-area stereographic scatter plot and an equal-area stereographic contour plot (Figure 8.12). Clasts were sampled in the lower unit at Site 1, in the bouldery unit at Site 2 and in the lower unit at Site 3. Orientation of particles at Sites 1 and 2 tend to be downslope, although there is considerable variation in orientation at both sites. In contrast, clasts at Site 3 show preferred orientation parallel to the channel of the Sehonghong River. Most clasts at Sites 1 and 2 tend to dip between 10º and 30º, whilst at Site 3, clasts dip between 20º and 50º. The chi-square test was used in order to determine whether clast orientation is statistically significant. Clasts at Site 1 and 2 have a probability of being randomly distributed at a level >0.05%, whilst those at Site 3 have a statistically significant orientation (<0.05%). Clast orientation at Site 3 was only sampled at approximately 460 cm depth as it was impossible to sample accurately and safely in the upper units. However, in order to obtain an idea of clast orientation in the bouldery unit, visual observations were recorded and clasts appear to be randomly oriented, with a variety of dips.

S_1 values, which measure the strength of clustering about the mean axis for the three sites, are fairly high and range from 0.621 at Site 2 to 0.749 at Site 3. S_2 and S_3 values are much lower which indicates that the clast fabrics represent linear clusters, whereby all observations are approximately parallel and $S_1 \gg S_2 \approx S_3$.

The normalised eigenvalues for the three sites were plotted onto a general shape diagram (Figure 8.13), and indicate that the sediment at all three sites has low isotropy values (0.03 to 0.11) and moderate elongation values in the case of Sites 1 and 2 (0.53 to 0.42 respectively) and a high elongation value at Site 3 (0.72). Fabric shape ellipsoids are compared with plotted data from various published sources (Figure 8.13C) which indicate that the sediment at Site 1 falls within the sediment gravity flows, undeformed lodgement till and gelifluction deposit envelopes, whilst the sediment at Site 2 fails to fall within any envelopes. In contrast, the sediment at Site 3 falls within the undeformed lodgement till and basal ice envelopes. When compared with Figure 8.12D, the sediment at Site 1 falls within the boundaries of lodgement till, whilst the sediment at Site 3 falls within the boundaries of melt-out

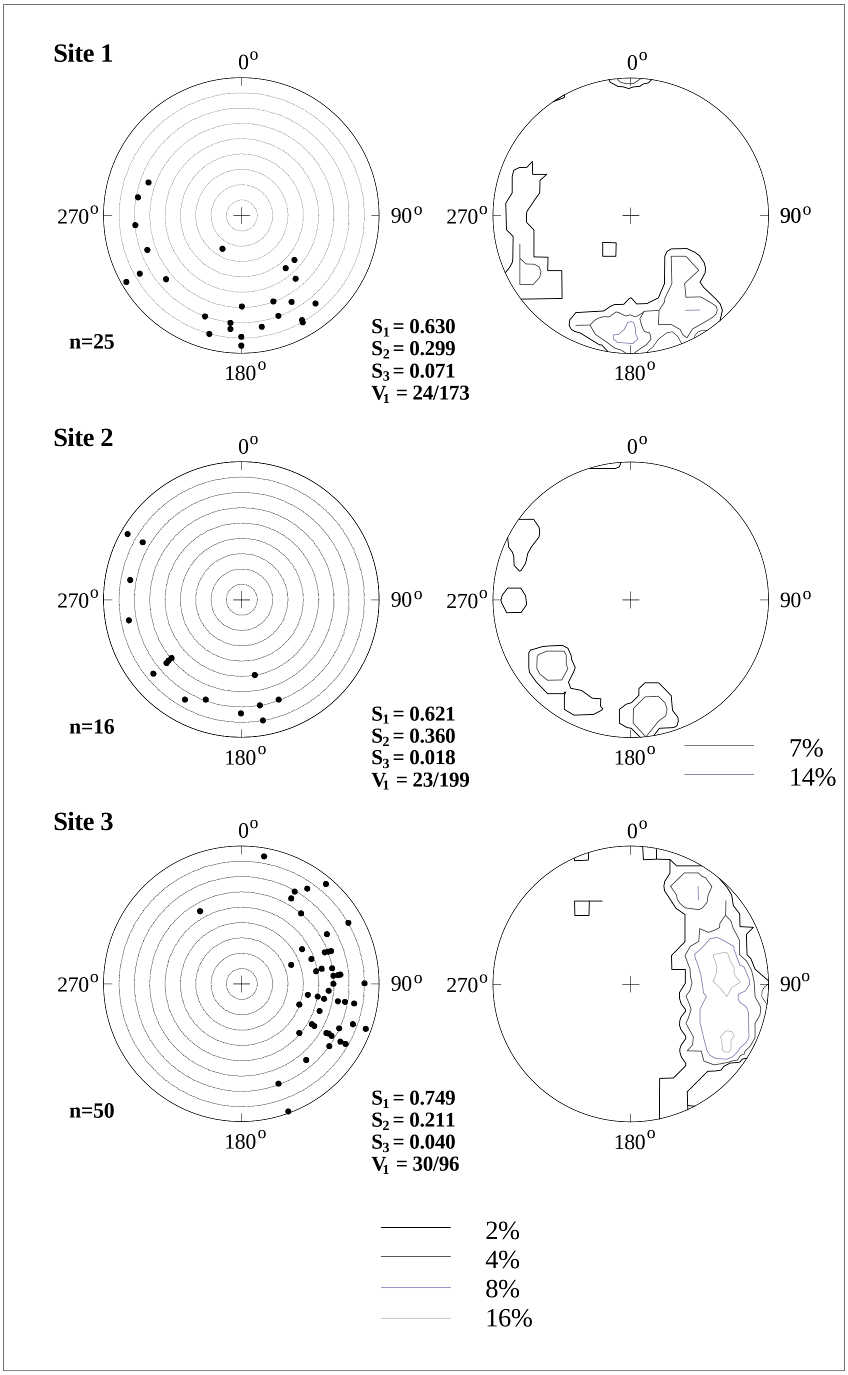

Figure 8.12 Clast orientation, dip and contouring at Sites 1, 2 and 3 at Sehonghong.

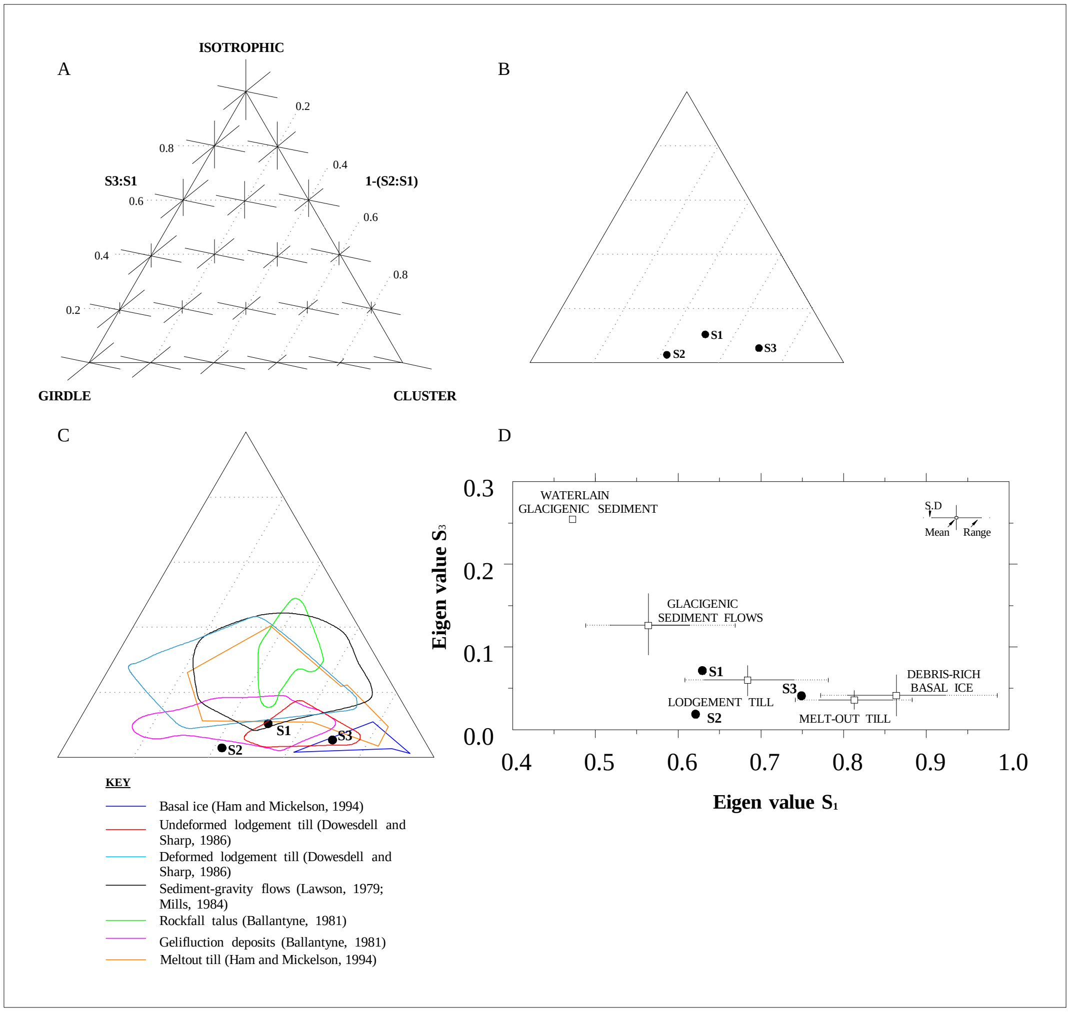

Figure 8.13 Till fabric using eigenvalue data for the Sehonghong River deposits. (A) The range of orthorhombic fabric shapes. (B) Fabric data from the three trenches. (C) Comparison with envelopes from a range of deposits. (D) Comparison with modern data fabrics from various environments (Dowdeswell *et al.*, 1985).

till. Once again the sediment at Site 2 fails to fall within any boundary. A triangular plot of normalised eigenvalues was also generated (Figure 8.14) in order to further compare the Sehonghong eigenvalues to envelopes produced by previous authors for various deposits. The sediment at Site 1 falls within the debris flow envelope produced by Lawson (1979), whilst the sediment at Site 3 falls within the melt- out till envelope. Both sites also fall within the internal fabric of rock glaciers envelope; however the sediment at Site 2 fails to fall within any envelopes.

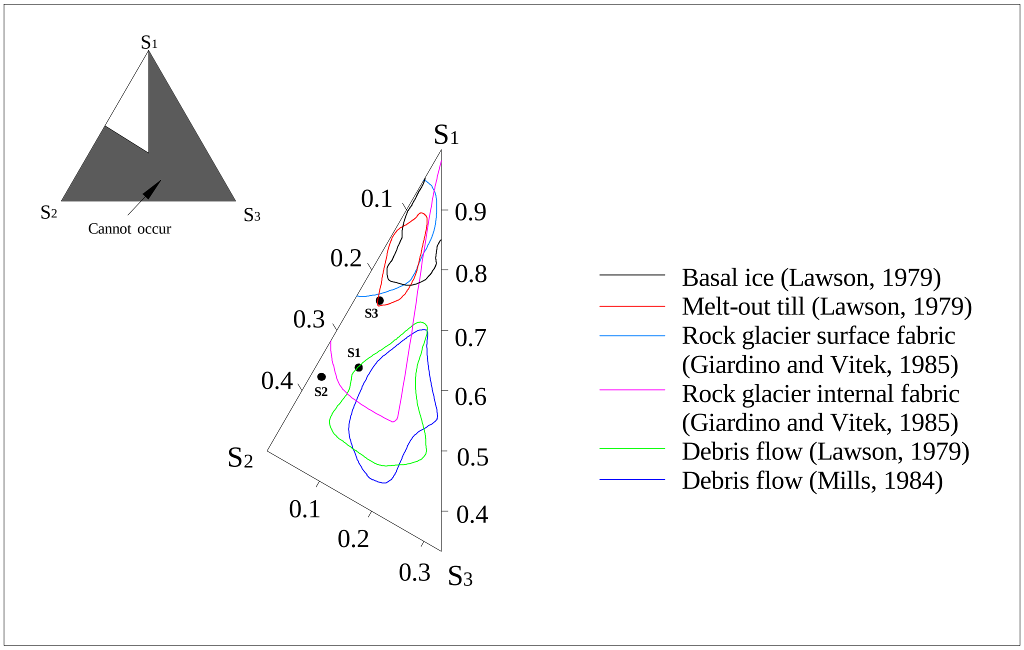

Figure 8.14 Triangular plot of normalised eigenvalues for the Sehonghong river deposits, showing envelopes suggested by various authors. The usable field diagram occupies one sixth of the diagram because $S_1 > S_2 > S_3$.

8.6 PARTICLE SHAPE

Particle form was plotted onto triangular diagrams using Tri-plot v1.3 (Graham and Midgley, 2000) and represents the descriptive classes defined by Sneed and Folk (1958) (Figure 8.15) and the isolines of the Oblate-prolate (OP) index of Dobkins and Folk (1970) (Figure 8.16).

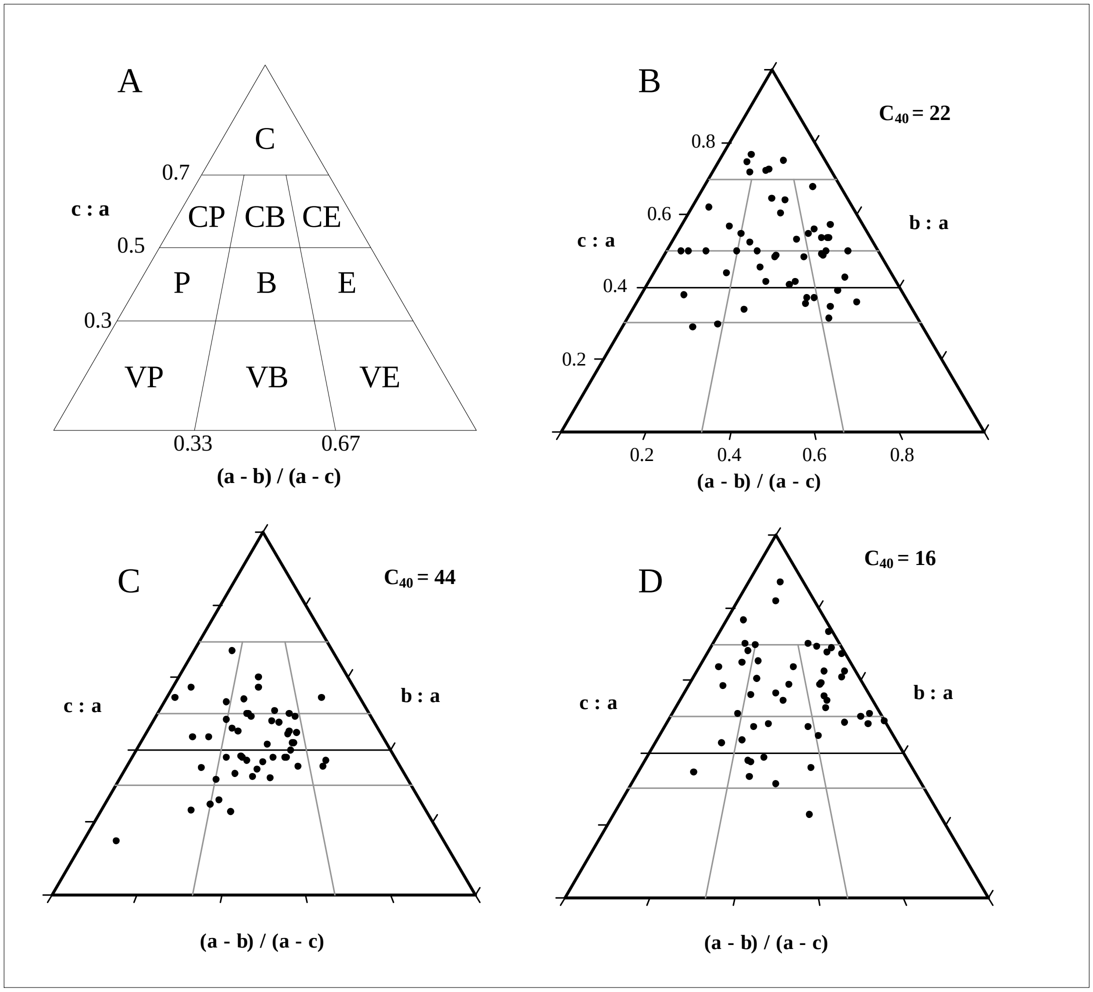

Figure 8.15 Triangular diagrams after Sneed and Folk (1958). (A) The descriptive classes according to Sneed and Folk (1958) where C = compact, P = platy, B = bladed, E = elongate and V = very. (B-D) Triangular diagrams for Trenches 1, 2 and 3 respectively at the Sehonghong River Site. C_{40} is the percentage of sample with c:a ≤ 0.4 (Benn and Ballantyne, 1993) (n = 50).

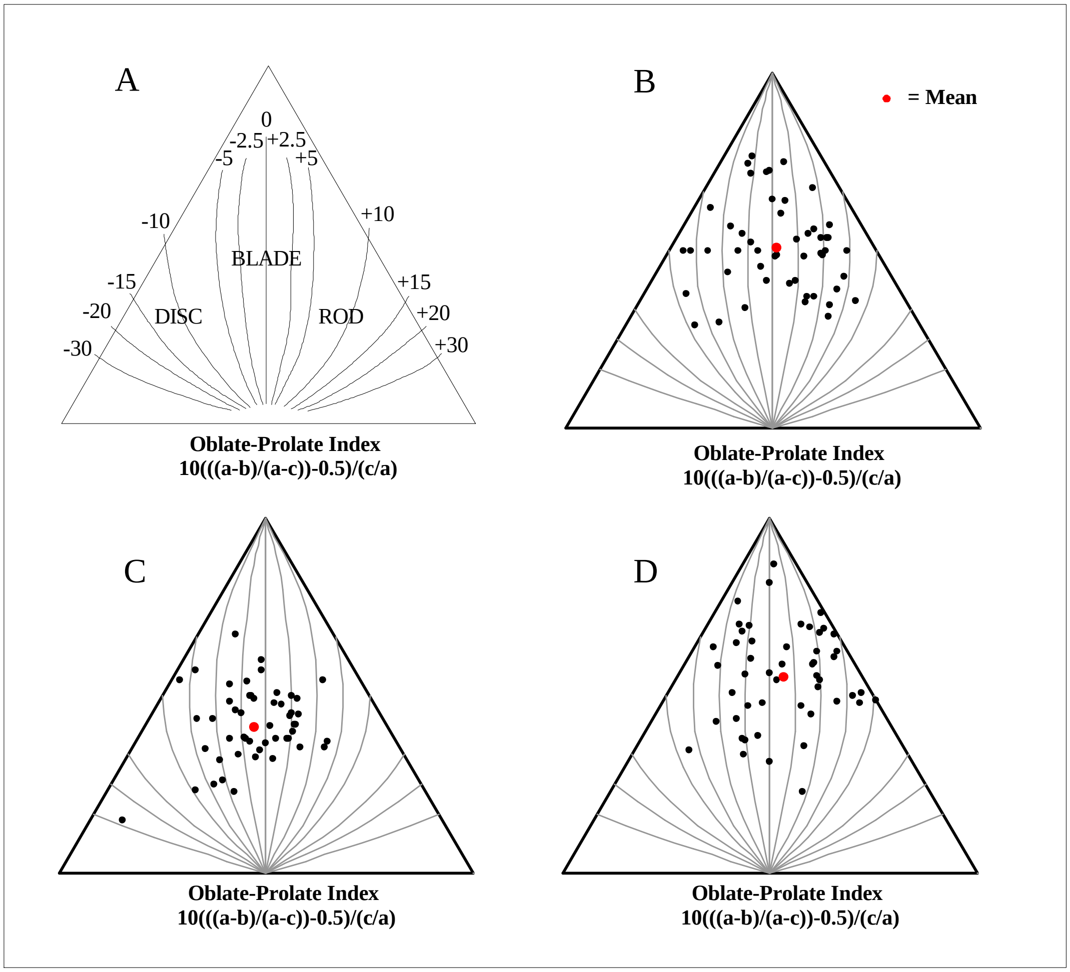

Figure 8.16 Triangular diagrams after Sneed and Folk (1958). (A) Isolines of the Oblate-prolate index according to Dobkins and Folk (1970). Triangular diagrams for Sites 1, 2 and 3 respectively at Sehonghong.

Clasts for Site 1 were sampled in the lower unit at approximately 150 cm depth. This site displays a variety of clast shapes; however clasts are predominantly bladed (36%), with elongate clasts being the second most common clast shape (32%) (Figure 8.15 and Table 8.4). Alternatively, clasts at Site 2 were sampled in the bouldery unit and are less compact in shape. Bladed clasts are once again the prevalent clast shape, with 72% of the total sample falling in this category. Clasts at Site 3 also tend to fall within the compact categories and bladed and elongate shapes form the majority (36% each). The greater amount of compact shapes is also reflected in the C_{40} index, which ranges from 16 at Site 3 to 44 at Site 2.

Table 8.4 The percentage of clasts falling within the various shape categories at the Sehonghong Site.

Shape	Site 1 (%)	Site 2 (%)	Site 3 (%)
Compact	12	-	14
Platy	20	22	14
Bladed	36	72	36
Elongate	32	6	36

Figure 8.16 once again indicates the wide variety of clast shapes at Site 1 with the presence of mostly bladed shapes but also some disc-like and rod-like shapes. Alternatively, there are practically no rod-like shapes at Site 2 and once again a variety of shapes at Site 3. The mean shape however at all three sites falls within the blade category, which is further reinforced by the values in Table 8.5, where the Oblate-prolate index falls between -1.56 and 1.34, which represents bladed shapes. The maximum projection sphericity is represented in Figure 8.17 and indicates that clasts at Site 1 fall between 0.4 and 0.9, whilst those at Site 2 fall between 0.3 and 0.8. In contrast, clasts at Site 3 have a greater sphericity, with clasts falling between 0.4 and 1. This is further reflected in Table 8.5 where mean maximum projection sphericity is 0.74 at Site 3. Once again it was not possible to sample clasts in the bouldery unit at Site 3 as a result of accuracy and safety, however visual observations were recorded and clasts appear to be predominantly more angular than those measured in the lower unit.

Table 8.5 The shape of clasts measured at Sehonghong. (*x* = mean, *s* = standard deviation).

	Number In Sample	Oblate-prolate Index		Maximum Projection Sphericity		Visual Roundness (Powers, 1953)	
		x	*s*	*x*	*s*	*x*	*s*
Site 1	50	0.52	4.72	0.70	0.10	1.62	0.64
Site 2	50	-1.56	5.32	0.62	0.10	1.24	0.72
Site 3	50	1.34	4.56	0.74	0.11	2.54	1.16

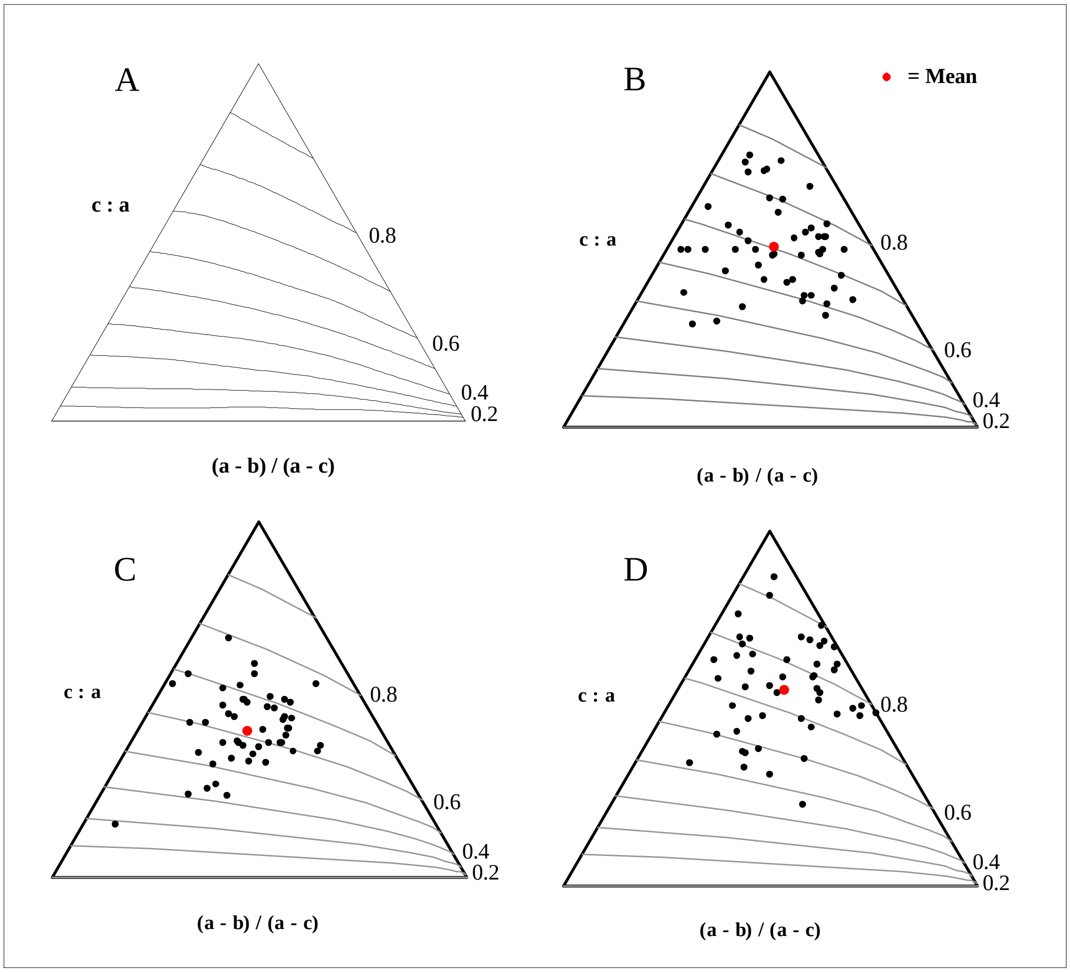

Figure 8.17 Triangular diagrams after Sneed and Folk (1958). (A) Isolines of the maximum projection sphericity according to Sneed and Folk (1958). Solid lines represent the classes defined by Zingg (1935). Triangular diagrams for Sites 1, 2 and 3 respectively at Sehonghong.

Clast roundness was obtained using the images of Powers (1953), where a roundness category is assigned to each clast (Figure 8.18 and Table 8.6). The majority of clasts at Site 1 fall within the angular and subangular categories (92%), with 8% falling in the subrounded category of roundness. Alternatively, clasts at Site 2 are slightly more angular, with 16% of clasts falling in the very angular category. Angular clasts form the modal class at this Site with 44%. In contrast, Site 3 contains much more rounded clasts. Subangular clasts form the modal class (34%); however there is also the presence of 28% subrounded clasts, as well as 20% rounded and well rounded clasts.

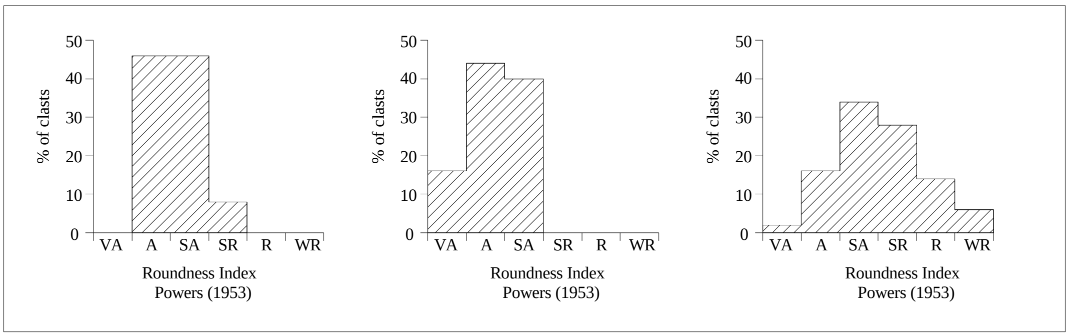

Figure 8.18 Graphs representing visual roundness of clasts (after Powers 1953) at Site 1 (A), 2 (B) and 3 (C) at Sehonghong. VA = Very Angular, A = Angular, SA = Sub Angular, SR = Sub Rounded, R = Rounded, WR = Well Rounded (n = 50).

Table 8.6 The percentage of clasts falling in the roundness categories at Sehonghong.

	VA (%)	A (%)	SA (%)	SR (%)	R (%)	WR (%)
Site 1	-	46	46	8	-	-
Site 2	16	44	40	-	-	-
Site 3	2	16	34	28	14	6

The t-test was performed in order to determine whether the sediment sampled at the three sites for form, sphericity and roundness were statistically significant (<0.05%) (Table 8.7). The sediment sampled at Site 1 and Site 3 is statistically significant for the Oblate-prolate index and maximum projection sphericity, whilst the sediment is not statistically significant for visual roundness. Sites 1 and 2 and Sites 2 and 3 are not significant in all cases, suggesting that different processes have led to their formation.

Table 8.7 The statistical significance calculated by the t-test of the shape of clasts sampled at the three Sehonghong Sites (SS = Statistically significant, NS = Not significant).

Trenches	Oblate Prolate Index	Maximum Projection Sphericity	Visual Roundness
S1-S2	NS	NS	NS
S1-S3	**SS**	**SS**	NS
S2-S3	NS	NS	NS

The t-test was also used in order to compare the three sites along the Sehonghong River to the linear deposits at the Tsatsa-La-Mangaung, Sekhokong and Leqooa Valley sites (Table 8.8). Although there are a few cases where the Oblate-prolate index is not significant between sites, in general most sites are statistically significant. The Oblate-prolate index describes the shape of clasts, and the clasts at all sites tend to have a mean bladed shape, therefore one would not expect there to be a great difference between sites (Figures 5.20, 6.13, 6.31, 7.23, 7.27 and 8.16). In contrast, several samples are not significant for maximum projection sphericity. This tends to occur between the linear deposits and Sites 1 and 3 along the Sehonghong River, whilst clasts at Site 2 compared to the linear deposits are predominantly statistically significant. Furthermore, a trend can once again be observed between Site 3 along the Sehonghong River and the linear deposits, where visual roundness is not significant in almost all cases. This once again indicates that different processes may have occurred at this site.

8.7 MICROMORHOLOGY

One thin section was sampled at each site, with the exception of Site 3 as the material was too hard to insert a Kubiena tin. Samples for thin section were taken at 220 cm depth at Site 1 and 100 cm depth at Site 2 and are represented in Table 8.9. The fabric pattern for the Sehonghong deposit (Sites 1 and 2) is random and the grains have a broad angle of parallelism which is weakly expressed. The c/f related distribution is single spaced porphyric in the case of Site 1 and double spaced porphyric at Site 2 and the dominant fraction is coarse sand. The particles are poorly sorted to unsorted, blocky, subangular with a smooth surface at Site 1 and an undulating surface at Site 2. The aggregates in the thin sections are spheroidal peds which are weakly separated. Void type is channel and vughy, with a predominantly channel microstructure. The total percentage area occupied by voids ranges from 10% at Site 2 to 15% at Site 1.

Table 8.8 The statistical significance calculated by the t-test of the shape of clasts sampled at the three sites at Sehonghong, compared to those for the Tsatsa-La-Mangaung, Sekhokong Sites 1 and 2 and Leqooa western and eastern deposits (SS = Statistically significant, NS = Not significant).

Site and Trenches	Oblate Prolate Index	Maximum Projection Sphericity	Visual Roundness
S1 – TsatsaT1	**SS**	NS	**SS**
S1 – TsatsaT2	**SS**	NS	**SS**
S1 – TsatsaT3	**SS**	NS	**SS**
S2 – TsatsaT1	NS	**SS**	**SS**
S2 – TsatsaT2	NS	**SS**	**SS**
S2 – TsatsaT3	NS	**SS**	NS
S3 – TsatsaT1	**SS**	NS	NS
S3 – TsatsaT2	**SS**	NS	NS
S3 – TsatsaT3	**SS**	NS	NS
S1 – SEK1T1	**SS**	NS	NS
S1 – SEK1T2	**SS**	NS	**SS**
S1 – SEK1T3	**SS**	**SS**	**SS**
S2 – SEK1T1	**SS**	**SS**	**SS**
S2 – SEK1T2	**SS**	**SS**	**SS**
S2 – SEK1T3	**SS**	NS	NS
S3 – SEK1T1	**SS**	NS	NS
S3 – SEK1T2	**SS**	NS	NS
S3 – SEK1T3	**SS**	NS	NS
S1 – SEK2T1	**SS**	NS	**SS**
S1 – SEK2T2	NS	**SS**	**SS**
S1 – SEK2T3	**SS**	**SS**	NS
S2 – SEK2T1	**SS**	**SS**	NS
S2 – SEK2T2	NS	**SS**	NS
S2 – SEK2T3	**SS**	NS	NS
S3 – SEK2T1	**SS**	NS	NS
S3 – SEK2T2	NS	NS	NS
S3 – SEK2T3	NS	NS	**SS**
S1 – LEQWT1	**SS**	NS	**SS**
S1 – LEQWT2	**SS**	NS	**SS**
S1 – LEQWT3	**SS**	**SS**	**SS**
S2 – LEQWT1	**SS**	**SS**	**SS**
S2 – LEQWT2	**SS**	**SS**	NS
S2 – LEQWT3	NS	**SS**	NS
S3 – LEQWT1	**SS**	NS	NS
S3 – LEQWT2	**SS**	**SS**	NS
S3 – LEQWT3	**SS**	NS	NS
S1 – LEQET1	**SS**	NS	NS
S1 – LEQET2	**SS**	**SS**	**SS**
S1 – LEQET3	**SS**	NS	**SS**
S2 – LEQET1	**SS**	**SS**	**SS**
S2 – LEQET2	NS	**SS**	**SS**
S2 – LEQET3	**SS**	**SS**	NS
S3 – LEQET1	**SS**	NS	NS
S3 – LEQET2	**SS**	NS	NS
S3 – LEQET3	**SS**	NS	NS

Table 8.9 Micromorphological description of the Sehonghong samples.

Micromor-logical features →	Skeleton									Aggregates		Voids			Parent material				Groundmass				Pedofeatures								
	Fabric						Shape										Fine											Infillings		Crystals	
Sample No. ↓	Pattern	Degree of parallelism	Quantity of oriented particles	C/F related distribution	Dominant size fraction	sorting	Shape	Degree of roundness	surface roughness	peds	ped seperation and pedality	Void type	Microstructure	% total area occ-upied by voids	Rock type	Average size um	Colour	Limpidity	C/F 2mm	C/F 10um	C/F related distribution	Cappings	Texture	laminated	Coatings	Texture	laminated	Classification	Descriptive criteria	Crystals	Crystal intergrowth
S1 220	R	BA	W-E	SSP	CS	P/U	B	SA	S	S	WS	C&V	CM	15	B	3000	YB	SP	4:1	7:3	DSP	●●●	SL	NL		-	-	LD	PF	●	P
S2 100	R	BA	W-E	DSP	CS	P/U	B	SA	U	S	WS	C&V	CM	10	B	2880	YB	SP	3:2	4:1	DSP	●●	SL	NL	●	CL	NL	LD	PF	●	P

KEY:

Pattern:
R = Random

Degree of parallelism:
BA = Broad angle

Quantity of oriented particles:
WE = Weakly expressed:<33% of particles are oriented

C/F related distribution:
SSP = Single spaced porphyric
DSP = Double spaced porphyric

Size:
CS = Coarse sand

Sorting:
PS = Porly sorted
U = Unsorted

Shape:
P = Platy
B = Blocky

Degree of roundness:
A = Angular
SA = Subangular

Surface roughness:
U= Undulating
S = Smooth

Peds:
S = Spheroidal Peds

Ped seperation and pedality:
WS = Weakly seperated

Void type:
C = Channels
CM = Chambers
V = Vughs
VCM = Vugh and Chamber

Microstructure:
VM = Vughy microstructure
CM = Channel microstructure

Mineral type
B = Basalt

Colour:
YB = Yellowish Brown

Limpidity:
SP = Speckled

Cappings/coatings:
● <10%
●● <10-20%
●●● >20%

Texture:
SL = Silt
CL = Clay

Laminated:
NL = Nonlaminated
L = Laminated

Infillings classification:
LD = Loose discontinuous

Descriptive criteria:
PF = Passage features

Crystals:
● Few
●● Some
●● Many

Crystal intergrowth:
P = Parallel

The main rock type in the south-facing deposit is basalt, which averages approximately 3000 μm in length at Site 1 and 2880 μm in length at Site 2. The colour of the fine material is yellowish brown and has a speckled limpidity. The c/f ratio indicates that the material is predominantly coarse-grained, with very few fractions finer than 10 μm. The c/f related distribution of the groundmass is double-spaced porphyric at both sites. The pedofeatures present in thin section are cappings at both sites as well as coatings at Site 2. Site 1 contains more than 20% of particles with cappings (approximately 80%). These are made up of silt and are non-laminated. In some cases the cappings encircle the particles (Figure 8.19). Site 2 contains between 10% and 20% of silt cappings on particles, however only the upper surface of grains are capped. Site 2 also contains clay coatings which line voids (Figure 8.20 and 8.21). These coatings are limpid, which are uniform fine clay without inclusions of microparticles (Stoops, 2003). Their limpidity is speckled and these clay coatings occur on less than 20% of voids. Infillings at Sites 1 and 2 are loose discontinuous passage features and crystals are few and parallel.

8.8 RADIOCARBON DATING

No samples were collected for radiocarbon dating due to lack of funding and the fact that several dates had already been obtained for Site 3 along the Sehonghong River by Prof. Stefan Grab. These dates were obtained for the eastern side (left) of the exposure (Figure 8.5) and will help reconstruct the time period of the various processes involved in the formation of the deposit at Site 3. Eleven units of alternating sand and gravel have been identified by Grab *et al.* (in prep) (Figure 8.21). The ages are represented in Table 8.10 and range from 19 800 ± 580 radiocarbon years BP at 6.4 m depth to 36 600 ± 1400 radiocarbon years BP at 8.5 m depth. The lowermost unit consisting of massive sand with clay and silt lenses yielded a calibrated age of 43 085 yrs BP. The radiocarbon date obtained at 7.5 m depth within an organic horizon yielded a calibrated age of 27 410 yrs BP. Finally, the sample at 6.4 m depth sampled in an organic sand unit produced a calibrated age of 23 055 yrs BP.

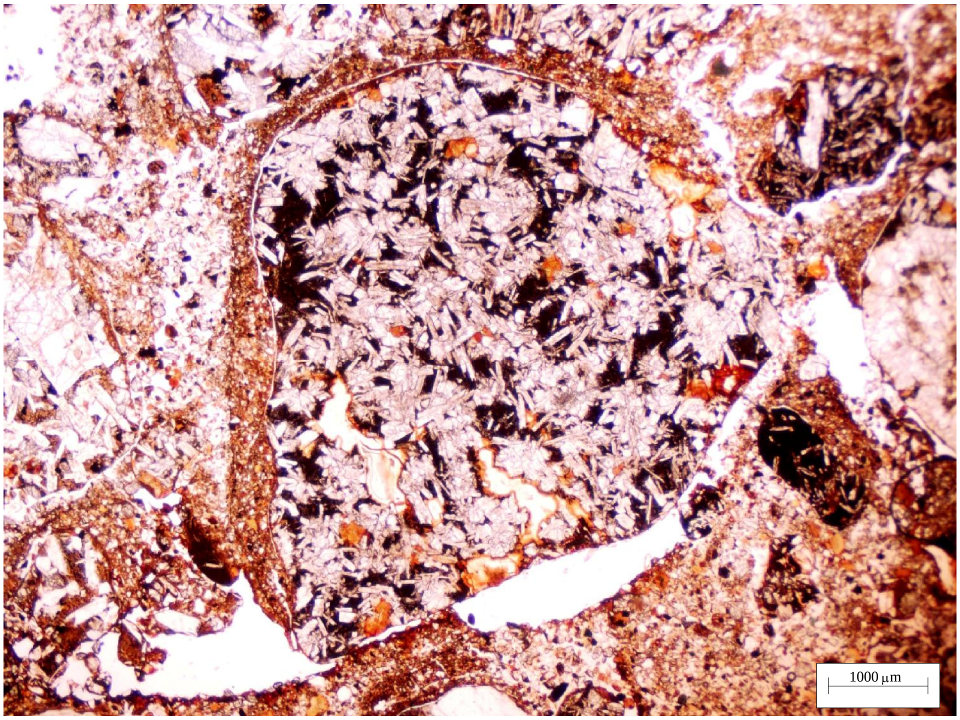

Figure 8.19 Silt capping encircling basal grain taken in PPL at Sehonghong Site 1.

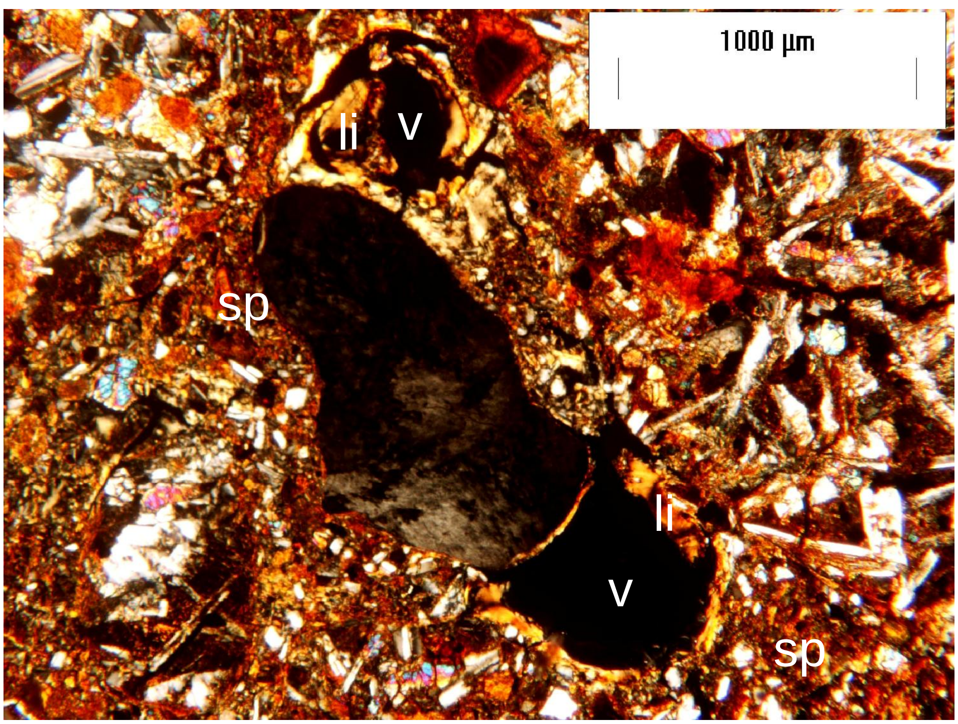

Figure 8.20 Clay coatings at Sehonghong Site 2 taken in XPL (li = Limpid, sp = speckled, V = void).

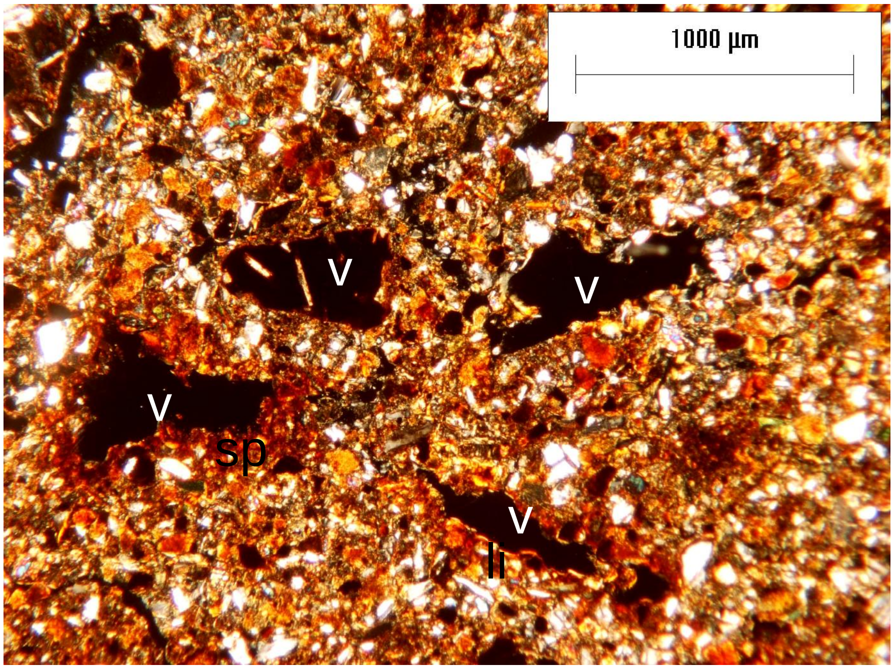

Figure 8.21 Clay coatings at Sehonghong Site 2 taken in XPL (li = Limpid, sp = speckled, V = void).

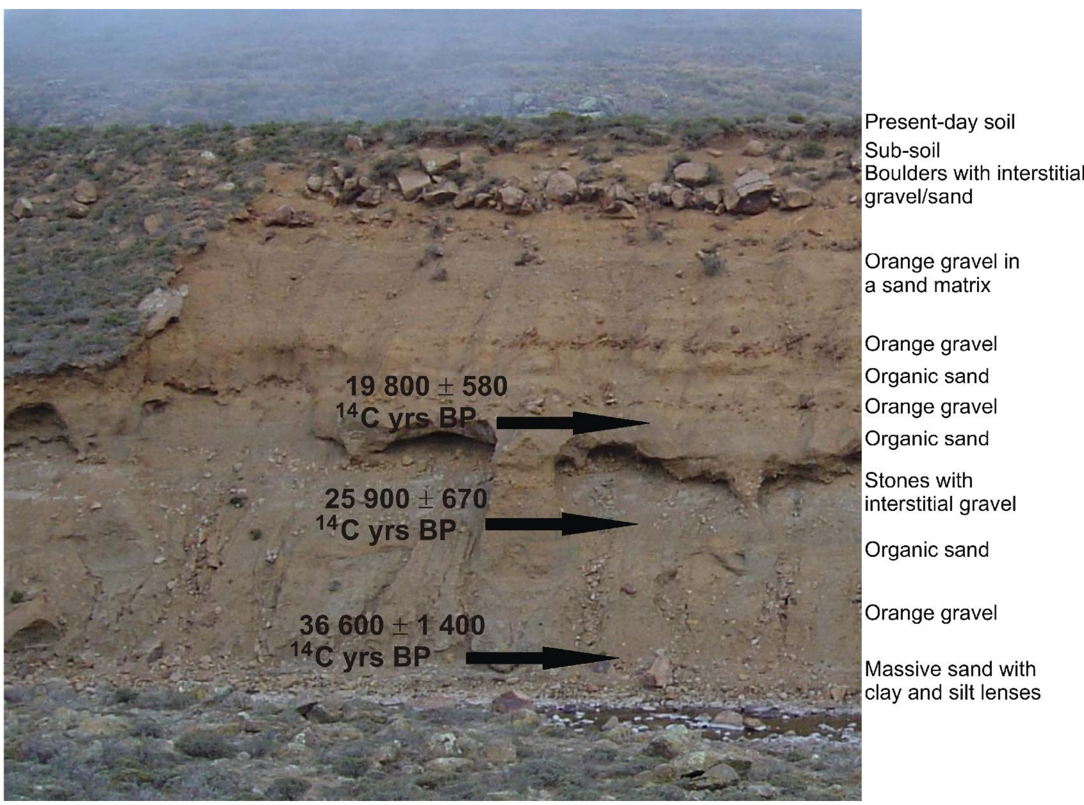

Figure 8.22 The site stratigraphy and Radiocarbon dates for the exposure at Site 3 described by Grab *et al*. (in prep).

Table 8.10 Radiocarbon and calibrated ages for the Sehonghong Site 3 deposit (sampling depths: 6.4 m, 7.5 m, 8.5 m).

Anal. No. [1] Gr-A	**Sample designation**	**$\delta^{13}C$ (‰ PDB)**	**Radiocarbon Age yrs BP**	**1σ yrs BC**	**2σ yrs BC**	**Calibrated yrs BP**
7813	Sehonghong A Un 2	-16.2	19 800 ± 580	21 794 – 20 348	22 434 – 19 432	23 055
7814	Sehonghong B Un 4	-19.8	25 900 ± 670	26 016 – 24 954	26 653 – 24 480	27 410
7816	Sehonghong C Un 6	-19.3	36 600 ± 1400	42 039 – 39 781	42 784 – 37 666	43 085

8.9 TEMPERATURE DATA FOR NHLANGENI

Temperature data have been recorded at Nhlangeni (approximately 2 km east of the Sehonghong Site) on a south- and north-facing slope at altitudes between 3200 m a.s.l. and 2650 m a.s.l. for the years 2000 to 2002 by Prof. Stefan Grab (Figure 8.23 and Table 8.11). The missing data during 2000 and 2001 is a result of faulty data loggers. The average annual air temperature over the 3 years ranges between 4.7ºC and 5.3°C on the south-and north-facing slopes at 3200 m a.s.l. There is also a difference of 4°C between the south-facing slope at 3200 m a.s.l. and the north-facing slope at 2650 m a.s.l.

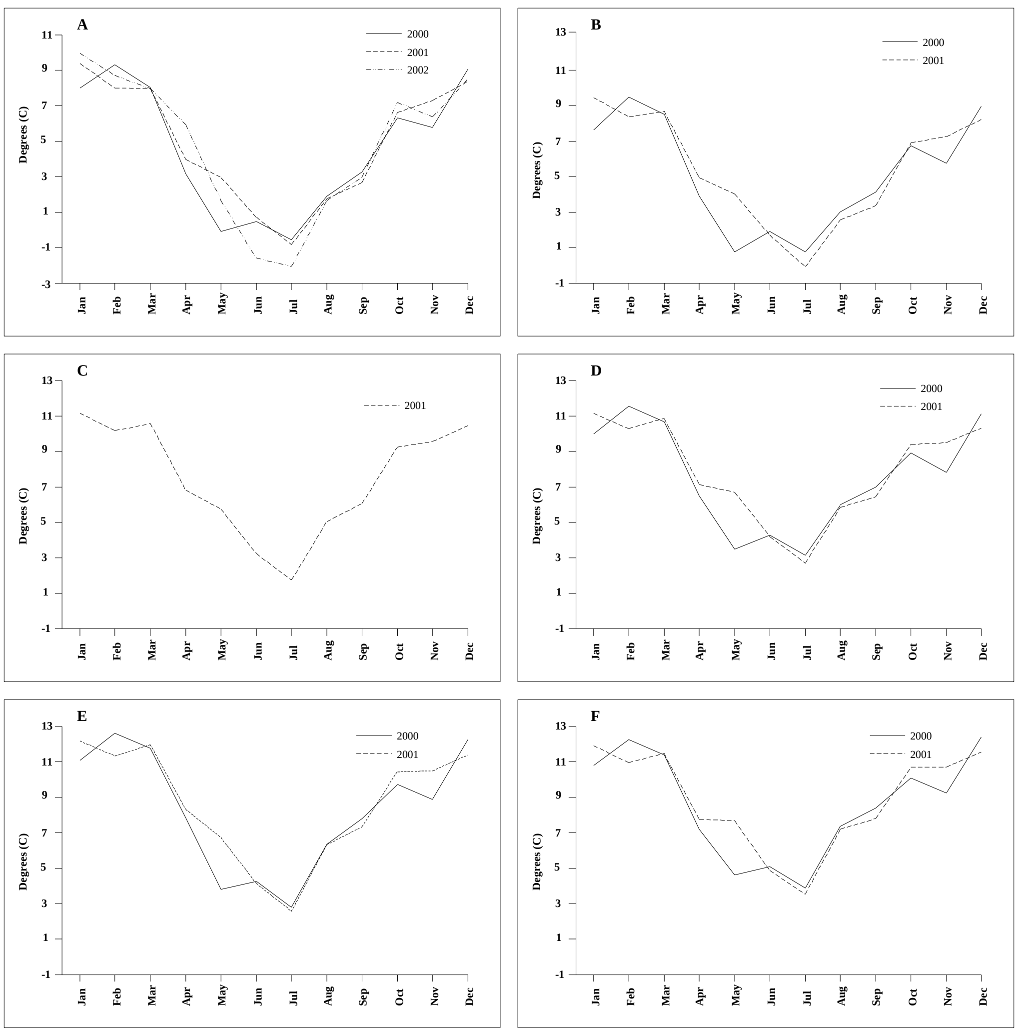

Figure 8.23 Mean monthly temperatures for Nhlangeni for the period 2000 to 2002 (A = south-facing slope 3200 m a.s.l., B = north-facing slope 3200 m a.s.l., C = south-facing slope 2900 m a.s.l., D = north-facing slope 2900 m a.s.l., E = south-facing slope 2650 m a.s.l., F = north-facing slope 2650 m a.s.l.).

Table 8.11 Mean annual air temperatures at Nhlangeni during the period 2000 to 2002.

Site	2000 (º C)	2001 (º C)	2002 (º C)	Av. Temp (ºC)
South-facing 3200 m a.s.l.	4.5	4.9	4.8	4.7
North-facing 3200 m a.s.l.	5.1	5.5	-	5.3
South-facing 2900 m a.s.l.	-	7.5	-	7.5
North-facing 2900 m a.s.l.	7.5	7.9	-	7.7
South-facing 2650 m a.s.l.	8.3	8.6	-	8.5
North-facing 2650 m a.s.l.	8.6	8.8	-	8.7

8.10 SUMMARY

A Site summary of the sedimentary characteristics of the three sites along the Sehonghong River is presented in Table 8.12. The sediment at Sites 1 and 2 is very similar and consists of a clastic/bouldery horizon overlying a gravely/sandy unit. Sediment sorting is poorly to very poorly sorted and clast orientation is random. Clasts tend to dip between 10° and 30°. Clasts are predominantly bladed in shape and fall in the angular and subangular categories at Site 1 and the angular category at Site 2. Clasts contain cappings in thin section at both sites and Site 2 also contains some clay coatings. In contrast, Site 3 consists of a bouldery unit overlying silts, both of which are poorly to very poorly sorted. Clast orientation is parallel to the Sehonghong River and clasts tend to dip between 20° and 50°. Clasts tend to be bladed and elongate and predominantly fall in the subangular category of roundness. Calibrated AMS ages indicate that the silty units located between 8.5 m 6.5 m were deposited between 43 085 yrs BP and 23 055 yrs BP.

Table 8.12 A summary of the sedimentary characteristics at Sehonghong.

	Site 1	**Site 2**	**Site 3**
Lithofacies	Clastic horizon overlying sandy sediment	Clastic horizon overlying sandy sediment	Boulders overlying silty sediment
Particle Size	-1 Phi (Gravel)	-1 Phi (Gravel)	-1 Phi (Gravel), 6 Phi, 5 Phi (Silt)
Sorting	Poorly – very poorly sorted	Poorly – very poorly sorted	Poorly - very poorly sorted
Fabric	Random	Random	Parallel to Sehonghong River
Dip	10° - 30°	10° - 30°	20° - 50°
Shape	Bladed	Bladed	Bladed and elongate
Roundness	Angular and subangular	Angular	Subangular
Micromorphology	Many cappings	Some cappings, few clay coatings	-
AMS dating			23 055 yrs BP, 27 410 yrs BP, 43 085 yrs BP